NIKE2D:

A Nonlinear, Implicit, Two-Dimensional Finite Element Code for Solid Mechanics - User Manual

Bruce E. Engelmann
Methods Development Group
Mechanical Engineering

John O. Hallquist
Originator

April 1991

TABLE OF CONTENTS

PREFACE

NIKE2D has been used extensively at the Lawrence Livermore National Laboratory for more than ten years to study the response of two-dimensional solids and structures undergoing finite deformations. The code was originated by Dr. John O. Hallquist of the Methods Development Group. Over the years, Dr. Hallquist has responded to evolving analysis requirements with software development that has continued to be at the forefront of technology. In 1988, Dr. Hallquist left the Laboratory to pursue a career in private business. The author wishes to thank Dr. Hallquist for his extensive contributions to the field, and pledges to keep NIKE2D on the leading edge of technology as we enter the new decade.

NIKE2D:
A Nonlinear, Implicit, Two-Dimensional Finite Element Code for Solid Mechanics - User Manual

ABSTRACT

This report is an updated user manual to the 1991 version of NIKE2D, and serves as a temporary theoretical manual. NIKE2D is an implicit finite element code for analyzing the finite deformation, static and dynamic response of two-dimensional, axisymmetric, plane strain, and plane stress solids. The code is fully vectorized and available on several computer platforms. A number of material models are incorporated to simulate a wide range of material behavior including elasto-plasticity, anisotropy, creep, thermal effects, and rate dependence. Slideline algorithms model gaps and sliding along material interfaces, including interface friction and single surface contact. Interactive graphics and rezoning is included for analyses with large mesh distortions. In addition to quasinewton and arc-length procedures, adaptive algorithms can be defined to solve the implicit equations using the solution language ISLAND. Each of these capabilities and more make NIKE2D a robust analysis tool.

1.0 INTRODUCTION

NIKE2D is an implicit finite element code for analyzing the finite deformation, quasistatic and dynamic response of two-dimensional, axisymmetric, plane strain, and plane stress solids. The finite element formulation accounts for both material and geometric nonlinearities. A number of material models are incorporated to simulate a wide range of material behavior including elasto-plasticity, anisotropy, creep, thermal effects, and rate dependence. Arbitrary contact between independent bodies is handled by a variety of slideline algorithms. These algorithms model gaps and sliding along material interfaces, including interface friction and single surface contact. Interactive graphics and rezoning is included for analyses with large mesh distortions.

The NIKE2D code has been used extensively at the Lawrence Livermore National Laboratory for more than ten years. It has been applied to a wide range of large deformation, inelastic response calculations. As a public domain code, NIKE2D's use outside the Laboratory has grown rapidly as well. The code has developed to meet evolving analysis requirements and utilize improved computer hardware. Algorithms have been optimized, and nearly all of the code is vectorized. Recent developments include a variety of new material models and a vastly improved solution capability. In addition to quasinewton and arc-length procedures, adaptive algorithms can be defined to solve the implicit finite element equations using the new solution control language called ISLAND (Interactive Solution Language for an Adaptive Nike Driver). Developed by Engelmann and Whirley (1991), ISLAND can be used to adapt the time step, the solution procedure, the rezoning strategy, etc., as a nonlinear analysis evolves. It is hoped that these improvements will expand the class of problems that can be solved with NIKE2D, while improving both accuracy and efficiency.

Versions of NIKE2D are available on several platforms: CRAY/UNICOS and NLTSS, VAX/VMS, and SUN/UNIX. The code has been ported to several other machines, and the extensive use of X-windows graphics allows the SUN/UNIX version to port easily to other UNIX based computers such as CONVEX and Silicon Graphics. A new double precision version of NIKE2D is available for VMS and UNIX systems. This is in response to the widely held belief that implicit analysis codes should be run in double precision on 32-bit machines to prevent large errors due to roundoff. Excellent speed performance has been reported with double precision NIKE2D on the new 64-bit IBM RS/6000 where single precision is represented by 32-bit words. The use of “single source control” has ensured that developments made in this rapidly evolving code are available on all platforms.

NIKE2D is part of a suite of codes developed in the Methods Development Group at LLNL. Other analysis codes include the three dimensional implicit NIKE3D code (Maker, Ferencz, and Hallquist [1990]), and the explicit finite element codes DYNA2D (Hallquist [1987]), and DYNA3D (Whirley and Hallquist [1991]). TOPAZ2D (Shapiro and Edwards [1990]) and TOPAZ3D (Shapiro [1985]) are finite element codes for nonlinear heat transfer calculations. PALM2D (Engelmann, Whirley and Shapiro [1990]) is a recently developed, fully coupled thermo-mechanical analysis code. Pre- and post-processors include MAZE (Hallquist [1983]) and ORION (Hallquist and Levatin [1985]) for two dimensions, and INGRID (Stillman and Hallquist [1985]) and TAURUS (Spelce and Hallquist [1991]) for three dimensions. The interactive pre-processor MAZE can be used to generate the full analysis model for NIKE2D. The graphical post-processor ORION may be used to display and plot NIKE2D analysis results. Thermomechanical calculations with NIKE2D can be driven by temperature profiles generated by the TOPAZ2D code.

Over the years, the wide user base of NIKE2D users has inspired continued development, and has kept the code on the forefront of technology. Feedback from analysts has been invaluable to the rapid and successful development of the code thus far. It is hoped that this type of feedback will continue, and that improvements made by others will be made available to the author for possible incorporation into the public domain version.

2.0 OVERVIEW OF NIKE2D

NIKE2D has a wide variety of capabilities that allow the analyst to solve most two-dimensional solid mechanics problems. The algorithms are optimized for speed and robustness, and most are vectorized for optimal performance on vector machines such as the CRAY. The NIKE2D code has a number of material models that include:

- elasticity and plasticity,
- anisotropy,
- creep,
- thermal effects,
- rate dependence.

Element formulations that:

- handle geometric nonlinearities,
- do not lock for isochoric materials.

A wide variety of boundary conditions and loads including:

- prescribed displacements,
- body force loads,
- concentrated nodal loads and follower forces,
- pressure and shear loads,
- loads due to thermal expansion.

Three types of analysis capability:

- quasistatic analysis,
- dynamic analysis,
- eigenvalue analysis.

Iterative solution techniques including:

- quasinewton stiffness updates,
- force or displacement control,
- arc-length control.

Two types of solution strategies:

- fixed step strategies,
- adaptive solution strategies with ISLAND templates.

A general interface contact capability including:

- sliding with or without separation,
- friction,
- single surface contact,
- tied slidelines for mesh grading,
- tie breaking slidelines for simulation of failure.

Rezoning capability including:

- interactive or automatic command execution,
- mesh smoothing and remap,
- graphics to display current results.

The following sections highlight these capabilities and give a brief description of theory and algorithms used in their implementation.

2.1 FINITE ELEMENT EQUATIONS

In solid mechanics, the governing equations are those of momentum conservation. These are often referred to as the equations of motion and can be written as

$$\tau_{ij,\,j} + b_i = \rho \ddot{u}_i \qquad \text{in } \Omega, \tag{1}$$

where τ_{ij} is the Cauchy stress tensor b_i is the body force per unit volume, ρ is the density, u_i are the displacements, Ω represents the continuum domain, superimposed dots denote differentiation with respect to time, and repeated indices are summed over the range of spatial dimensions. The continuum has a boundary Γ which can be divided into a boundary Γ_u where displacements are prescribed and Γ_τ where stresses are prescribed. Conditions on the boundary may be written as

$$u_i = \bar{u}_i \quad \text{on } \Gamma_u, \tag{2}$$

$$\tau_{ij} n_j = \bar{\tau}_i \quad \text{on } \Gamma_\tau . \tag{3}$$

The initial conditions are

$$u_i(0) = u_{oi} , \tag{4}$$

$$\dot{u}_i(0) = \dot{u}_{oi} . \tag{5}$$

Equations (1)-(5) represent the strong form of the initial/boundary value problem of the dynamics of solid continua. The rate of deformation tensor $\dot{d}_{ij}$ is defined in terms of velocity $\dot{u}_i$ as

$$\dot{d}_{ij} = \frac{1}{2}(\dot{u}_{i,j} + \dot{u}_{j,i}) . \tag{6}$$

The Cauchy stress is, in general, a function of the rate of deformation $\dot{d}_{ij}$ a set of history variables $\mathbf{H}$, and the temperature $\mathbf{T}$,

$$\tau_{ij} = \tau_{ij}(\dot{d}_{ij}, \mathbf{H}, \mathbf{T}) . \tag{7}$$

For two-dimensional analysis, each of the above relations are modified under the postulates of axisymmetry, plain strain, or plane stress.

To develop the finite element equations, a weak form of the governing equations is constructed, and the resulting weak form is semidiscretized. The spatial discretization and temporal solution are performed independently in a semidiscretization. In NIKE2D, quadrilateral elements are used for the spatial discretization, yielding a coupled system of ordinary differential equations,

$$\mathbf{M}\ddot{\mathbf{u}} + \mathbf{F}^{int}(\mathbf{u}, \dot{\mathbf{u}}, \mathbf{T}) = \mathbf{P}(\mathbf{u}, \mathbf{b}, t, \mathbf{T}) , \tag{8}$$

where $\mathbf{M}$ is the mass matrix, $\mathbf{F}^{int}$ is the internal nodal force vector, and $\mathbf{P}$ is the external nodal force vector. Note that the external load $\mathbf{P}$ may be a function of nodal displacement $\mathbf{u}$, body force per unit volume $\mathbf{b}$, time t, and nodal temperature $\mathbf{T}$. For a dynamic analysis, (8) is solved by the Newmark-β time integration scheme. The finite element equations for a quasistatic analysis are obtained by eliminating inertial effects in (8), and thus have the form

$$\mathbf{F}^{int}(\mathbf{u}, \dot{\mathbf{u}}, \mathbf{T}) = \mathbf{P}(\mathbf{u}, \mathbf{b}, t, \mathbf{T}) . \tag{9}$$

An eigenvalue analysis in NIKE2D involves solving the eigenproblem

$$(\mathbf{K} - \omega^2 \mathbf{M})\mathbf{u} = 0 , \tag{10}$$

where $\mathbf{K}$ is the tangent matrix and ω is the natural frequency. Note that $\mathbf{K}$ is the derivative of the nodal force with respect to nodal displacements evaluated at the original (reference) configuration.

$$\mathbf{K} = \left.\frac{\partial \mathbf{F}}{\partial \mathbf{u}}\right|_{t=0} . \tag{11}$$

2.2 MATERIAL MODELS

A number of material models are incorporated in NIKE2D to simulate a wide range of material behavior including plasticity, thermal effects and rate dependence. The following is a list of currently implemented models:

1.	Elasticity	0,1,2
2.	Orthotropic elasticity	0,1,2
3.	Elastoplasticity	0,1,2
4.	Thermal-elastoplasticity	0,1,2
5.	Soil and crushable foam	0,1
6.	Viscoelasticity	0,1,2
7.	Thermal-orthotropic elasticity	0,1,2
8.	Thermoelastic-creep	0,1
9.	Blatz-Ko rubber	0,1,2
10.	Power law plasticity with failure	0,1,2
11.	Unified creep plasticity	0,1,2
12.	Power law thermoplasticity	0,1,2
13.	Strain rate sensitive elastoplasticity	0,1,2
14.	Circumferentially cracked elastoplasticity	0
15.	Extended two invariant cap	0,1
16.	Ramberg-Osgood elastoplasticity	0,1,
17.	Thermal-elastoplasticity with 8-curves	0,1
18.	Three phase thermal elastoplasticity	0,1
19.	Strain rate sensitive power law plasticity	0,1,2
20.	Power law thermoplasticity with failure	0,1

21.	Nonlinear elastoplasticity	0,1
22.	Polynomial hyperelastic rubber	0,1,2
23.	Primary, secondary, tertiary creep	0,1,2
24.	Deformation mechanism	0,1,2
25.	Gurson-Tvergaard void growth plasticity	0,1
26.	Mooney-Rivlin rubber	0,1

The numbers 0, 1, and 2 following each model name denote that model's availability for axisymmetric, plane strain, and plane stress geometries, respectively. A brief description of the theory and applicable references for each of the NIKE2D materials are given in Section 4.4 on page 113.

2.3 ELEMENT FORMULATION

A rate formulation is used for many of the material models in NIKE2D. For these models, stresses are updated using an implementation of the Green-Naghdi rate. The total Lagrangian formulation is used for the rubber models. A majority of the material models include isochoric plasticity or other incompressible behavior. To present mesh locking with these materials, a mean dilatational formulation is used for axisymmetric and plane strain geometries. The assumed displacement formulation is used for the orthotropic material models and for plane stress geometries. This section briefly describes the element formulation used in NIKE2D. First, the NIKE2D implementation of the mean dilatational formulation and the Green-Naghdi stress rate is discussed. Then, the form of the element contributions to the finite element equations are given. Finally, the introduction of generalized Rayleigh damping at the element level is shown.

The coordinate system used in NIKE2D is shown in Figure 1. The plane is defined by the r and z axes, the x axis represents the transverse direction for plane strain and plane stress geometries, and z is the axis of symmetry for axisymmetry. Displacement increments Δv and Δw corresponding to the r and z directions, are computed from nodal values.

In a rate formulation, stresses at time t_{n+1} are found from quantities at time t_n. The incremental displacement gradient $\Delta\mathbf{d}$ is required for the stress update and is related to the rate of deformation tensor by

$$\Delta\mathbf{d} = \Delta t\dot{\mathbf{d}}, \tag{12}$$

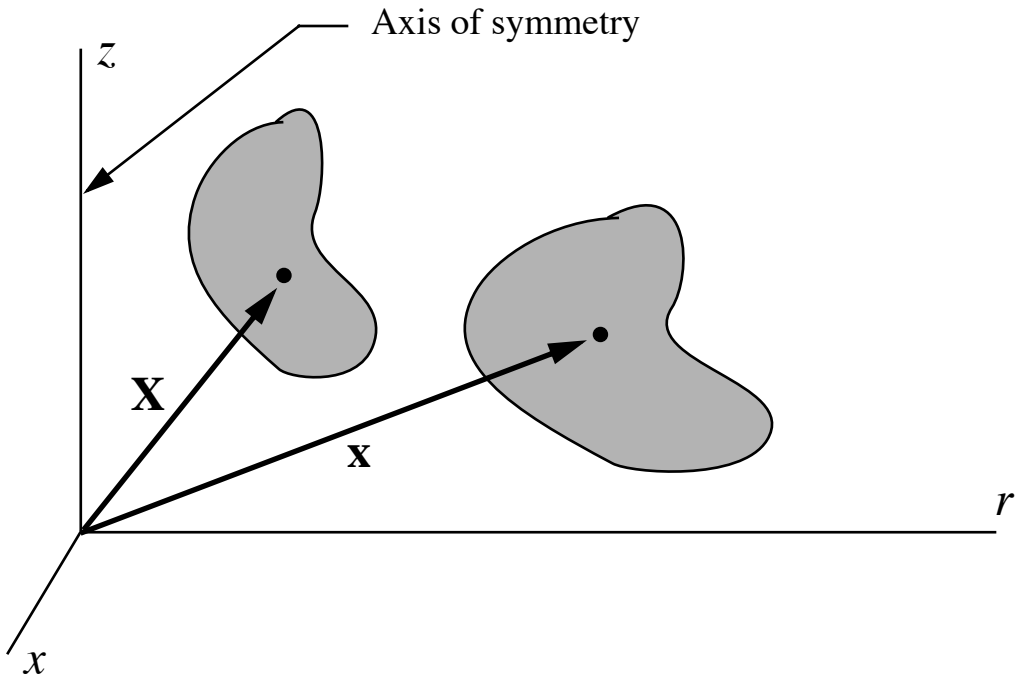

Figure 1
Coordinate system used in NIKE2D.

where Δt is the time step, $\Delta t = t_{n+1} - t_n$. For axisymmetric geometries, the mean dilatational components of the incremental displacement gradient are

$$\Delta d_{rr} = \frac{\partial \Delta v}{\partial r_{n+1/2}} + \phi, \tag{13}$$

$$\Delta d_{zz} = \frac{\partial \Delta w}{\partial z_{n+1/2}} + \phi, \tag{14}$$

$$\Delta d_{rz} = \frac{\Delta v}{r_{n+1/2}} + \phi, \tag{15}$$

$$\Delta d_{rz} = \frac{1}{2}\left(\frac{\partial \Delta v}{\partial z_{n+1/2}} + \frac{\partial \Delta w}{\partial r_{r+1/2}}\right), \tag{16}$$

where

$$\phi = \Delta d^{v}_{n+1/2} - \frac{1}{3}\left(\frac{\partial \Delta v}{\partial r_{n+1/2}} + \frac{\partial \Delta w}{\partial z_{n+1/2}} + \frac{\Delta v}{r_{n+1/2}}\right) , \tag{17}$$

$$\Delta d^{v}_{n+1/2} = \frac{\frac{1}{3}\int\limits_{v_{n+1/2}} \left(\frac{\partial \Delta v}{\partial r_{n+1/2}} + \frac{\partial \Delta w}{\partial z_{n+1/2}} + \frac{\Delta v}{r_{n+1/2}}\right) \partial V}{\int\limits_{v_{n+1/2}} dV} , \tag{18}$$

and

$$r_{n+1/2} = \frac{1}{2}(r_n + r_{n+1/2}) , \tag{19}$$

$$z_{n+1/2} = \frac{1}{2}(z_n + z_{n+1/2}) . \tag{20}$$

The geometry of the midstep is used in the gradient calculation so that rigid body motions cause zero straining. The mean dilatational components for plane strain are defined in an analogous manner.

The Green-Naghdi stress rate $\mathbf{t}^{\nabla}$ is defined as

$$\mathbf{t}^{\nabla} = \dot{\boldsymbol{t}} + \boldsymbol{t}\boldsymbol{W} - \boldsymbol{W}\boldsymbol{t} \quad , \tag{21}$$

where

$$\mathbf{W} = \dot{\mathbf{R}}\mathbf{R}^{T}, \tag{22}$$

R is the orthogonal rotation tensor, and dots denote time differentiation. The deformation gradient **F** is given by

$$\mathbf{F} = \frac{\partial \mathbf{x}}{\partial \mathbf{X}}, \tag{23}$$

where **X** represents the undeformed geometry and **x** represents the deformed geometry as shown in Figure 1. The rotation tensor **R** is obtained by the polar decomposition of **F**,

$$\mathbf{F} = \mathbf{R}\mathbf{U}, \tag{24}$$

and can be computed in closed form (see Marsden and Hughes [1983]).

The NIKE2D implementation of the Green-Naghdi rate is equivalent to (21) but differs slightly in form. First, the orthogonal rotation tensor **R** is computed at the beginning of the step,

$$\mathbf{F}_n = \frac{\partial \mathbf{x}_n}{\partial \mathbf{X}} = \mathbf{R}_n \mathbf{U}_n, \tag{25}$$

at the midstep

$$\mathbf{F}_{n+1/2} = \frac{\partial \mathbf{x}_{n+1/2}}{\partial \mathbf{X}} = \frac{1}{2}(\mathbf{F}_n + \mathbf{F}_{n+1}) = \mathbf{R}_{n+1/2}\mathbf{U}_{n+1/2} \quad , \tag{26}$$

and at the end of the step

$$\mathbf{F}_{n+1} = \frac{\partial \mathbf{x}_{n+1}}{\partial \mathbf{X}} = \mathbf{R}_{n+1}\mathbf{U}_{n+1}. \tag{27}$$

Next, the "unrotated" Cauchy stress $\boldsymbol{s}$ is computed by

$$\boldsymbol{s}_n = \mathbf{R}_n^T \boldsymbol{t}_n \mathbf{R}_n \ . \tag{28}$$

Increments in unrotated stress are computed by the appropriate constitutive relation

$$\Delta \boldsymbol{s}_{n+1/2} = \mathbf{C}\Delta \boldsymbol{e}_{n+1/2} \ , \tag{29}$$

where $\Delta \boldsymbol{e}_{n+1/2}$ is the unrotated strain increment and **C** is the constitutive tensor. The unrotated strain is defined in terms of the incremental displacement gradient by

$$\Delta \boldsymbol{e}_{n+1/2} = \mathbf{R}_{n+1/2}^T \Delta \mathbf{d}_{n+1/2} \mathbf{R}_{n+1/2}. \tag{30}$$

Since constitutive models are evaluated in the unrotated configuration, it is not necessary to transform history variables such as a back stress. The unrotated stress is updated by

$$\boldsymbol{s}_{n+1} = \boldsymbol{s}_n + \Delta \boldsymbol{s}_{n+1/2} \ . \tag{31}$$

Finally, the Cauchy stress at t_{n+1} is given by

$$\boldsymbol{t}_{n+1} = \mathbf{R}_{n+1}\boldsymbol{s}_{n+1}\mathbf{R}_{n+1}^{T} \ . \tag{32}$$

The element contribution $\mathbf{F}_e^{int}$ to the internal nodal force vector $\mathbf{F}^{int}$ is of the form

$$\mathbf{F}_e^{int} = \int_{V_{n+1}} \mathbf{B}_{n+1}^{T}\boldsymbol{t}_{n+1}dV \ , \tag{33}$$

where $\mathbf{B}$ is the symmetric displacement gradient operator. The element tangent stiffness matrix $\mathbf{K}_e$ is the sum of the material stiffness $\mathbf{K}_e^M$ and the geometric stiffness $\mathbf{K}_e^G$,

$$\mathbf{K}_e = \mathbf{K}_e^M + \mathbf{K}_e^G. \tag{34}$$

The material stiffness for a mean dilatational element is given by

$$\mathbf{K}_e^M = \int_{V_{n+1}} \bar{\mathbf{B}}_{n+1}^{T}\mathbf{E}_{n+1}\bar{\mathbf{B}}_{n+1}dV, \tag{35}$$

where

$$\mathbf{E}_{n+1} = \bar{\mathbf{T}}_{n+1}\mathbf{C}_{n+1}\bar{\mathbf{T}}_{n+1}^{T} \tag{36}$$

is the transformation that brings $\mathbf{C}$ into the rotated configuration, and $\bar{\mathbf{B}}$ is the modified strain displacement operator given by Hughes (1980). Since numerical experience has shown its inclusion to impede convergence in quasinewton solution strategies, the use of the geometric stiffness is optional in NIKE2D.

For dynamic analysis, damping can be incorporated into the model at the element level in two ways: through the specification of dissipative material behavior or by a nonlinear adaptation of Rayleigh damping termed generalized Rayleigh damping. Dissipative mechanisms in material behavior are pointwise in nature and include viscoelasticity and hysteretic damping caused by cyclic plasticity. Generalized Rayleigh damping is more global in nature. However, it is implemented at the element level to maximize computational efficiency. The NIKE2D implementation of generalized Rayleigh damping is discussed in Whirley and Engelmann (1991d).

Stiffness proportional Rayleigh damping is introduced by replacing the incremental stress computation (29) by

$$\Delta \boldsymbol{s}_{n+1/2} = \mathbf{C}\Delta \boldsymbol{e}_{n+1/2} + \frac{\alpha_{stiff}}{\Delta t}\mathbf{C}^{elas}\Delta \boldsymbol{e}_{n+1/2} \ , \tag{37}$$

where α_{stiff} is the stiffness proportional damping coefficient, Δt is the time step, and $\mathbf{C}^{elas}$ is the elastic constitutive tensor. The stiffness proportional damping coefficient is specified by material. Mass proportional damping is added be replacing (33) with

$$\mathbf{F}_e^{int} = \int_{V_{n+1}} \mathbf{B}_{n+1}^T \boldsymbol{t}_{n+1} dV + \frac{\alpha_{mass}}{\Delta t}\mathbf{M}_e \Delta \mathbf{u}_e \ , \tag{38}$$

where α_{mass} is the mass proportional damping coefficient, $\mathbf{M}_e$ is the element mass matrix, and $\Delta \mathbf{u}_e$ is the vector of nodal incremental displacements. In the NIKE2D implementation, a unique stiffness proportional damping coefficient may be specified for each material. However, one mass proportional damping coefficient operates on the entire model mass. The damping force is proportional to a midstep velocity approximation.

2.4 LOADS AND BOUNDARY CONDITIONS

A number of types of applied loads and boundary conditions are available for both quasistatic and dynamic analysis. Various combinations of these can be used to model almost any two-dimensional solid mechanics problem. Many of the loads and boundary conditions can be functions of time. In NIKE2D, these functional relationships are specified by tabulated "load curves." The available options are described in the following. References will be made to the governing equations where applicable.

Displacement boundary conditions which are specified at boundary nodes, are the discrete analog to Eq. (2). In NIKE2D, displacements can also be specified at nodes within the domain. Each of the degrees-of-freedom may be fixed, or prescribed according to a time function. Either a global or user-defined coordinate system may be used for specification of prescribed displacements. For dynamic problems, initial conditions are required for all nodes in the finite element mesh. Displacement initial conditions (4) at nodes are zero, except when nonzero nodal displacements are prescribed at $t = 0$. Nonzero velocity initial conditions (5) can be specified for each nodal degree-of-freedom. Alternatively, an initial angular velocity about the x axis may be specified for plane strain and plane stress geometries. It should be noted that initial velocities not equal to the time derivative of prescribed displacements will result in a highly dynamic response.

Loads can be specified at nodes, along boundary segments (element sides), and within element domains. Concentrated nodal loads can be specified at any node in the model according to a time function. These loads can be prescribed for each degree-of-freedom, or may be defined to move with the mesh as a follower force. The discrete analog to the traction boundary condition (3) are pressure and shear loads. These are prescribed along boundary segments according to a time function. Pressure and shear loads follow the mesh motion throughout the analysis. Body force loads can be specified within elements to represent various physical phenomena such as magnetism. Alternatively, body force loads are applied as a "base acceleration." In this case, the body force per unit volume b_i is given by

$$b_i = \rho a_i , \tag{39}$$

where a_i are given prescribed accelerations in the r and z directions. Body forces due to an angular acceleration about the x axis can also be specified for plane strain and plane stress geometries. All body force loads are prescribed according to a time function.

Thermal loads are applied with changes in temperature. These loads are associated with strains caused by thermal expansion. Thermal loading is invoked by specifying temperature profiles and using material models that include thermal expansion. Nodal temperature profiles can be manually input or determined from plotfiles generated by a TOPAZ2D heat transfer analysis. Manually input nodal temperature profiles, $\mathbf{T}(t)$, are of the form

$$\mathbf{T}(t) = \mathbf{T}^B + f(t)\mathbf{T}^M , \tag{40}$$

where $\mathbf{T}^B$ is a vector of nodal base temperatures, $f(t)$ is a time function, and $\mathbf{T}^M$ is a vector of nodal load curve multipliers. As an option, nodal reference temperatures, $\mathbf{T}^R$, may be used to "thermally stress" the model at the zeroth time step, before the mechanical analysis begins. Note that nodal reference temperatures are clearly different from material reference temperatures. Material reference temperatures (specified by material) are used only as a reference value for secant coefficients of thermal expansion.

2.5 QUASISTATIC ANALYSIS

For a quasistatic analysis, the finite element equations (9) are solved incrementally by an iterative strategy. In absence of viscous and thermal effects, a temporal discretization of (9) yields

$$\mathbf{F}^{int}(\mathbf{u}_{n+1}) = \mathbf{P}_{n+1} , \tag{41}$$

where $\mathbf{u}_{n+1}$ and $\mathbf{P}_{n+1}$ are the nodal displacements and external load evaluation at t_{n+1}. At each time step, quantities are known at t_n, and the solution involves finding the displacement $\mathbf{u}_{n+1}$ that satisfies (44). This new equilibrium solution is found by iteration.

Either a fixed step strategy or an adaptive solution strategy is used for the incremental procedure. In a fixed step strategy, the time step and the iterative algorithm are fixed throughout the analysis. Step size is often limited by accuracy and convergence considerations. Adaptive solution strategies allow the step size and algorithm to change as the analysis evolves. Adaptive strategies are defined by ISLAND templates which are described in Section 2.7 on page 19.

The following fixed step iterative schemes are available:

1. BFGS (default)
2. Broyden
3. Davidon-Fletcher-Powell (DFP)
4. Davidon-symmetric
5. modified Newton
6. modified constant arc length
7. modified constant arc length with line search
8. modified constant arc length with BFGS
9. modified constant arc length with Broyden
10. modified constant arc length with DFP
11. modified constant arc length with modified BFGS
12. modified constant arc length with Davidon

Schemes 1–4 are quasinewton methods. In quasinewton methods, the factored stiffness matrix is updated in each iteration for a better approximation to the true Jacobian. The BFGS and Broyden updates are described in Matthies and Strang (1979) and Walker (1979), respectively. The DFP and Davidon symmetric updates were implemented with the consultation of Schweizerhof (1986). The stiffness is not updated or refactored with scheme 5, modified Newton. Because quasinewton methods may have superlinear local convergence, they generally require fewer iterations than the modified Newton method. Schemes 6–12 are arc-length methods which are suited for problems involving snap through buckling and global instabilities. Arc-length methods have been proposed by many authors including Riks (1979), Ramm (1980), and Crisfield (1981). The implementation in NIKE2D represents a cooperative effort with Schweizerhof (1986), and is based on work by Simo and coworkers (1984), Schweizerhof and Ramm (1986), and Schweizerhof and Wriggers

(1987). To avoid divergence, a line search is used with each of the above schemes, along with automatic stiffness reformations as needed. The solution algorithm for schemes 1-5 is summarized in the following.

To obtain the solution at t_{n+1}, the finite element equations (9) are first linearized about the configuration at t_n,

$$\mathbf{K}(\mathbf{u}_n)\Delta\mathbf{u}^0 = \mathbf{P}_{n+1} - \mathbf{F}^{int}(\mathbf{u}_n) \ , \tag{42}$$

where $\mathbf{K}$ is the stiffness matrix based on the configuration at t_n, $\Delta\mathbf{u}^0$ is the increment in displacement, and superscripts denote iteration number. Solving (42) for $\Delta\mathbf{u}^0$, the displacement is updated by

$$\mathbf{u}_{n+1} = \mathbf{u}_n + s^0\Delta\mathbf{u}^0, \tag{43}$$

where s^0 is a parameter between 0 and 1 that is determined by a line search procedure. Equilibrium iterations are performed by solving

$$\mathbf{K}^i\Delta\mathbf{u}^i = \mathbf{P}_{n+1} - \mathbf{F}^{int}(\mathbf{u}^i_{n+}) = \mathbf{Q}^i_{n+1} \tag{44}$$

for $\Delta\mathbf{u}^i$, where $\mathbf{Q}^i_{n+1}$ is the residual, and $\mathbf{K}^i$ is an estimate to the Jacobian which depends on the solution scheme used. Convergence is determined by examining both the displacement norm

$$\frac{\|\Delta\mathbf{u}^i\|}{u_{max}} \le e_d \ , \tag{45}$$

and the energy norm

$$\frac{(\Delta\mathbf{u}^i)^T\mathbf{Q}^i_{n+1}}{(\Delta\mathbf{u}^o)^T\mathbf{Q}^o_{n+1}} \le e_e \ . \tag{46}$$

In the above, vertical bars denote an Euclidean norm, u_{max} is the maximum displacement norm obtained over all of the n steps including the current iterate, and e_d and e_e are tolerances that are typically 10^{-2} to 10^{-3} or smaller. Convergence tolerances are discussed in Bathe (1982). Divergence in NIKE2D is determined by a comparison of residual norms,

$$\|\mathbf{Q}^0_{n+1}\| < \|\mathbf{Q}^{i+1}_{n+1}\| \ . \tag{47}$$

If convergence is not attained and the solution is not divergent, the displacement is updated by

$$\mathbf{u}_{n+1}^{i+1} = \mathbf{u}_{n+1}^{i} + s^i \Delta \mathbf{u}^i \tag{48}$$

and iterations continue. When the solution diverges, or convergence fails to occur within a specified number of iterations, the tangent matrix $\mathbf{K}$ is reformed using the current estimate of geometry before continuing equilibrium iteration.

Although computationally intensive, the line search is an essential part of the quasinewton or modified Newton procedures. The implementation follows that of Matthies and Strang (1979). The value of s^i is found by iteration such that the inner product

$$(\Delta \mathbf{u}^i)^T \mathbf{Q}^i{}_{n+1} \rightarrow 0 \, . \tag{49}$$

Up to 10 iterations are allowed in NIKE2D to find s^i. For stiffening systems where $s^i < 1$, the scaling of the displacement update (48) is required for stability of the solution.

The quasinewton update procedure is recursive. Conceptually, the stiffness inverse is recursively updated for the BFGS method by

$$(\mathbf{K}^i)^{-1} = (\mathbf{I} + \mathbf{w}^i (\mathbf{v}^i)^T)(\mathbf{K}^{i-1})^{-1}(\mathbf{I} + \mathbf{v}^i (\mathbf{w}^i)^T) \quad , \tag{50}$$

and for the Broyden update by

$$(\mathbf{K}^i)^{-1} = (\mathbf{I} + \bar{\mathbf{w}}^i (\bar{\mathbf{v}}^i)^T)(\mathbf{K}^{i-1})^{-1} \quad . \tag{51}$$

where $\mathbf{w}^i$, $\mathbf{v}^i$, $\bar{\mathbf{w}}^i$, and $\bar{\mathbf{v}}^i$ are easily computed vectors. In the NIKE2D implementation, the matrix-vector multiplications in (50) and (51) are equivalently done as vector-vector multiplications on the right hand side, requiring substantially less computational effort.

2.6 DYNAMIC ANALYSIS

The Newmark-β method is used to integrate the semidiscretized finite element equations (8) in time. The Newmark-β family of methods is given by

$$\mathbf{u}_{n+1} = \mathbf{u}_n + \Delta t \dot{\mathbf{u}}_n + (1/2 - \beta)\Delta t^2 \ddot{\mathbf{u}}_n + \beta \Delta t^2 \ddot{\mathbf{u}}_{n+1} \, , \tag{52}$$

$$\dot{\mathbf{u}}_{n+1} = \dot{\mathbf{u}}_{n+1} + (1-\gamma)\Delta t\ddot{\mathbf{u}}_n + \gamma\Delta t\ddot{\mathbf{u}}_{n+1} \quad , \tag{53}$$

where β and γ are free parameters governing the accuracy and stability of the time integration. The time integration algorithm is unconditionally stable for

$$2\beta \geq \gamma \geq 1/2 \, . \tag{54}$$

The default setting of the parameters in NIKE2D is $\beta = 1/4$ and $\gamma = 1/2$. This choice of parameters represents the trapezoidal rule which is second order accurate in time, is energy conserving for linear problems, and does not introduce numerical dissipation. Algorithmic damping is introduced when $\gamma = 1/2$. Since the higher modes of the semidiscrete finite equations are artifacts of the discretization process, it is generally desirable to limit the participation of the high frequency modes (see Hughes [1987]). High frequency dissipation is maximized when

$$\beta = \frac{1}{4}(\gamma + 1/2)^2 \, . \tag{55}$$

However, for any choice of parameters where $\gamma > 1/2$, accuracy drops to first order.

Other types of damping include concentrated nodal dampers and generalized Rayleigh damping. Conceptually, Rayleigh damping is incorporated by replacing the internal nodal force vector $\mathbf{F}^{int}$ by

$$\mathbf{F}^{int} \leftarrow \mathbf{F}^{int} + \alpha_{mass}\mathbf{M}\dot{\mathbf{u}} + \alpha_{stiff}\mathbf{K}\dot{\mathbf{u}} . \tag{56}$$

For a linear elastic model, the modal fraction of critical damping can be specified at two natural frequencies. The fraction of critical damping ξ_r in each mode r is determined by the mass and stiffness proportionality coefficients, α_{mass} and α_{stiff}, and the natural frequency ω_r, by the relation

$$\xi_r = \frac{1}{2}(\alpha_{mass}/\omega_r + \alpha_{stiff}\omega_r) \quad . \tag{57}$$

A major drawback of Rayleigh damping is that the amount of damping in all of the other modes cannot be controlled. For purely mass proportional damping, the damping ratio is inversely proportional to the frequency of vibration. In the case of purely stiffness proportional damping, the damping ratio is directly proportional to the frequency, and the highest modes of the system will be heavily damped.

To obtain the dynamic solution at t_{n+1}, the finite element equations (8) are first linearized about the configuration at t_n,

$$\mathbf{M}\ddot{\mathbf{u}}_{n+1} + \mathbf{D}\dot{\mathbf{u}}_{n+1} + \mathbf{K}(\mathbf{u}_n)\Delta\mathbf{u}^0 = \mathbf{P}_{n+1} - \mathbf{F}^{int}(\mathbf{u}_n) \ , \tag{58}$$

where **D** is the damping matrix. Substituting (52) and (53) into (58), yields a system of equations similar to (41),

$$\mathbf{K}^*\Delta\mathbf{u}^0 = \mathbf{P}_{n+1} - \mathbf{F}^*(\mathbf{u}_n) \ , \tag{59}$$

where

$$\mathbf{K}^* = \mathbf{K} + \frac{1}{\beta\Delta t^2}\mathbf{M} + \frac{\gamma}{\beta\Delta t}\mathbf{D} \, , \tag{60}$$

$$\mathbf{F}^* = \mathbf{F}^{int} - \mathbf{M}\left[\frac{1}{\beta\Delta t}\dot{\mathbf{u}}_n + \frac{1}{\beta}\left(\frac{1}{2} - \beta\right)\ddot{\mathbf{u}}_n\right] - \mathbf{D}\left[\frac{\gamma}{\beta}\dot{\mathbf{u}}_n + \frac{\gamma}{\beta}\left(\frac{1}{2} - \beta\right)\Delta t\ddot{\mathbf{u}}_n\right] \quad . \tag{61}$$

Solving (59) for $\Delta\mathbf{u}^0$, the nodal acceleration, velocity, and displacement are updated by

$$\ddot{\mathbf{u}}_{n+1} = \frac{1}{\beta\Delta t^2}\Delta\mathbf{u}^0 - \frac{1}{\Delta t}\dot{\mathbf{u}}_n - \frac{1}{\beta}\left(\frac{1}{2} - \beta\right)\ddot{\mathbf{u}}_n \quad , \tag{62}$$

$$\dot{\mathbf{u}}_{n+1} = \dot{\mathbf{u}}_n + (1-\gamma)\Delta t\ddot{\mathbf{u}}_n + \gamma\Delta t\ddot{\mathbf{u}}_{n+1} \quad , \tag{63}$$

$$\mathbf{u}_{n+1} = \mathbf{u}_n + \Delta\mathbf{u}^0. \tag{64}$$

Equilibrium iterations are then performed with

$$\mathbf{K}^*\Delta\mathbf{u}^i = \mathbf{P}_{n+1} - \mathbf{F}^*(\mathbf{u}^i{}_{n+1}) \, , \tag{65}$$

where

$$\mathbf{F}^* = \mathbf{F}(\mathbf{u}^i{}_{n+1}) + \mathbf{M}\ddot{\mathbf{u}}^i{}_{n+1} + \mathbf{D}\dot{\mathbf{u}}^i_{n+1} \, . \tag{66}$$

The iteration procedure is analogous to that described in Section 2.5 on page 13. Fixed step iterative schemes 1-5 may be used for a dynamic analysis. Alternatively, an adaptive solution strategy may be defined by including an ISLAND template.

2.7 ADAPTIVE SOLUTION STRATEGIES WITH ISLAND

The development of effective solution strategies to solve the implicit, global finite element equations is one of the most important challenges in computational mechanics. Efficient strategies make good use of computational resources, and allow larger and more complex analysis models to be solved. Robust algorithms are essential to solve the complex nonlinearities typically tackled by NIKE2D analysts. Experience has shown that no single algorithm is optimal for all problem classes, and that adaptivity and flexibility are necessary to maximize efficiency and robustness of the solution process. This adaptivity and flexibility has been incorporated into NIKE2D through the development of the ISLAND language (Interactive Solution Language for an Adaptive Nike Driver). A complete description of ISLAND is given in Engelmann and Whirley (1991), and only certain aspects are highlighted in this manual. Therefore users interested in adaptive algorithms are encouraged to consult this reference.

The ISLAND language has a flexible control structure that allows the step size, the solution algorithm, and the convergence measures to vary as the solution evolves. This degree of adaptivity is necessary since the degree and form of nonlinearities change throughout most analyses. A number of iteration procedures are available, and each of these may be optimal in different instances. Optimal time step or increment size is based on accuracy and global convergence considerations, which often vary throughout an analysis and definitely change from problem class to problem class. Modeling capabilities in NIKE2D include some very strong nonlinearities such as contact. The accuracy of the required linearization must be balanced with computational efficiency when defining an optimal strategy.

Adaptive strategies are specified by including an ISLAND solution template with the input file. The solution template is a file containing commands, variable definitions, and parameters which completely define the solution strategy. Predefined solution templates are available in which only a few problem class dependent parameters need be specified. Therefore, with a given ISLAND template, the use of NIKE2D with adaptive solution strategies is as easy as with a fixed step strategy. Advanced analysts and ISLAND users may wish to modify existing templates for their specific application.

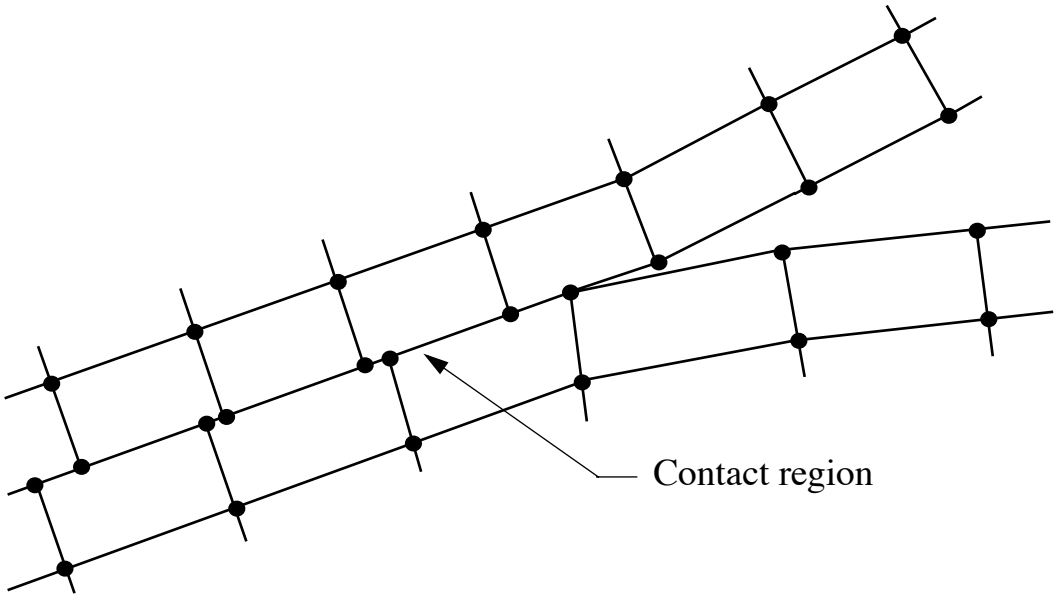

Figure 2
Typical slideline.

2.8 SLIDELINES

A general slideline capability is implemented in NIKE2D that includes both sliding and tied interfaces with arbitrary mesh refinement on adjacent sides of the interface. Sliding with no separation or sliding with separation, closure, and friction is available. All of the contact algorithms in NIKE2D are based on a penalty formulation which is described briefly in the following.

A slideline is defined in the input file by a list of node numbers lying along the interface. One side of the contact surface is referred to as the master surface and the other side is the slave surface. Since a symmetric treatment is used, the designation of the slave and master surface is arbitrary. However, the slave surface must lie to the left of the master surface as one moves along the master surface, encountering the master nodes in the order they are defined. If this restriction is violated, the numerical algorithms that determine penetration are invalid.

Consider the portion of a slideline shown in Figure 2. In the region of contact, interface springs are used to preclude penetration. Any node that penetrates through its respective contact surface causes a linear interface spring to be inserted into the stiffness matrix that couples the penetrating

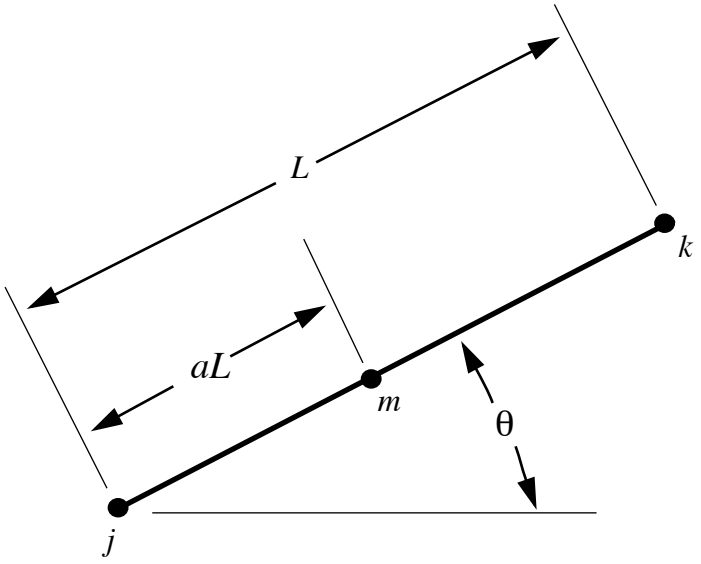

Figure 3
Contact of node *m* with segment of *jk*.

node to two adjacent nodes on the contact surface. Except in the case where the slideline is frictional or tied, the interface spring acts normal to the contact surface, and the sliding is unaffected. The test for penetration, as well as the determination of the penetration depth and points of contact, are described in Hallquist (1978), and Hallquist, Goudreau, and Benson (1985).

Consider the case of frictionless sliding with separation and closure. The following illustrates the argumentation of the stiffness matrix $\mathbf{K}$ and the internal nodal force $\mathbf{F}^{int}$ when penetration is detected. Figure 3 shows an isolated portion of the interface where node *m* is penetrating through segment *jk*. A local equilibrium relationship can be written as

$$\mathbf{K}^S \Delta\mathbf{u}^S = \mathbf{P}^S - \mathbf{F}^S, \tag{67}$$

where $\Delta\mathbf{u}^S$ is the incremental displacement vector containing the penalty spring degrees-of-freedom, $\mathbf{K}^S$ is the spring stiffness, $\mathbf{F}^S$ is spring internal force, and $\mathbf{P}^S$ is the external force arising from internal states of stress in the interface elements. The spring degrees-of-freedom are ordered

$$\Delta\mathbf{u}^S = [\Delta v_m, \Delta w_m, \Delta v_j, \Delta w_j, \Delta v_k, \Delta w_k]. \tag{68}$$

The spring stiffness matrix $\mathbf{K}^s$ is defined as

$$\mathbf{K}^s = \kappa \begin{bmatrix} s^2 & -sc & -(1-a)s^2 & (1-a)sc & -as^2 & asc \\ & c^2 & (1-a)sc & -(1-a)c^2 & asc & -ac^2 \\ & & (1-a)^2 s^2 & -(1-a)^2 sc & (1-a)as^2 & -(1-a)asc \\ & & & (1-a)^2 c^2 & -(1-a)asc & (1-a)ac^2 \\ & & & & a^2 s^2 & -a^2 sc \\ & & & & & a^2 c^2 \\ symmetric & & & & & \end{bmatrix}, \tag{69}$$

where $c = \cos\theta$, $s = \sin\theta$, and κ is the penalty stiffness. The spring internal force $\mathbf{F}^s$ is defined by

$$\mathbf{F}^s = \kappa\delta \begin{Bmatrix} -s \\ c \\ (1-a)s \\ -(1-a)c \\ as \\ -ac \end{Bmatrix} \tag{70}$$

where $-\delta$ is the amount of penetration of node *m* through segment *jk*. The spring stiffness $\mathbf{K}^s$ and force $\mathbf{F}^s$ are computed for all active slideline nodes and segments, and are assembled into the global finite element equations. Thus, the stiffness profile changes as analyses with slidelines evolve. Bandwidth minimization accounts for the variety of profiles possible with arbitrary contact.

The penalty stiffness κ is unique for each segment, and is based on the contact area and material properties of the element containing the segment. The value of κ may be changed by a scale factor defined in the input file. If noticeable penetration is observed, the scale factor should be increased. However, high penalty scale factors can be detrimental to the convergence of global iterations. The default value of κ has been chosen to balance global convergence rate with slideline constraint enforcement on a wide variety of problems. To aid in global convergence, a penalty spring stiffness matrix is assembled whenever an interface node is threatening to penetrate and is less than $10^{-3}\ L$ away from a segment of length *L*. Although the early insertion of the spring stiffness can slow convergence, it has shown to improve the stability of the code. In addition, early insertion often removes rigid body modes in quasistatic analyses.

2.9 REZONING ALGORITHMS

Implicit Lagrangian codes are well suited for problems with moderate element distortions. When distortions become excessive, Eulerian approaches may become necessary. However, Lagrangian formulations are usually preferred for solid mechanics for various reasons, including history dependent material models and contact. Rezoning may be used to extend the domain of application for Lagrangian codes to problems with large distortions.

The NIKE2D implementation for rezoning is based on that in DYNA2D (see Hallquist [1982b] and Goudreau and Hallquist [1982]). Rezoning is performed in three phases:

1) Generate nodal values on the old mesh for all variables to be remapped.
2) Rezone one or more materials either interactively or automatically via a command file.
3) Perform the remapping by interpolating from nodal point values of the old mesh.

When rezoning interactively, current results can be interactively displayed. Automatically rezoning via a command file requires an understanding of the response *a prori*. However, automatic rezoning has proven to be an important option for performing parameter studies.

Nodal values of all Gauss point variables, such as stress, are computed in Phase 1. A global variable to be remapped is approximated piecewise by a continuous field g, defined over each element in terms of nodal variables as

$$g = \boldsymbol{f}\mathbf{g}_e, \tag{71}$$

where are shape functions of the same order as those used in the finite element analysis, and $\mathbf{g}_e$ is a vector of nodal point values. Given a variable h to be remapped, a least squares fit is obtained by minimizing the functional

$$\Pi = \sum_e \int_{\Omega_e} (g-h)^2 d\Omega_e \ , \tag{72}$$

with respect to nodal values. The minimization

$$\frac{\partial \Pi}{\partial g_i} = 0 \qquad i = 1, 2, \ldots, n, \tag{73}$$

requires the solution of the set of linear equations

$$\mathbf{Mg} = \mathbf{f}, \tag{74}$$

where

$$\mathbf{M} = \sum_e \mathbf{m}^e = \sum_e \int_{\Omega_e} \boldsymbol{f}^T \boldsymbol{f} d\Omega_e , \tag{75}$$

$$\mathbf{f} = \sum_e \mathbf{f}^e = \sum_e \int_{\Omega_e} \boldsymbol{f}^T h d\Omega_e . \tag{76}$$

If the "mass" matrix is lumped as

$$\hat{M}_i = \sum_{j=1}^{a} M_{ij}, \tag{77}$$

the calculation of the desired nodal values is simply

$$g_i = \frac{f_i}{\hat{M}_i} . \tag{78}$$

Equation (78) provides an initial guess for $\boldsymbol{g}$. This is used as a starting vector to iterate for a solution that ultimately satisfies Eq. (74), while avoiding matrix inversion (see Zienkiewicz, Xi-Kui and Nakazowa (1985). Iterations are performed using the recursive relation

$$\mathbf{g}^{i+l} = \hat{\mathbf{M}}^{-1}[\mathbf{f} - (\mathbf{M} - \hat{\mathbf{M}})\mathbf{g}^i] , \tag{79}$$

where convergence is determined by

$$\frac{\|\mathbf{g}^{i+1} - \mathbf{g}^i\|}{\|\mathbf{g}^{i+1}\|} \le e_r . \tag{80}$$

The value of e_r may be specified in the input file, and has a default of 0.01. Tighter tolerances lead to nodal values that are only marginally more accurate but at the cost of many more iterations. Convergence to $e_r = 0.01$ is typically achieved in less than 5 iterations, and is monotonic. Tighter

tolerances, for example $e_r = 0.0001$, can require up to forty iterations to attain convergence. Cost per iteration, however, is relatively inexpensive since the element consistent "mass" matrices are computed once and stored.

In the output file of NIKE2D, each Gauss point variable is compared with its interpolated value from the nodes. A percentage error is computed at each Gauss point by

percent error

$$\text{percent error} = \frac{|h_g - \tilde{g}|}{h_{max} - h_{min}} \times 100 \tag{81}$$

where h_g is the actual Gauss point value, $\tilde{g}$ is the interpolated value from the fit, h_{max} is the maximum value in the material, and h_{min} is the minimum value in the material.

An average value over all Gauss points is computed and printed. The errors are usually under 5% which is well within the range of acceptable accuracy for most calculations.

After element consistent mass matrices are computed and stored, Eqs. (74)-(79) are applied to each history variable, i.e., stress, plastic strain, energy, density, etc., for each material. This necessitates $m \times n$ applications of these latter equations where m is the number of materials used in the analysis and n is the number of history variables. The resulting $m \times n$ nodal vectors are stored on disk for possible use in the third phase of rezoning. The efficient implementation of the first phase makes its cost insignificant relative to third phase remap.

Phase two is performed either interactively or automatically using a rezone command file. Interactive rezoning includes graphics that can be used to study current including the capability to display:

- color fringes,
- contour lines,
- vector plots,
- principal stress lines,
- deformed meshes and material outlines,
- profile plots,
- reaction forces,
- interface pressures along slidelines.

All relevant variables can be plotted including constitutive model state variables that are not available in the output database for post-processing. Copies of the plots can be obtained as viewgraphs, 35mm slides from the Dicomed, or hardcopy from the FR80.

Rezoning involves dekinking slidelines and material boundaries, adjusting the spacing of boundary nodes, and moving the interior nodes to achieve a smooth mesh. The total number of nodes and elements is preserved. Three methods are available in NIKE2D for smoothing interior nodes. They are the equipotential method, isoparametric interpolation, and a combination of the two obtained by a linear blending. Other methods have been proposed. The QMESH manual (see Jones [1974]), provides an excellent description and evaluation of a variety of techniques. In applying the relaxation, the new nodal positions are given by

$$r = \frac{\sum_{i=1}^{8} \zeta_i r_i}{\sum_{i=1}^{8} \zeta_i}, \tag{82}$$

$$z = \frac{\sum_{i=1}^{8} \zeta_i z_i}{\sum_{i=1}^{8} \zeta_i}, \tag{83}$$

where r_i and z_i are the nodal positions relative to the node being moved as shown in Figure 4.

The weights for equipotential smoothing are

$$\zeta_1 = \zeta_5 = \frac{1}{4}[(r_7 - r_3)^2 + (z_7 - z_3)^2] \quad ,$$

$$\zeta_3 = \zeta_7 = \frac{1}{4}[(r_1 - r_5) + (z_1 - z_5)^2] \quad ,$$

$$\zeta_2 = \zeta_6 = \frac{1}{2}[(r_1 - r_5) + (z_1 - z_5)(z_7 - z_3)] \quad ,$$

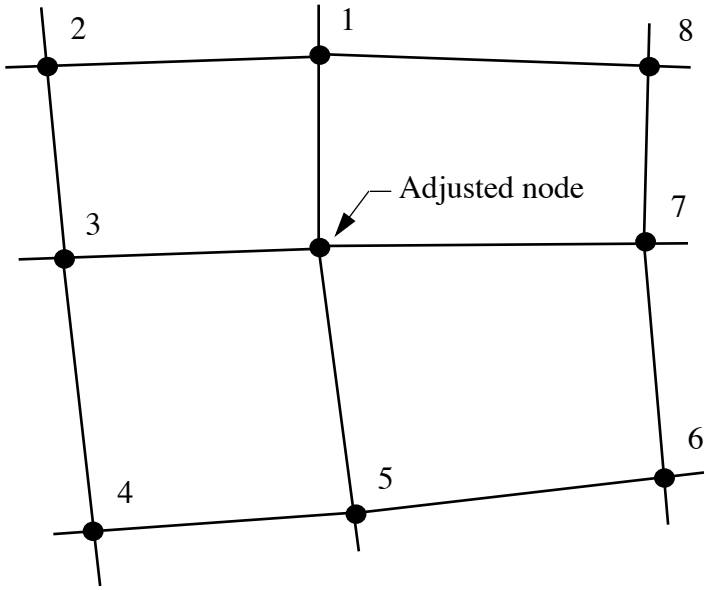

Figure 4
Nodal stencil for smoothing.

$$\zeta_4 = \zeta_8 = -\zeta_2 , \tag{84}$$

and for isoparametric smoothing are

$$\zeta_1 = \zeta_3 = \zeta_5 = \zeta_7 = 0.50 , \tag{85}$$

$$\xi_2 = \zeta_4 = \zeta_6 = \zeta = \zeta_8 = -0.25 .$$

Since logical regularity is not assumed in the mesh, the nodal stencil is constructed for each interior node, and then relaxed. The nodes are iteratively moved until convergence is obtained.

In phase three, new element Gauss point values in the rezoned regions are found by interpolation from the nodal values on the old mesh. Nodal quantities are likewise determined by interpolation.

3.0 ANALYSIS WITH NIKE2D

Various aspects of running an analysis with NIKE2D are discussed in the following sections. These include a description of the procedure to start, to interactively control, and to restart an analysis. Specifics on the use of both interactive and automatic rezoning are given. The use of the MAZE pre-processor to create NIKE2D input files, and the ORION post-processor to graphically interpret analysis results is also discussed.

3.1 PRE-PROCESSING

Development of the two-dimensional, interactive mesh generator, MAZE, has significantly reduced the amount of manual preparation of the NIKE2D input file. The format for the NIKE2D input file is given in Section 3.4 on page 32. MAZE will generate the input file and supports most of the options including the material input and slideline definition. Where appropriate in Section 3.4 on page 32, MAZE commands required to generate specific input options are enclosed in square brackets. A subset of maze command definitions is given in Chapter 8. Input options not supported by MAZE must be entered manually. It is hoped that future versions of MAZE will completely support the current NIKE2D input file format.

3.2 STARTING A NIKE2D ANALYSIS

The execution sequence for NIKE2D varies slightly from platform to platform. On CRAY (NLTSS and UNICOS) and SUN (UNIX) systems, the execution line is:

nike2d i=*inf*, **h**=*itf*, **o**=*otf*, **g**=*ptf*, **d**=*dpf*, **f**=*fdf*, **t**=*tpf*, **c**=*rcf*

where

inf = input file name

itf = ISLAND solution template file name

otf = printed output file name

ptf = binary plot file name (for post-processing)

dpf = binary regular dump file name (for restarting)

fdf = binary running dump file name (for restarting)

tpf = binary TOPAZ2D plot file name (for temperature profiles)

rcf = rezone command file name

On VAX (VMS) systems, the execution line is:

run nike2d

The user then types the file name specifications when prompted:

i=*inf*, **b**=*itf*, **o**=*otf*, **g**=*pft*, **d**=*dpf*, **f**=*rdf*, **t**=*tpf*, **c**=*rcf*

VMS file name extensions should not be included in the file name specification. File names must be unique and can have up to six characters. When starting an analysis, the input file name must be specified. For example,

nike2d i=*inf*

is a valid execution line. Specification of other file names is optional, except when noted below.

Running an analysis with an adaptive solution strategy requires the specification of an ISLAND solution template file, and therefore **h=***itf* must be included. A TOPAZ2D plot file name, **t**=*tpf* should be included when temperature profiles are to be determined from a TOPAZ2D heat transfer analysis. A rezone command file, **c**=*rcf*, should be specified if automatic rezoning is desired.

The default file names for the output file, the binary plot file, and the binary regular dump file are `n2hsp`, `n2plot`, and `n2dump`, respectively. File sizes are set depending on the computer platform used. NIKE2D uses a familied file system in which a root file is augmented by additional "family members" when data to be written exceeds the set file length. New family members are named by appending the root name by a two digit number. For example, following an analysis with data for several steps written to the plot database, the resulting family of binary plot files might be

```
n2plot
n2plot01
n2plot02
n2plot03
n2plot04
```

If instead of the default, the binary plot file name **g**=`great` is specified, the resulting family is

```
great
great01
great02
great03
great04
```

Note that file names are specified by root name.

Two types of restart dump files are created by NIKE2D: a regular dump file and a running dump file. Their use and function is different, depending on whether a fixed step strategy or an adaptive ISLAND strategy is invoked:

1. For a fixed step strategy, restart data is written to the regular dump file at a step interval specified in the input file. This restart data is saved for each step it is written. In addition, restart data is overwritten at each solution step in a running dump file if **f**=*rdf* is included on the execute line.
2. For an adaptive ISLAND strategy, restart data is written to the regular dump file when indicated in the ISLAND solution template, and is saved for each step it is written. The running dump file may contain several of the latest solution steps as indicated in the ISLAND solution template. With a adaptive ISLAND strategy, neither **d**=*dpf* or **f**=*rdf* has to be included in the execution line as default names will be used.

In either fixed step or adaptive strategies, family members are added for each step restart data is written to the regular dump file. For the first step in which restart data is written, the ....01 family member is used. For the second step, the ....02 family member is used and so on.

3.3 INPUT FILE CONVERSION

Over the past 10 years, three distinct input file formats were used. These were referred to as the `on`, `nn`, and `nr` formats. This user manual introduces a new format, denoted the `91` format. As in the past, the new version of NIKE2D will run using input files with old formats. However, it is advantageous to use the new format as more functionality is available. Since many NIKE2D users have old but valuable input files with old formats, an input format conversion utility is included in

NIKE2D. The conversion utility converts input files with either the `on`, `nn`, or `nr` to the `91` format. To convert an old file, first change its name to `convert`. Then run NIKE2D using the execution line

NIKE2D **i**=`convert`, **h**=*nwf*

The code will convert the input file and terminate. File *nwf* will contain the converted input file in the `91` format.

3.4 INTERACTIVE CONTROL

Several sense switch controls are included to "cleanly" stop a run, or briefly interrupt an analysis for status reports, interactive rezoning, etc. To use sense switch controls on CRAY/NLTSS machines, simply enter the desired switch while NIKE2D is executing. On CRAY/UNICOS, VAX/VMS, and SUN/UNIX machines, first interrupt execution by entering `<ctrl>c`, and then enter the desired switch at the prompt. For fixed step solution strategies, the following six sense switches are available.

Type	Response
`sw1.`	A restart file is written and NIKE2D terminates.
`sw2.`	NIKE2D responds with time, iteration, and convergence information.
`sw3.`	NIKE2D responds every step with time, and iteration summary (enabled /disabled with repeated entry).
`sw4.`	A restart file is written and the analysis continues.
`sw5.`	Enter interactive graphics and rezoning phase.
`sw6.`	NIKE2D requests user to input a new time step value.

A number of sense switch controls are also available for adaptive solution strategies using ISLAND templates. These will not be discussed in this manual. However, ISLAND allows a high level of interactivity throughout the analysis and interested users should see Engelmann and Whirley (1991).

3.5 RESTARTING A NIKE2D ANALYSIS

The procedure for restarting a NIKE2D analysis depends on whether a fixed step or an adaptive ISLAND strategy is used. For fixed step strategies, the execution line for restarting NIKE2D is:

nike2d i=*irf*, **r**=*rtf*, **o**=*otf*, **g**=*ptf*, **d**=*dpf*, **f**=*fdp*, **t**=*tpf*, **c**=*rcf*

where

irf = restart input file name,

rtf = binary restart input file name,

and the other file designations are identical to those in Section 3.2 on page 29. Using this execution line, NIKE2D will restart the analysis from the step represented by the restart data in the **r**=*rtf* file. Therefore, specification of this file name is required. When restarting from a periodic, binary regular dump file, the desired family member should be specified (see Section 3.2 on page 29) for **r**=*rtf*. The root name should be specified when restarting from a binary running dump file. The restart input file, **i**=*irf*, is optional. This file may be used to redefine output intervals for plotted and printed data, iteration parameters, integration constants, time step size, damping parameters, load curves, and material properties, The format of the restart input file is described in Chapter 5.0.

The flexibility of the restart procedure is much greater for ISLAND adaptive solution strategies. As with fixed strategies, regular dump files can be used for restarting by specifying the desired family member, **r**=*rtf*. In this case, the **h**=*itf* specification must be excluded. Alternatively, a restart ISLAND template, **h**=*itf*, can be specified along with the original **d**=*dpf* and **f**=*fdf* root names. For example, a valid restart line with a restart ISLAND template is:

nike2d h=*itf*, **d**=*dpf*, **f**=*fdf*

where *dpf* and *fdf* are the file names specified for the original analysis. If default names were used, an equivalent execution line is:

nike2d h=*itf*

When a restart ISLAND template is used, the analyst can interactively select from lists of steps available for restarting.

3.6 REZONING

Rezoning in NIKE2D may be performed either interactively or automatically. The mesh may be interactively rezoned any number of times throughout an analysis. Interactive rezoning is initiated by typing the `sw5`. sense switch control. Commands can then be typed to study current results and rezone the mesh. A complete list and description of graphics and rezoning commands is given in Chapter 6.0. The analysis will continue with the rezoned finite element mesh after the interactive phase is completed.

Automatic rezoning is invoked by specifying a rezone command file, **c**=*rcf*, and by indicating an automatic rezoning interval in the input file. The rezone command file should contain an ordered list of commands to properly rezone the mesh. The list should echo that which would have been typed had the rezoning been done interactively. Definition of the command file usually requires an understanding of the response *apriori*. Therefore, it is recommended that rezoning first be done interactively. Automatic rezoning can then be used for subsequent parameter studies.

3.7 POST-PROCESSING

The ORION post-processor may be used to produce graphical output of NIKE2D analysis results. The familied binary plot files generated by NIKE2D are read by ORION to plot deformed shapes, contours and fringes, and time histories. Contour and fringe plots may be made of nearly 100 different quantities, including a variety of strain measures. In addition, interface pressure and shear profiles can be plotted along slidelines. If numerical output is desired, printed output options may be specified in the NIKE2D input file to print analysis results to the **o=***otf* file**.**

4.0 INPUT FILE FORMAT

The following sections describe the format of the NIKE2D input file. MAZE commands for generating input options are given in square brackets where applicable. Explanatory notes appear throughout.

4.1 PROBLEM DEFINITION

Card 1

Columns	Quantity	Format
1-72	Heading to appear in output [TITLE]	12A6
73-74	Input form EQ. "91" input follows 1991 manual	A2

Card 2

Columns	Quantity	Format
1-5	Number of materials	I5
6-10	Number of nodes, NUMNP	I5
11-15	Number of elements, NUMEL	I5
16-20	Not used	I5
21-25	Number of slidelines, NSL	I5
26-30	Total number of slave nodes	I5
31-35	Total number of master nodes	I5
36-40	Number of nodal printout blocks, NNPB	I5
41-45	Number of element printout blocks, NEPB	I5
46-50	Number of constrained nodal pairs, NCNP	I5

Card 3

Columns	Quantity	Format
1-5	Number of load curves, NLC	I5
6-10	Maximum number of points in any load curve	I5
11-15	Number of concentrated nodal load and follower force cards, NCNL	I5
16-20	Number of element sides with either pressure or shear loading applied, NPSL	I5
21-25	Number of displacement boundary conditions, NDBC	I5
26-30	Body force loads due to base acceleration in *r*-direction, IBFR EQ.0: no *r*-acceleration EQ.1: *r*-acceleration	I5
31-40	Body force loads due to base acceleration in *z*-direction, IBFZ EQ.0: no *z*-acceleration EQ.1: *z*-acceleration	I5
41-50	Body force loads due to angular velocity, IBFA LT.0: angular velocity about the *x*-axis EQ.0: no angular velocity GT.0: angular velocity about the *z*-axis	I5
51-55	Number of concentrated nodal masses, NCNM	I5
56-60	Number of concentrated nodal dampers, NCND	I5
61-65	Initial condition flag, INC LT.0: initialize angular velocity EQ.0: initialize nodal velocities to zero GT.0: initialize angular velocities	I5

Card 4

Columns	Quantity	Format
1-5	Element formulation flag [SMOPT] EQ.0: B-bar EQ.1: NIKE2D formulation	I5
6-10	Integration order flag [EFF] EQ.0: 2×2 Gauss integration EQ.1: 1 point integration	I5
11-15	Number of element body force loads, NBFL	I5
16-20	Thermal option flag [TEO] EQ.0: no thermal effects EQ.1: nodal temperatures are spatially invariant and are determined from load curve ITCURV at each time step. EQ.2: nodal temperatures are determined from specified nodal vectors $\mathbf{T}^B$ and $\mathbf{T}^M$, and load curve ITCURV at each time step. EQ.-1: nodal temperatures are determined by reading in a new temperature state from a TOPAZ2D plotfile at each time step. The time word at the beginning of each temperature state is ignored. EQ.-2: nodal temperatures are interpolated from temperature states in a TOPAZ2D plotfile at each time step. EQ.-3: initial nodal temperatures are defined as $\mathbf{T}^R$ and final nodal temperatures are determined from a steady-state TOPAZ2D plotfile. At each intermediate step, nodal temperatures are interpolated from these two states.	I5
21-25	Load curve number for temperature vs. time, [ITCURV]	I5
26-30	Nodal reference temperature flag, ITREF [ITRF] EQ.0: nodal reference temperatures are not specified EQ.1: nodal reference temperatures $\mathbf{T}^R$ are specified on node cards	I5
31-35	Element plot database flag [IEPD] EQ.0: element energy is stored in the plot database. EQ.1: element thickness (plane stress) is stored in the plot database. EQ.2: element temperature is stored in the plot database.	I5

Card 5

Columns	Quantity	Format
1-5	Geometry type [IGM] EQ.0: axisymmetric EQ.1: plane strain EQ.2: plane stress	I5
6-10	Analysis flag [AF] EQ.-2: dynamic analysis, statically initialized EQ.-1: dynamic analysis EQ.0: quasistatic analysis EQ.N: eigenvalue analysis with N eigenvalues and eigenvectors to be extracted	I5
11-15	Bandwidth minimization flag [BWMO] EQ.0: no EQ.1: yes	I5
16-20	Out-of-core solution flag [OOCSF] EQ.0: in-core solution EQ.1: out-of-core solution	I5
21-25	Percent of computer memory to be used [PCM]	I5
26-30	Solution method [SM] EQ.0: fixed step strategy EQ.1: adaptive ISLAND strategy	I5
31-40	Newmark parameter γ [NIP1] EQ.0.0: default set to 0.5	E10.0
41-50	Newmark parameter β [NIP2] EQ.0.0: default set to 0.25	E10.0
51-60	Mass proportional coefficient α_{mass} for Rayleigh damping	E10.0

Problem Definition Notes

(card):(field)	Comments
1 : 2	See Section 3.3 on page 31 for the automatic conversion of old NIKE2D input files to the new 91 format.
2 : 1	Material parameters for each material are specified as described in Section 4.3 on page 46.
2 : 2	Nodal coordinates and attributes are specified as described in Section 4.4 on page 113.
2 : 3	Element connectivity and attributes are specified as described in Section 4.5 on page 115.
2 : 5-7	Slidelines are defined as described in Section 4.6 on page 117 and Section 4.7 on page 118.
2 : 8,9	The specification of printout blocks can be used to limit the often voluminous printed output to only sets of nodes and elements of particular interest. Printout blocks are defined as described in Section 4.8 on page 122 and Section 4.9 on page 123.
2 : 10	Constrained nodal pairs may be used to define constraint relations between various degrees-of-freedom in the model, and are defined as described in Section 4.10 on page 124.
3 : 1,2	Load curves are used to define functional relationships for loads, boundary conditions, and material parameters. They are defined as described in Section 4.11 on page 125.
3 : 3-5	External loads and displacement boundary conditions are specified as described in Section 4.12 on page 126, Section 4.13 on page 127, and Section 4.14 on page 129.
3 : 6-8	The acceleration histories associated with these body force loads are specified as described in Section 4.15 on page 130, Section 4.16 on page 131, and Section 4.17 on page 132.
3 : 9,10	Concentrated nodal masses and dampers may be defined for dynamic analysis, and are defined as described in Section 4.18 on page 133 and Section 4.19 on page 134.
3 : 11	Nonzero initial velocity conditions for dynamic analysis are specified as described in Section 4.20 on page 135 and Section 4.21 on page 136.

(card):(field)	Comments
4 : 1	This option applies only to axisymmetric and plane strain geometries, and affects only the formation of the material tangent matrix $\mathbf{K}^M$. The B-bar formulation (default) is the most consistent approximation to the true Jacobian.
4 : 2	For accuracy and mesh stability, 2 x 2 integration (default) should always be selected. One point integration is implemented primarily as a tool for comparison to explicit finite element methodologies such as those used in DYNA2D.
4 : 3	Element body force loads may be used to represent various physical phenomena such as magnetism. Their magnitude and time history is specified as described in Section 4.22 on page 137.
4 : 4	Thermal effects are incorporated in NIKE2D by specifying material models which include temperature dependent material parameters or thermal expansion (see Section 2.4 on page 12). At each time step, material temperatures are derived from nodal temperature profiles which are determined from TOPAZ2D plotfiles or from information in this file. For TEO=2, nodal temperatures are determined by Eq. (37), and vectors $\mathbf{T}^B$ and $\mathbf{T}^M$ are specified as described in Section 4.23 on page 138.
4 : 5	Load curve ITCURV must be defined when thermal option flag TEO > 0.
4 : 6	Nodal reference temperatures may be used to "thermally stress" the modal at the zeroth time step (see Section 2.4 on page 12). For ITREF=1, nodal reference temperatures should be defined as described in Section 4.4 on page 113. Flag ITREF must be defined greater than zero for thermal option TEO= -3 since, for this case, the initial temperatures are taken to be the nodal reference temperatures.
4 : 7	This option determines which scalar field variable, energy, thickness, or temperature is written to the plot database and can be plotted as component 20 with the ORION post-processor.
5 : 1	The definition of concentrated loads is different for each geometry assumption (see Section 4.12 on page 126). The initial thickness for plane stress geometries are specified by material as described in Section 4.3 on page 46.
5 : 2	For an eigenvalue analysis, cards in Section 4.2 on page 42 should be left blank. Eigenvalues and eigenvectors can be displayed using the ORION post-processor with each time state representing a mode. For each state i= 1,2,...,N, the time word represents the frequency ω_i, and the mesh configuration represents the displacement mode $\mathbf{u}_i$.

(card):(field)	Comments
5 : 3	The computational work required for linear equation solving is proportional to the bandwidth of the global stiffness matrix **K**. Therefore, bandwidth minimization can result in substantial computational savings. In NIKE2D, bandwidth minimization is performed using the Gibbs, Poole, and Stockmeyer (1976) algorithm. It is done only at initialization (thus a small relative cost), and its use is transparent to the user.
5 : 4	If machine memory is not sufficient for an in-core solution, the more expensive, out-of-core option should be selected. The profile FISSILE solver (see Taylor, Wilson, and Sackett [1980]) is used for both in-core and out-of-core schemes.
5 : 5	This option is not used for currently supported computer platforms.
5 : 6	Fixed step and adaptive strategies are discussed throughout Chapter 2.0. For fixed step strategies, solution parameters should be specified as described in Section 4.2 on page 42. If an adaptive strategy is used, solution parameters are specified by including an ISLAND solution template.
5 : 7,8	The Newmark-β parameters govern the accuracy and stability of the time integration for dynamic problems, and their selection is discussed in Section 2.6 on page 16.
5 : 9	Rayleigh damping may be used to introduce dissipation for dynamic problems. Stiffness and mass proportional Rayleigh damping is discussed in Section 2.3 on page 7 and Section 2.6 on page 16.

4.2 SOLUTION DEFINITION

If an adaptive ISLAND solution strategy is used, the following 3 cards should be left blank, as algorithmic parameters are specified in the solution template. For fixed step strategies, these cards should be defined as described.

Card 1

Columns	Quantity	Format
1-10	Time step size [DELT]	E10.0
11-15	Number of time steps [NSTEP]	I5
16-20	Step interval for printing [PRTI] EQ.0: no printed output	I5
21-25	Step interval for plotting [PLTI] EQ.0: data written to plot file every step	I5
26-30	Step interval for regular restart dumps [SBRF] EQ.0: restart data written upon normal termination	I5
31-35	Step interval for automatic rezoning [SIAR] EQ.0: no automatic rezoning	I5
36-40	Standard solution method flag [NSMD] LE.1: BFGS EQ.2 Broyden EQ.3: Davidon-Fletcher-Powell (DFP) EQ.4: Davidon symmetric EQ.5: modified newton EQ.6: arc length EQ.7: arc length with line search EQ.8: arc length with BFGS EQ.9: arc length with Broyden EQ.10: arc length with DFP EQ.11: arc length with modified BFGS EQ.12: arc length with Davidon	I5
41-50	Convergence tolerance on displacements [DCTOL] EQ.0.0: default set to 0.001	E10.0
51-60	Convergence tolerance on energy [ECTOL] EQ.0.0: default set to 0.01	E10.0

Columns	Quantity	Format
61-65	Number of steps between stiffness matrix reformations [NBSR] EQ.0: default set to 1	I5
66-70	Number of steps between equilibrium iterations [NBEI] EQ.0: default set to 1	I5
71-75	Maximum number of equilibrium iterations allowed between stiffness matrix reformations [NIBSR] EQ.0: default set to 10	I5
76-80	Maximum number of stiffness matrix reformations per time step [MSRF] EQ.0: default set to 15	I5

Card 2

Columns	Quantity	Format
1-5	Number of arc length unloading steps [NAUS]	I5
6-10	Arc length unloading method [IAUM] LE.1: BFGS EQ.2: Broyden EQ.3: Davidon-Fletcher-Powell (DFP) EQ.4: Davidon symmetric EQ.5: modified newton	I5
11-15	Arc length displacement control flag [IADC] EQ.0: displacement norm is used GT.0: node number for arc length displacement control	I5
16-20	Direction for nodal arc length displacement control [IADR] EQ.1: r direction EQ.2: z direction	I5
21-25	Arc length constraint method [IACN] EQ.0: Crisfield EQ.1: Ramm	I5
26-30	Arc length damping flag [IADM] EQ.0: no EQ.1: yes	I5
31-40	Initial arc length size [ASIZ] EQ.0: arc length size based on time step size	E10.0

Card 3

Columns	Quantity	Format
1-10	Line search tolerance [LST] ($0.5 \le LST \le 0.95$) EQ.0.0: default set to 0.90	E10.0
11-20	Slideline stiffness insertion tolerance [SST] EQ.0.0: default set to 0.001	E10.0
21-30	Reduction factor for frictional slideline [RFFC] EQ.0.0: default set to 0.01	E10.0
31-40	Rezoner least squares fit tolerance [RLT] EQ.0.0: default set to 0.01	E10.0
42-45	Geometric stiffness flag [IGS] EQ.0: no EQ.1: yes	I5

Solution Definition Notes

(card):(field)	Comments
1 : 1,2	The number and size of time steps must be specified for all quasistatic and dynamic problems solved using fixed step strategies. For quasistatic analyses that do not include rate dependent material models, time is simply a parameter that specifies the load incrementation for the incremental solution strategy, and may or may not be physically motivated. For dynamic problems, time step size should be chosen to accurately time integrate the equations of motion. In any case, time step size should be limited to achieve convergence in each of the solution increments.
1 : 3-6	Step intervals for each function have defaults as described.
1 : 7	Because quasinewton methods may have superlinear convergence, they generally require fewer iterations than the modified Newton method. Arc length methods are suitable for problems involving snap through buckling or other global instabilities, and can only be used for quasistatic analysis.
1 : 8,9	Default convergence tolerances have been set based on extensive numerical experience. The "loosening" or "tightening" of tolerances may improve the convergence rate, or increase the accuracy in achieving global equilibrium. The optimal value of convergence tolerances is generally determined by trial and error. Variable convergence measures may be defined by using ISLAND solution templates.

(card):(field)	Comments
1 : 10	This parameter should always be set to 1, with one possible exception. When performing a completely **linear** dynamic analysis, this parameter may be set to a larger number to increase computational efficiency. Note that any problem involving slidelines in **not linear**.
1 : 11	This parameter should always be set to 1.
1 : 12,13	The default values of these parameters are based on extensive numerical experience. Optimal values are different for each problem class.
2 : 1	Nonzero values of this parameter result in unloading after the specified number of steps NSTEP is taken using an arc length method.
2 : 2	Unloading is performed without the augmented arc length constraint.
2 : 3,4	The arc length constraint equation is defined in terms of either a displacement norm or the displacement of a particular degree-of-freedom.
2 : 5	This parameter specifies the form of the arc length constraint equation. Crisfield's method represents a spherical constraint in load-displacement space, while Ramm's method is a linearized constraint.
2 : 6	With arc length methods, the incrementation of the external load changes from iteration to iteration in an attempt to satisfy the arc length constraint equation. Arc length damping may be used to "damp out" oscillations in the load incrementation which adversely affect the convergence of the global system.
3 : 1-4	Default tolerances are based on numerical experience.
3 : 5	Numerical experience has shown the inclusion of the geometric stiffness to impede convergence in quasinewton solution strategies.

4.3 MATERIALS

Repeat the following set of cards for each material model.

Card 1

Columns	Quantity	Format
1-5	Material identification number	I5
6-10	Material type	I5
	EQ.l: elasticity	
	EQ.2: orthotropic elasticity	
	EQ.3: elastoplasticity	
	EQ.4: thermal-elastoplasticity	
	EQ.5: soil and crushable foam	
	EQ.6: viscoelasticity	
	EQ.7: thermal-orthotropic elasticity	
	EQ.8: thermoelastic-creep	
	EQ.9: Blatz-Ko rubber	
	EQ.10: power law plasticity with failure	
	EQ.11: unified creep plasticity	
	EQ.12: power law thermoplasticty	
	EQ.13: strain rate sensitive elastoplasticity	
	EQ.14: circumferentially cracked elastoplasticity	
	EQ.15: two-invariant cap	
	EQ.16: Ramberg-Osgood elastoplasticity	
	EQ.17: thermal-elastoplasticity with 8-curves	
	EQ.18: thermal-elastoplastic quench	
	EQ.19: strain rate sensitive power law plasticity	
	EQ.20: power law thermoplasticity with failure	
	EQ.21: nonlinear elastoplastic	
	EQ.22: polynomial hyperelastic rubber	
	EQ.23: primary-secondary-tertiary creep	
	EQ.24: deformation mechanism	
	EQ.25: Gurson -Tvergaard void growth plasticity	
	EQ 26: Mooney-Rivlin rubber	

Columns	Quantity	Format
11-20	Density	E10.0
21-30	Thickness for plane stress analysis EQ.0.0: default set to 1.0	E10.0
31-40	Material reference temperature T_{ref}	E10.0
41-50	Stiffness proportional coefficient α_{stiff} for Rayleigh damping	E10.0

Card 2

Columns	Quantity	Format
1-72	Material identification	12A6

Cards 3,4,...,8

Material Type 1 (Elasticity)

Columns		Quantity	Format
1-10	Card 3	Young's modulus E	E10.0
1-10	Card 4	Poisson's ratio ν	E10.0
1-10	Card 5	Blank	
1-10	Card 6	Blank	
1-10	Card 7	Blank	
1-10	Card 8	Blank	

Material Type 2 (Orthotropic Elasticity)

Columns		Quantity	Format
1-10	Card 3	Elastic modulus E_a	E10.0
11-20		Elastic modulus E_b	E10.0
21-30		Elastic modulus E_c	E10.0
1-10	Card 4	Poisson's ratio ν_{ba}	E10.0
11-20		Poisson's ratio ν_{ca}	E10.0
21-30		Poisson's ratio ν_{cb}	E10.0
1-10	Card 5	Shear modulus G_{ab}	E10.0
1-10	Card 6	Material axes option, AOPT EQ.0.0: locally orthotropic with material axes determined by angle Ψ and element nodes n_1 and n_2 specified on each element card. EQ.1.0: locally orthotropic with material axes determined by a point in space and the global location of Gauss integration points EQ.2.0: globally orthotropic with material axes determined by angle Ψ_G.	E10.0
1-10	Card 7	Coordinate y_p (define for AOPT = 1.0)	E10.0
11-20		Coordinate z_p (define for AOPT = 1.0)	E10.0
1-10	Card 8	Angle Ψ_G (define for AOPT = 2.0)	E10.0

The constitutive matrix $\mathbf{C}$ relating increments in stress to increments in strain is defined as

$$\mathbf{C} = \bar{\mathbf{T}}^T \mathbf{C}_L \bar{\mathbf{T}}, \tag{86}$$

where $\bar{\mathbf{T}}$ is the appropriate transformation matrix and $\mathbf{C}_L$ is the constitutive matrix defined in terms of the orthogonal material axes, a and b,

$$\mathbf{C}_L^{-1} = \begin{bmatrix} \frac{1}{E_a} & -\frac{\nu_{ba}}{E_b} & -\frac{\nu_{ca}}{E_c} & 0 \\ -\frac{\nu_{ab}}{E_a} & \frac{1}{E_b} & -\frac{\nu_{cb}}{E_c} & 0 \\ -\frac{\nu_{ac}}{E_a} & -\frac{\nu_{bc}}{E_b} & \frac{1}{E_c} & 0 \\ 0 & 0 & & \end{bmatrix}. \tag{87}$$

Poisson's ratios are defined as

$$\nu_{ij} = \frac{\varepsilon_j}{\varepsilon_i}, \tag{88}$$

which represents the strain ratio resulting from a uniaxial stress applied in the *i-th* direction. Note that $\nu_{ab}/E_a = \nu_{ba}/E_b$, $\nu_{ca}/E_c = \nu_{ac}/E_c$ and $\nu_{cb}/E_c = \nu_{bc}/E_b$.

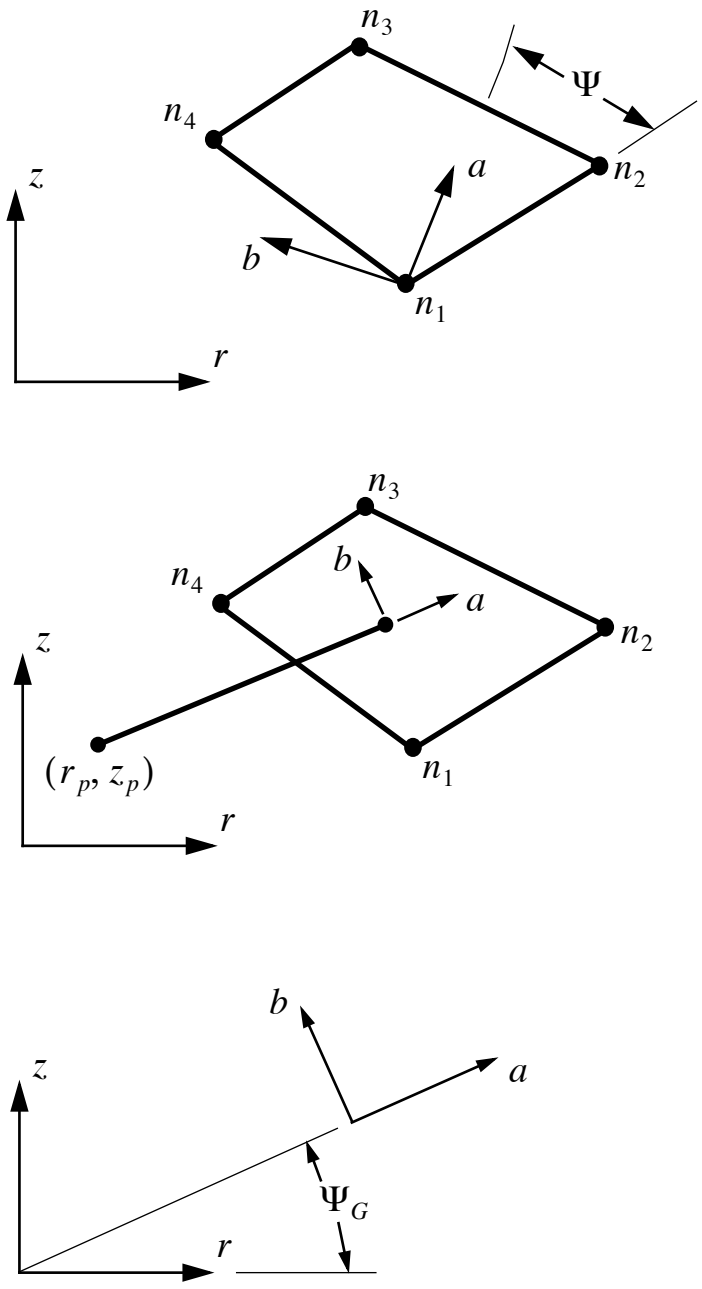

Figure 5
Options for determining the principal material axes
(a) AOPT = 0.0; (b) AOPT = 1.0; (c) AOPT = 2.0.

Material Type 3 (Elastoplasticity)

Columns		Quantity	Format
1-10	Card 3	Young's modulus E	E10.0
1-10	Card 4	Poisson's ratio ν	E10.0
1-10	Card 5	Yield stress σ_o	E10.0
1-10	Card 6	Hardening modulus E_p	E10.0
11-20		Hardening parameter β	E10.0
1-10	Card 7	Effective plastic strain $\bar{\varepsilon}_1^p$	E10.0
11-20		Effective plastic strain $\bar{\varepsilon}_2^p$	E10.0
.		.	.
.		.	.
.		.	.
71-80		Effective plastic strain $\bar{\varepsilon}_8^p$	E10.0
1-10	Card 8	Yield stress σ_{y1} at $\bar{\varepsilon}_1^p$	E10.0
11-20		Yield stress σ_{y2} at $\bar{\varepsilon}_2^p$	E10.0
.		.	.
.		.	.
.		.	.
71-80		Yield stress σ_{y8} at $\bar{\varepsilon}_8^p$	E10.0

The material behavior is elastoplastic and includes either linear or nonlinear strain hardening. Linear hardening is selected by leaving cards 7 and 8 blank. The specification of hardening parameter β, where $0 \le \beta \le 1$, results in either kinematic, isotropic, or a combination of kinematic and isotropic linear hardening, as shown in Figure 6. Purely kinematic or purely isotropic hardening is obtained by setting β to 0.0 or 1.0, respectively. The linear hardening law has the form

$$\sigma_y = \sigma_o + \beta E_p \bar{\varepsilon}^p \tag{89}$$

where σ_y is the current yield stress and the effective plastic strain $\bar{\varepsilon}^p$ is given by

$$\bar{\varepsilon}^p = \int^t d\bar{\varepsilon}^p. \tag{90}$$

Increment $d\bar{\varepsilon}^p$ defined in terms of the plastic strain tensor $d\varepsilon_{ij}^p$ as

$$d\bar{\varepsilon}^p = \left(\frac{2}{3} d\varepsilon_{ij}^p d\varepsilon_{ij}^p\right)^{\frac{1}{2}}. \tag{91}$$

For isotropic hardening, the effective stress σ is given by

$$\sigma = \left(\frac{3}{2} s_{ij} s_{ij}\right)^{\frac{1}{2}}, \tag{92}$$

where s_{ij} is the deviatoric stress tensor. For kinematic hardening,

$$\sigma = \left(\frac{3}{2} \eta_{ij} \eta_{ij}\right)^{\frac{1}{2}}, \tag{93}$$

where the translated stress η_{ij} is defined as

$$\eta_{ij} = s_{ij} - \alpha_{ij}, \tag{94}$$

and α_{ij} is the back stress tensor. The hardening modulus E_p, which represents the slope of the yield stress σ_y vs. effective plastic strain $\bar{\varepsilon}^p$ curve, can be written in terms of the tangent modulus E_T as

$$E_p = \frac{E E_T}{E - E_T}. \tag{95}$$

The tangent modulus E_T is the slope of the inelastic portion of a uniaxial stress vs. strain curve (or equivalently the effective stress σ vs. effective strain ε curve). An isotropic, nonlinear hardening law may be specified by defining the $\sigma_y - \bar{\varepsilon}^p$ relationship on cards 7 and 8. For this case, $\bar{\varepsilon}_1^p$ must be zero, and the data on cards 5 and 6 is ignored.

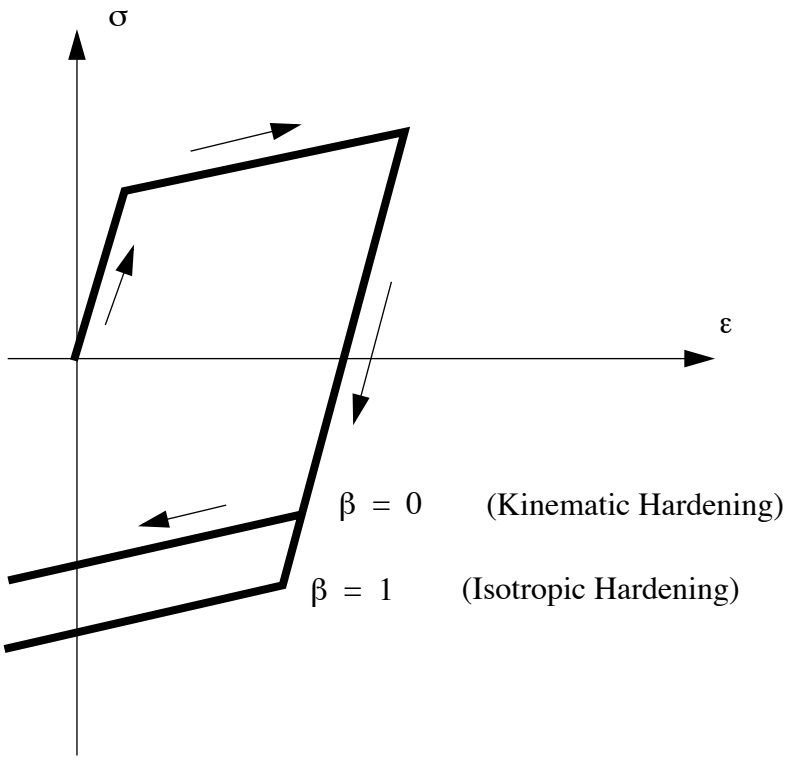

Figure 6
Elastic-plastic behavior with isotropic and kinematic hardening

Kinematic and isotropic hardening models yield identical behavior under monotonic loading. Under cyclic loading, kinematic hardening predicts a hysteretic energy dissipation, while isotropic hardening predicts no energy dissipation after the first cycle. The isotropic model is somewhat faster in computation time, however.

Material Type 4 (Thermal-Elastoplasticity)

Columns		Quantity	Format
1-10	Card 3	Temperature T_1	E10.0
11-20		Temperature T_2	E10.0
.		.	.
.		.	.
.		.	.
71-80		Temperature T_3	E10.0
1-10	Card 4	Young's modulusE_1 at T_1	E10.0
11-20		Young's modulus E_2 at T_2	E10.0
.		.	.
.		.	.
.		.	.
71-80		Young's modulus E_8 at T_8	E10.0
1-10	Card 5	Poisson's ratioν_1 at T_1	E10.0
11-20		Poisson's ratio ν_2 at T_2	E10.0
.		.	.
.		.	.
.		.	.
71-80		Poisson's ratioν_8 at T_8	E10.0
1-10	Card 6	Secant coefficient of thermal expansion $\bar{\alpha}_1$ to T_1	E10.0
11-20		Secant coefficient of thermal expansion $\bar{\alpha}_2$ to T_2	E10.0
.		.	.
.		.	.
.		.	.
71-80		Secant coefficient of thermal expansion $\bar{\alpha}_8$ to T_8	E10.0
1-10	Card 7	Yield stress σ_{01} at T_1	E10.0

Columns		Quantity	Format
11-20		Yield stress σ_{02} at T_2	E10.0
.		.	.
.		.	.
.		.	.
71-80		Yield stress σ_{08} at T_8	E10.0
1-10	Card 8	Hardening modulus E_{p1} at T_1	E10.0
11-20		Hardening modulus E_{p2} at T_2	E10.0
.		.	.
.		.	.
.		.	.
71-80		Hardening modulus E_{p8} at T_8	E10.0

The material behavior is elastoplastic with isotropic, linear strain hardening. Material parameters E, ν, σ_0, and E_p can all be functions of temperature. Thermal expansion due to temperature change is included when nonzero values of $\bar{\alpha}$ are specified. The secant coefficient of thermal expansion $\bar{\alpha}$ can also be a function of temperature. Total thermal strain ε_{ij}^T is defined in terms of the secant coefficient $\bar{\alpha}$ as

$$\varepsilon_{ij}^T = \bar{\alpha}(T - T_{ref})\delta_{ij} , \tag{96}$$

where T is the current temperature and T_{ref} is the material reference temperature. Therefore, temperature dependent, secant coefficients of thermal expansion $\bar{\alpha}$ should be defined as the value **to** that temperature, not the value **at** that temperature. The secant coefficient $\bar{\alpha}$ is related to the tangent coefficient of thermal expansion α at a temperature T by

$$\bar{\alpha}(T) = \frac{1}{T - T_{ref}} \int_{T_{ref}}^{T} \alpha(T) dT . \tag{97}$$

For temperature **independent** coefficients of thermal expansion, $\bar{\alpha}$ is identical to α, and the classical definition of thermal expansion is valid.

If all material parameters are temperature independent, one set of parameters may be defined with T_1 set to zero. This case commonly occurs when thermal expansion is the only temperature related effect of interest. In all other cases, at least two temperatures and their corresponding material parameters must be specified. The analysis will be terminated if a material temperature falls outside the defined range. A purely thermoelastic material is obtained by leaving cards 7 and 8 blank.

Material Type 5 (Soil and Crushable Foam)

Columns		Quantity	Format
1-10	Card 3	Shear modulus G	E10.0
11-20		Bulk unloading modulus K_u	E10.0
21-30		Yield function constant a_0	E10.0
31-40		Yield function constant a_1	E10.0
41-50		Yield function constant a_2	E10.0
51-60		Minimum pressure p_c, $(p_c < 0)$	E10.0
61-70		Unloading option, UOPT EQ.0.0: volumetric crushing EQ.1.0: no volumetric crushing	E10.0
1-10	Card 4	Volumetric strain ε_1^v	E10.0
11-20		Pressure p_1	E10.0
21-30		Volumetric strain ε_2^v	E10.0
31-40		Pressure p_2	E10.0
1-10	Card 5	Volumetric strain ε_3^v	E10.0
11-20		Pressure p_3	E10.0
21-30		Volumetric strain ε_4^v	E10.0
31-40		Pressure p_4	E10.0
.		.	.
.		.	.
.		.	.
1-1	Card 8	Volumetric strain ε_9^v	E10.0
11-20		Pressure p_9	E10.0
21-30		Volumetric strain ε_{10}^v	E10.0
31-40		Pressure p_{10}	E10.0

This model, adapted from the HONDO code (see Key [1974]), allows for the specification of a nonlinear pressure p vs. volumetric strain ε^v relationship as shown in Figure 7. Here, pressure is positive in compression, and volumetric strain is negative in compression. The tabulated data should be specified in the order of increasing compression. Volumetric crushing is optional, and

represents the unloading behavior illustrated in Figure 7. For volumetric crushing, the unloading modulus is K_u. Without volumetric crushing, unloading follows the specified pressure-volumetric strain curve. A minimum pressure p_c ($p_c < 0$) may also be defined. If the pressure drops below this cutoff value, it is reset to the cutoff value.

The deviatoric behavior is elastic, perfectly plastic, with a pressure dependent yield function ϕ given by

$$\phi = J_2 - (a_0 + a_1 p + a_2 p^2), \tag{98}$$

where

$$J_2 = \frac{1}{2} s_{ij} s_{ij}. \tag{99}$$

For nonzero a_1 and a_2, the flow is nonassociative. On the yield surface, $J_2 = (1/3)\sigma_y^2$, where σ_y is the uniaxial yield stress (or equivalently the effective yield stress). Therefore, constants a_0, a_1, and a_2 may be determined from uniaxial test data and

$$\sigma_y = [3(a_0 + a_1 p + a_2 p^2)]^{\frac{1}{2}}. \tag{100}$$

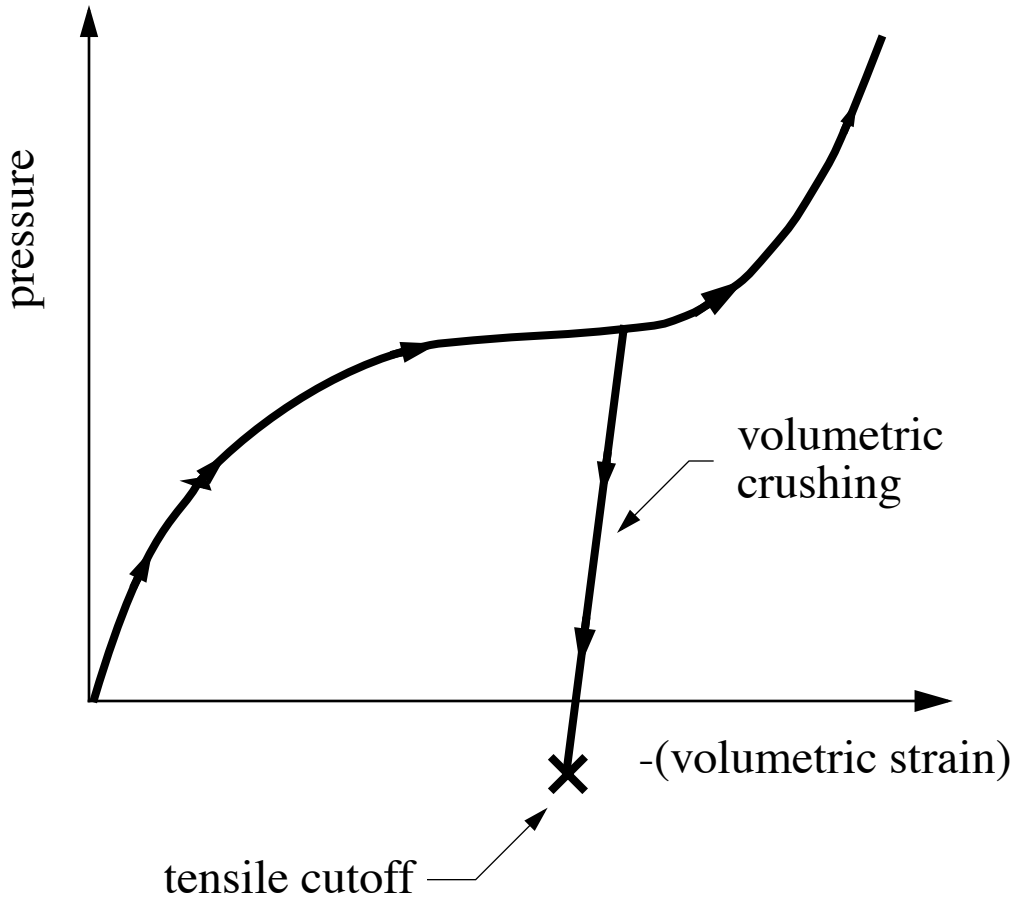

Figure 7
Pressure-volumetric strain curve for the soil and crushable foam model.

Material Type 6 (Viscoelasticity)

Columns		Quantity	Format
1-10	Card 3	Bulk modulus K	E10.0
1-10	Card 4	Instantaneous shear modulus G_G	E10.0
1-10	Card 5	Long time shear modulus G_R	E10.0
1-10	Card 6	Time parameter MFLAG.EQ.0.0: decay constant β MFLAG.EQ.1.0: time relaxation constant τ	E10.0
	Card 7	Model formulation flag MFLAG EQ.0.0: standard NIKE2D formulation EQ.1.0: Kelvin viscoelastic formulation	
	Card 8	Blank	

Two types of viscoelastic formulations are available. For the standard NIKE2D formulation (MFLAG = 0.0), the deviatoric stress rate $\dot{s}_{ij}$ is given by

$$\dot{s}_{ij} = 2\int_0^t G(t-\tau)\dot{e}_{ij}d\tau \ , \tag{101}$$

where the shear relaxation modulus $G(t)$ is defined by

$$G(t) = G_R + (G_G - G_R)e^{-\beta t} \ , \tag{102}$$

and $\dot{e}_{ij}$ is the deviatoric strain rate. The evolution of components of deviatoric stress for the Kelvin formulation (MFLAG = 1.0) are governed by

$$\dot{s}_{ij} + \frac{1}{\tau}s_{ij} = (1+\delta_{ij})G_G\dot{e}_{ij} + (1+\delta_{ij})\frac{G_R}{\tau}e_{ij} \qquad \text{(no sum)}. \tag{103}$$

These computed componenets are projected into the deviatoric stress space.

The standard NIKE2D formulation is adapted from the HONDO code. The implementation of the Kelvin formulation, as well as the relation of the model parameters to stiffness and damping properties over a frequency range of interest, is discussed in Whirley and Engelmann (1991a). The Kelvin formulation is primarily suited for problems dominated by shear response such as seismic applications. For each of the viscoelastic formulations, the volumetric response is elastic,

$$p = -K\varepsilon^{v}. \tag{104}$$

Material Type 7 (Thermal-Orthotropic Elasticity)

Columns		Quantity	Format
1-10	Card 3	Elastic modulus E_a	E10.0
11-20		Elastic modulus E_b	E10.0
21-30		Elastic modulus E_c	E10.0
1-10	Card 4	Poisson's ratio ν_{ba}	E10.0
11-20		Poisson's ratio ν_{ca}	E10.0
21-30		Poisson's ratio ν_{cb}	E10.0
31-40		Coefficient of thermal expansion α_a	E10.0
41-50		Coefficient of thermal expansion α_b	E10.0
51-60		Coefficient of thermal expansion α_c	E10.0

Cards 5-8 are identical to those for material type 2.

This model is similar to material type 2, except that orthotropic thermal expansion is included with the specification of α_a, α_b, and α_c.

Material Type 8 (Thermoelastic-Creep)

Columns		Quantity	Format
1-10	Card 3	Temperature T_1	E10.0
11-20		Temperature T_2	E10.0
.		.	.
.		.	.
.		.	.
71-80		Temperature T_8	E10.0
1-10	Card 4	Shear modulus $2G_1$ at T_1	E10.0
11-20		Shear modulus $2G_2$ at T_2	E10.0
.		.	.
.		.	.
.		.	.
71-80		Shear modulus $2G_8$ at T_8	E10.0
1-10	Card 5	Bulk modulus K_1 at T_1	E10.0
11-20		Bulk modulus K_2 at T_2	E10.0
.		.	.
.		.	.
.		.	.
71-80		Bulk modulus K_8 at T_8	E10.0
1-10	Card 6	Secant coefficient of thermal expansion $\bar{\alpha}_1$ to T_1	E10.0
11-20		Secant coefficient of thermal expansion $\bar{\alpha}_2$ to T_2	E10.0
.		.	.
.		.	.
.		.	.
71-80		Secant coefficient of thermal expansion $\bar{\alpha}_8$ to T_8	E10.0
1-10	Card 7	Creep coefficient a_1 at T_1	E10.0

Columns		Quantity	Format
11-20		Creep coefficient a_2 at T_2	E10.0
.		.	.
.		.	.
.		.	.
71-80		Creep coefficient a_8 at T_8	E10.0
1-10	Card 8	Creep exponent b_1 at T_1	E10.0
11-20		Creep exponent b_2 at T_2	E10.0
.		.	.
.		.	.
.		.	.
71-80		Creep exponent b_8 at T_8	E10.0

The implementation of this model was developed by Krieg (1977), and includes both thermoelastic and creep behavior. The instantaneous creep rate $\dot{\varepsilon}$ is given by a power law of the form

$$|\dot{\varepsilon}| = a|\sigma|^b , \tag{105}$$

where σ is effective stress. Material parameters G, K, a, and b can all be functions of temperature. Thermal expansion due to temperature change is included when nonzero values of $\bar{\alpha}$ are specified. The secant coefficient of thermal expansion $\bar{\alpha}$ can also be a function of temperature. Total thermal strain ε_{ij}^T is defined in terms of the secant coefficient $\bar{\alpha}$ as

$$\varepsilon_{ij}^T = \bar{\alpha}(T - T_{ref})\delta_{ij} , \tag{106}$$

where T is the current temperature and T_{ref} is the material reference temperature. Therefore, temperature dependent, secant coefficients of thermal expansion $\bar{\alpha}$ should be defined as the value **to** that temperature, not the value **at** that temperature. The secant coefficient $\bar{\alpha}$ is related to the tangent coefficient of thermal expansion α at a temperature T by

$$\bar{\alpha}(T) = \frac{1}{T - T_{ref}} \int_{T_{ref}}^{T} \alpha(T) dT . \tag{107}$$

For temperature **independent** coefficients of thermal expansion, $\bar{\alpha}$ is identical to α, and the classical definition of thermal expansion is valid.

At least two temperatures and their corresponding material parameters must be specified. The analysis will be terminated if a material temperature falls outside the defined range.

Material Type 9 (Blatz - Ko Rubber)

Columns		Quantity	Format
1-10	Card 3	Shear modulus G	E10.0
	Card 4	Blank	
.		.	.
.		.	.
.		.	.
	Card 8	Blank	

This model is hyperelastic and is defined in a total Lagrangian context. The second Piola-Kirchhoff stress S_{ij} is computed as

$$S_{ij} = G\left(\frac{1}{V_r}C_{ij} - \nu^{-\frac{1}{1-2\nu}}\delta_{ij}\right) , \tag{108}$$

where V_r is the relative volume, C_{ij} is the right Cauchy-Green strain tensor, and ν is Poisson's ratio which fixed at 0.463 . The Cauchy stress τ_{ij} is determined from the second Piola-Kirchhoff stress S_{ij} by the relationship

$$\tau_{ij} = \frac{1}{V_r}F_{ik}F_{jl}S_{kl}, \tag{109}$$

where F_{ij} is the deformation gradient.

Material Type 10 (Power Law Plasticity with Failure)

Columns		Quantity	Format
1-10	Card 3	Young's modulus E	E10.0
11-20		Poisson's ratio ν	E10.0
21-30		Strength coefficient k	E10.0
31-40		Hardening exponent n	E10.0
41-50		Strength to failure from tensile test σ_{tf}	E10.0
51-60		Strength to failure from shear test σ_{sf}	E10.0
61-70		Load curve number for shear strength to failure as a function of pressure, LSHEAR	E10.0
71-80		Failure option flag, IFAIL EQ.0.0: failure not modelled EQ.1.0: Mohr-Coulomb EQ.2.0: Drucker-Prager EQ.3.0: both Mohr-Coulomb and Drucker-Prager	E10.0
	Card 4	Blank	
.		.	.
.		.	.
.		.	.
	Card 8	Blank	

The material behavior is elastoplastic with isotropic, power law hardening. The nonlinear hardening law has the form

$$\sigma_y = k(\varepsilon_0 + \bar{\varepsilon}^p)^n \ , \tag{110}$$

where ε_0 is the initial yield strain given by

$$\varepsilon_0 = \left(\frac{E}{k}\right)^{\frac{1}{n-1}} \ . \tag{111}$$

Failure is included if IFAIL is specified as nonzero. When failure is reached at all Gauss points in an element, the strength of the element is reduced to nearly zero, and that element is deleted in the binary plot database. Several failure options are available and are defined as follows:

- If IFAIL = 1.0 and load curve number LSHEAR = 0.0, the Mohr-Coulomb failure criterion is invoked. Failure is initiated when stress values exceed the Mohr-Coulomb criterion

$$\sigma_{sf} = m\sigma_{tf} + b\,. \tag{112}$$

The slope m and itercept b are determined from tensile and shear test values, σ_{tf} and σ_{sf}, by

$$m = \frac{\frac{1}{2}\sigma_{tf} - \sigma_{sf}}{\sqrt{\sigma_{tf}\sigma_{sf} - \sigma_{sf}^2}}\,, \tag{113}$$

$$b = \frac{\sigma_{tf}\sigma_{sf}}{2\sqrt{\sigma_{tf}\sigma_{sf} - \sigma_{sf}^2}} = m\frac{\sigma_{tf}\sigma_{sf}}{\sigma_{tf} - 2\sigma_{sf}}\,. \tag{114}$$

The values of σ_{tf} and σ_{sf} are restricted to

$$\sigma_{sf} > 0\,, \tag{115}$$

$$\sigma_{tf} > \sigma_{sf}\,. \tag{116}$$

- If IFAIL = 1.0 and load curve number LSHEAR is nonzero, a modified Mohr-Coulomb criterion is used. Failure is initiated when the maximum shear stress exceeds the appropriate value from the shear strength to failure vs. pressure curve.
- If IFAIL = 2.0, the Drucker-Prager failure criterion is invoked. The Drucker-Prager surface is constructed from the tensile and shear strengths at failure, σ_{tf} and σ_{sf}.
- If IFAIL = 3.0, both the Drucker-Prager and the appropriate Mohr-Coulomb failure criteria are invoked.

Material Type 11 (Creep Plasticity)

Columns		Quantity	Format
1-10	Card 3	Young's modulus E	E10.0
11-20		Poisson's ratio ν	E10.0
21-30		Initial temperature T in $^\circ K$	E10.0
31-40		Density x specific heat ρC_v	E10.0
41-50		Hardening parameter β	E10.0
1-10	Card 4	Rate dependent yield stress coefficient C_1	E10.0
11-20		Rate dependent yield stress exponent C_2	E10.0
21-30		Rate independent yield stress coefficient C_3	E10.0
31-40		Rate independent yield stress exponent C_4	E10.0
1-10	Card 5	Transition coefficient C_5	E10.0
11-20		Transition exponent C_6	E10.0
21-30		Hardening coefficient C_7	E10.0
31-40		Hardening exponent C_8	E10.0
1-10	Card 6	Dynamic recovery coefficient C_9	E10.0
11-20		Dynamic recovery exponent C_{10}	E10.0
21-30		Diffusion recovery coefficient C_{11}	E10.0
31-40		Diffusion recovery exponent C_{12}	E10.0

This model represents a modified implementation of a unified creep plasticity model proposed by Bamman (1984). The original implementation is described by Hallquist (1986), and recent results and modifications are discussed by Bamman (1990), and Flower and Nikkel (1990). The current model implementation is briefly described in the following.

The history dependence of this model is characterized through the introduction of two internal state variables, a scalar κ, and a second order tensor $\boldsymbol{a}$. The governing constitutive equations are of the form

$$\dot{\boldsymbol{s}} = \frac{E\nu}{(1+\nu)(1-2\nu)} tr(\dot{\boldsymbol{e}})1 + \frac{E}{1+\nu}(\dot{\boldsymbol{e}} - \dot{\boldsymbol{e}}^p) \quad , \tag{117}$$

$$\dot{\boldsymbol{e}}^p = f(T)\sinh\left[\frac{|\boldsymbol{h}| - \kappa - Y(T)}{V(T)}\right]\frac{\boldsymbol{h}}{|\boldsymbol{h}|} \quad , \tag{118}$$

$$\dot{\boldsymbol{a}} = k(T)(1-\beta)\dot{\boldsymbol{e}}^p - \frac{(g(T) + h(T)|\dot{\boldsymbol{e}}^p|)|\boldsymbol{a}|\boldsymbol{a}}{1-\beta} \quad , \tag{119}$$

$$\dot{\kappa} = k(T)\beta|\dot{\boldsymbol{e}}^p| - \frac{(g(T) + h(T)|\dot{\boldsymbol{e}}^p|)\kappa^2}{\beta} \quad , \tag{120}$$

where the translated stress $\boldsymbol{h}$ is given by

$$\boldsymbol{h} = \mathbf{s} - \boldsymbol{a} \ , \tag{121}$$

and **s** is the deviatoric stress. The inelastic behavior of the model is governed by six temperature dependent parameter functions *V(T), Y(T), f(T), h(T), k(T),* and *g(T).* Each of the functions is an exponential and defined by two material parameters as follows:

$$V(T) = C_1 e^{-C_2/T} \quad \text{(rate dependent yield stress)}, \tag{122}$$

$$Y(T) = C_3 e^{C_4/T} \quad \text{(rate independent yield stress)}, \tag{123}$$

$$f(T) = C_5 e^{-C_6/T} \quad \text{(transition to rate dependent behavior)}, \tag{124}$$

$$h(T) = C_7 e^{-C_8/T} \quad \text{(hardening)}, \tag{125}$$

$$k(T) = C_9 e^{-C_{10}/T} \quad \text{(dynamic recovery)}, \tag{126}$$

$$g(T) = C_{11} e^{-C_{12}/T} \quad \text{(diffusion controlled static or thermal recovery)}. \tag{127}$$

The specification of hardening parameter β, where $0.0 \le \beta \le 1.0$, results in either kinematic, isotropic, or a combination of kinematic and isotropic hardening. Purely kinematic or purely isotropic hardening is obtained by setting $\beta = 0.0$ or $\beta = 1.0$, respectively. For these cases, numerical perturbations are used to prevent the governing equations from becoming singular. The model also accounts for adiabatic heating due to plastic work. Temperature rate $\dot{T}$ is defined in terms of the density ρ and specific heat C_v as

$$\dot{T} = \frac{0.95}{\rho C_v} \boldsymbol{s}\dot{\boldsymbol{e}}^p \ . \tag{128}$$

To help illustrate the use of this model, a sample set of material parameters for 21-6-9 stainless steel is given as follows.

Sample values for 21-6-9 stainless steel

Young's modulus E	2.00e+5	[MPa]
Poisson's ratio ν	0.30	
Initial temperature T	373	[$^\circ K$]
Density x specific heat ρC_v	2.68e-01	[MKg] or [(m^3 $^\circ K/MJ$)]
Hardening parameter β	0.0	
Rate dependent yield stress coefficient C_1	5.58e+01	[MPa}
Rate dependent yield stress exponent C_2	8.67e+01	[$^\circ K$]
Rate independent yield stress coefficient C_3	1.67e+01	[MPa]
Rate independent yield stress exponent C_4	4.68e+02	[$^\circ K$]
Transition coefficient C_5	1.02e+04	[s^{-1}]
Transition exponent C_6	3.48e+03	[$^\circ K$]
Hardening coefficient C_7	4.72e-03	[1/MPa]
Hardening exponent C_8	2.55e+02	[$^\circ K$]
Dynamic recovery coefficient C_9	1.81e+03	[MPa]
Dynamic recovery exponent C_{10}	5.23e+01	[$^\circ K$]
Diffusion recovery coefficient C_{11}	0.0	[1/$MPa \bullet s$]
Diffusion recovery exponent C_{12}	1.0	[$^\circ K$]

Material Type 12 (Power Law Thermoplasticity)

Columns		Quantity	Format
1-10	Card 3	Temperature T_1	E10.0
11-20		Temperature T_2	E10.0
.		.	.
.		.	.
.		.	.
71-80		Temperature T_8	E10.0
1-10	Card 4	Young's modulus E_1 at T_1	E10.0
11-20		Young's modulus E_2 at T_2	E10.0
.		.	.
.		.	.
.		.	.
71-80		Young's modulus E_8 at T_8	E10.0
1-10	Card 5	Poisson's ratio ν_1 at T_1	E10.0
11-20		Poisson's ratio ν_2 at T_2	E10.0
.		.	.
.		.	.
.		.	.
71-80		Poisson's ratio ν_8 at T_8	E10.0
1-10	Card 6	Coefficient of thermal expansion α_1 at T_1	E10.0
11-20		Coefficient of thermal expansion α_2 at T_2	E10.0
.		.	.
.		.	.
.		.	.
71-80		Coefficient of thermal expansion α_8 at T_8	E10.0

Columns		Quantity	Format
1-10	Card 7	Strength coefficient k_1 at T_1	E10.0
11-20		Strength coefficient k_2 at T_2	E10.0
.		.	.
.		.	.
.		.	.
71-80		Strength coefficient k_8 at T_8	E10.0
1-10	Card 8	Hardening exponent n_1 at T_1	E10.0
11-20		Hardening exponent n_2 at T_2	E10.0
.		.	.
.		.	.
.		.	.
71-80		Hardening exponent n_8 at T_8	E10.0

The material behavior is elastoplastic with isotropic, power law hardening. The nonlinear hardening law has the form

$$\sigma_y = k(\varepsilon_0 + \bar{\varepsilon}^p)^n \ , \tag{129}$$

where ε_0 is the initial yield strain given by

$$\varepsilon_0 = \left(\frac{E}{k}\right)^{\frac{1}{n-1}} \ . \tag{130}$$

Material parameters E, ν, k, and n can all be functions of temperature. Thermal expansion due to temperature change is included when nonzero values of α are specified. The coefficient of thermal expansion α can also be a function of temperature and, for this model, represents a tangent value. Thermal strain rate $\dot{\varepsilon}_{ij}^T$ is defined in terms of the tangent coefficient of thermal expansion α as

$$\dot{\varepsilon}_{ij}^T = \alpha(T)\dot{T}\delta_{ij} \ , \tag{131}$$

where T is the current temperature.

If all material parameters are temperature independent, one set of parameters may be defined with T_1 set to zero. This case commonly occurs when thermal expansion is the only temperature related effect of interest. In all other cases, at least two temperatures and their corresponding material parameters must be specified. The analysis will be terminated if a material temperature falls outside the defined range. A purely thermoelastic material is obtained by leaving cards 7 and 8 blank.

Material Type 13 (Strain Rate Dependent Isotropic Plasticity)

Columns		Quantity	Format
1-10	Card 3	Young's modulus E	E10.0
11-20		Poisson's ratio ν	E10.0
21-30		Load curve number for yield stress σ_0 vs. effective strain rate $\dot{\varepsilon}$	E10.0
31-40		Hardening modulus E_p	E10.0
	Card 4	Blank	
	Card 5	Blank	
.		.	
.		.	
.		.	
	Card 8	Blank	

The material behavior is elastoplastic with strain rate dependent, isotropic hardening. The hardening law has the form

$$\sigma_y = \sigma_0(\dot{\varepsilon}) + E_p\bar{\varepsilon}^p \ , \tag{132}$$

where $\bar{\varepsilon}^p$ is the effective plastic strain and σ_0 is determined by the load curve specification of σ_0 vs. $\dot{\varepsilon}$. The effective strain rate $\dot{\varepsilon}$ is defined as

$$\dot{\varepsilon} = \left(\frac{2}{3}\dot{e}_{ij}\dot{e}_{ij}\right)^{\frac{1}{2}} , \tag{133}$$

where $\dot{e}_{ij}$ is the deviatoric strain rate tensor. The hardening modulus E_p, which represents the slope of the yield stress σ_y vs. effective plastic strain $\bar{\varepsilon}^p$ curve, can be written in terms of the tangent modulus E_T as

$$E_p = \frac{EE_T}{E - E_T}. \tag{134}$$

The tangent modulus E_T is the slope of the inelastic portion of a uniaxial stress vs. strain curve.

Material Type 14 (Circumferentially Cracked Elastoplasticity)

Columns		Quantity	Format
1-10	Card 3	Young's modulus E	E10.0
1-10	Card 4	Poisson's ratio ν	E10.0
1-10	Card 5	Yield stress σ_0	E10.0
1-10	Card 6	Hardening modulus E_p	E10.0
11-20		Hardening parameter β	E10.0
1-10	Card 7	Effective plastic strain $\bar{\varepsilon}_1^p$	E10.0
11-20		Effective plastic strain $\bar{\varepsilon}_2^p$	E10.0
.		.	.
.		.	.
.		.	.
71-80		Effective plastic strain $\bar{\varepsilon}_8^p$	E10.0
1-10	Card 8	Yield stress σ_{y1} at $\bar{\varepsilon}_1^p$	E10.0
11-20		Yield stress σ_{y2} at $\bar{\varepsilon}_2^p$	E10.0
.		.	.
.		.	.
.		.	.
71-80		Yield stress σ_{y8} at $\bar{\varepsilon}_8^p$	E10.0

This model is applicable only to axisymmetric structures. The material behavior is identical to material type 3, except that elements of this material cannot carry tensile circumferential stress. By specifying an initial relative volume greater than one on the element cards, the development of compressive circumferential stresses can be delayed or prevented since a gap must close circumferentially before compressive hoop stress develops.

Material Type 15 (Extended Two Invariant Geologic Cap)

Columns		Quantity	Format
1-10	Card 3	Initial bulk modulus κ	E10.0
11-20		Initial shear modulus G	E10.0
1-10	Card 4	Failure envelope parameter α	E10.0
11-20		Failure envelope linear coefficient θ	E10.0
21-30		Failure envelope exponential coefficient γ	E10.0
31-40		Failure envelope exponent β	E10.0
41-50		Cap surface axis ratio R	E10.0
1-10	Card 5	Hardening law exponent D	E10.0
11-20		Hardening law coefficient W	E10.0
21-30		Hardening law parameter X_0	E10.0
31-40		Kinematic hardening coefficient $\bar{c}$	E10.0
41-50		Kinematic hardening parameter N	E10.0
1-10	Card 6	Plot database flag, IPLOT EQ.1.0: Hardening variable, κ EQ.2.0: Cap - J_1 axis intercept, $X(\kappa)$ EQ.3.0: Volumetric plastic strain, ε_v^p EQ.4.0: First stress invariant, J_1 EQ.5.0: Second stress invariant, $\sqrt{J_{2D}}$ EQ.6.0: Not used EQ.7.0: Not used EQ.8.0: Response mode number EQ.9.0: Number of iterations	E10.0
11-20		Load curve number for K/K_0 vs. V/V_0	E10.0
21-30		Load curve number for G/G_0 vs. V/V_0	
31-40		Load curve number for R/R_0 vs. V/V_0	
41-50		Load curve number for T/T_0 vs. V/V_0	

Columns		Quantity	Format
1-10	Card 7	Formulation flag, ITYPE EQ.1.0: Soil or Concrete (Cap surface may contract) EQ.2.0: Rock (Cap surface does not contract)	E10.0
11-20		Vectorization flag, IVEC EQ.0.0: Vectorized (fixed number of iterations) EQ.1.0: Fully iterative	E10.0
1-10	Card 8	Tension cutoff, $T < 0$ (positive in compression)	E10.0

The two-invariant cap model is widely used for modeling concrete, soil, and other granular materials. Other applications have included modeling metal powders in compaction studies.

The two-invariant cap model is widely used for modeling concrete, soil, and other granular materials. Other applications have included modeling metal powders in compaction studies. This implementation of an extended two invariant cap model was developed by Whirley and Engelmann (1991e) based on the formulations of Simo, Ju, Pister, and Taylor (1988) and Sandler and Rubin (1979). Modifications to the standard cap model are implemented to permit several material parameters to be functions of relative volume, including the bulk modulus K, the shear modulus G, the cap surface axis ratio R, and the tension cutoff limit T, as suggested by Krauss (1990). In addition, the two invariant cap theory is extended to include nonlinear kinematic hardening as suggested by Isenberg, Vaughn, and Sandler (1978). A brief discussion of the extended cap model and its parameters is given below.

The cap model is formulated in terms of the invariants of the stress tensor. The square root of the second invariant of the deviatoric stress tensor, $\sqrt{J_{2D}}$, is found from the deviatoric stresses $\boldsymbol{s}$ as

$$\sqrt{J_{2D}} \equiv \sqrt{\frac{1}{2} s_{ij} s_{ij}} \tag{135}$$

and is an objective scalar measure of the distortional or shearing stress. The first invariant of the stress, J_1, is simply the sum of the normal stresses, or equivalently, three times the pressure.

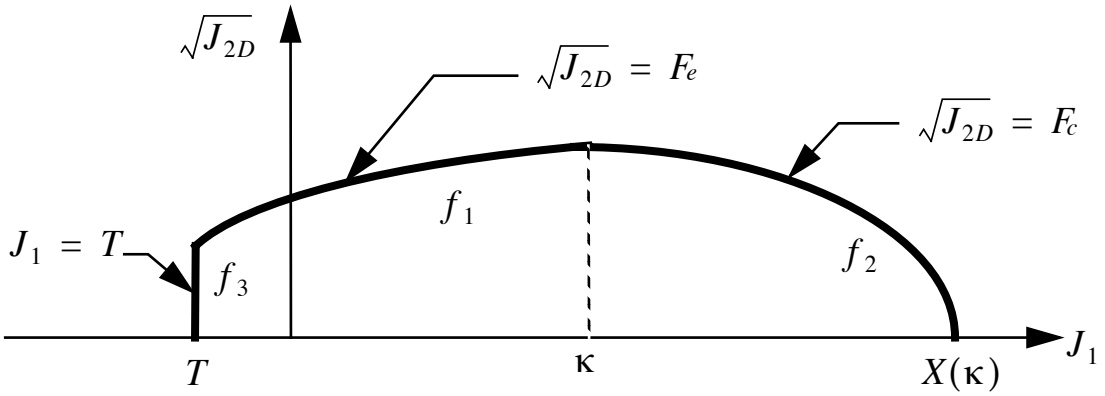

Figure 8
The yield surfaces of the two invariant cap.

The cap model consists of three surfaces in $\sqrt{J_{2D}}$ - J_1 space, as shown in Figure 8. First, there is a failure envelope surface, denoted f_1 in the figure. The functional form of f_1 is

$$f_1 = \sqrt{J_{2D}} - min(F_e(J_1), T_{mises})) \quad , \tag{136}$$

where F_e is given by

$$F_e(J_1) \equiv \alpha - \gamma exp(-\beta J_1) + \theta J_1 \tag{137}$$

and $T_{mises} \equiv |X(\kappa_n) - L(\kappa_n)|$. This failure envelope surface is fixed in $\sqrt{J_{2D}}$ - J_1 space, and therefore does not harden. Next, there is a cap surface, denoted f_2 in the figure, with f_2 given by

$$f_2 = \sqrt{J_{2D}} - F_c(J_1, \kappa) \, , \tag{138}$$

where F_c is defined by

$$F_c(J_1, \kappa) \equiv \frac{1}{R}\sqrt{[X(\kappa) - L(\kappa)]^2 - [J_1 - L(\kappa)]^2} \quad , \tag{139}$$

$X(\kappa)$ is the intersection of the cap surface with the J_1 axis,

$$X(\kappa) = \kappa + RF_e(\kappa) \ , \tag{140}$$

and $L(\kappa)$ is defined by

$$L(\kappa) \equiv \begin{cases} \kappa \ \text{ if } \ \kappa > 0 \\ 0 \ \text{ if } \ \kappa \le 0 \end{cases} \ . \tag{141}$$

The hardening parameter κ is related to the plastic volume change ε_v^p through the hardening law

$$\varepsilon_v^p = W\{1 - exp[-D(X(\kappa) - X_0)]\} \quad . \tag{142}$$

Geometrically, κ is seen in the figure as the J_1 coordinate of the intersection of the cap surface and the failure surface. Finally, there is the tension cutoff surface, denoted f_3 in the figure. The function f_3 is given by

$$f_3 \equiv T - J_1, \tag{143}$$

where T is an input material parameter which specifies the maximum hydrostatic tension sustainable by the material. The elastic domain in $\sqrt{J_{2D}}$ - J_1 space is then bounded by the failure envelope surface above, the tension cutoff surface on the left, and the cap surface on the right.

An additive decomposition of the strain into elastic and plastic parts is assumed:

$$\boldsymbol{e} = \boldsymbol{e}^e + \boldsymbol{e}^p \ , \tag{144}$$

where $\boldsymbol{e}^e$ is the elastic strain and $\boldsymbol{e}^p$ is the plastic strain. Stress is found from the elastic strain using Hooke's law,

$$\boldsymbol{s} = \mathbf{C}(\boldsymbol{e} - \boldsymbol{e}^p) \ , \tag{145}$$

where $\boldsymbol{s}$ is the stress and $\mathbf{C}$ is the elastic constitutive tensor.

The yield condition may be written

$$\begin{aligned} f_1(\boldsymbol{s}) &\le 0 \\ f_2(\mathbf{s}, \kappa) &\le 0 \\ f_3(\boldsymbol{s}) &\le 0 \end{aligned} \tag{146}$$

and the plastic consistency condition requires that

$$\begin{aligned} \dot{\lambda}_k f_k &= 0 \\ \dot{\lambda}_k &\ge 0 \end{aligned} \quad k = 1, 2, 3, \tag{147}$$

where λ_k is the plastic consistency parameter for surface k. If $f_k < 0$, then $\dot{\lambda}_k = 0$ and the response is elastic. If $f_k > 0$, then surface k is active and $\dot{\lambda}_k$ is found from the requirement that $\dot{f}_k = 0$.

Associated plastic flow is assumed, so using Koiter's flow rule the plastic strain rate is given as the sum of contributions from all of the active surfaces,

$$\dot{\boldsymbol{e}}^p = \sum_{k=1}^{3} \dot{\lambda}_k \frac{\partial f_k}{\partial \boldsymbol{s}}. \tag{148}$$

One of the major advantages of the cap model over other classical pressure-dependent plasticity models is the ability to control the amount of dilatency produced under shear loading. Dilatency is produced under shear loading as a result of the yield surface having a positive slope in $\sqrt{J_{2D}}$ - J_1 space, so the assumption of plastic flow in the direction normal to the yield surface produces a plastic strain rate vector that has a component in the volumetric (hydrostatic) direction (see Figure 8). In models such as the Drucker-Prager and Mohr-Coulomb, this dilatency continues as long as shear loads are applied, and in many cases produces far more dilatency than is experimentally observed in material tests. In the cap model, when the failure surface is active, dilatency is produced just as with the Drucker-Prager and Mohr-Coulomb models. However, the hardening law permits the cap surface to contract until the cap intersects the failure envelope at the stress point, and the cap remains at that point. The local normal to the yield surface is now vertical, and therefore the normality rule assures that no further plastic volumetric strain (dilatency) is created. Adjustment of the parameters that control the rate of cap contraction permits experimentally observed amounts of dilatency to be incorporated into the cap model, thus producing a constitutive law which better represents the physics to be modeled.

Another advantage of the cap model over other models such as the Drucker-Prager and Mohr-Coulomb is the ability to model plastic compaction. In these models all purely volumetric response is elastic. In the cap model, volumetric response is elastic until the stress point hits the cap surface. Thereafter, plastic volumetric strain (compaction) is generated at a rate controlled by the hardening law. Thus, in addition to controlling the amount of dilatency, the introduction of the cap surface adds another experimentally observed response characteristic of geological materials into the model.

The inclusion of kinematic hardening will result in hysteretic energy dissipation under cyclic loading conditions. Following the approach of (Isenberg, Vaughn, and Sandler, 1978), a nonlinear kinematic hardening law is used for the failure envelope surface when nonzero values of $\bar{c}$ and N are specified. In this case, the failure envelope surface is replaced by a family of yield surfaces bounded by an initial yield surface and a limiting failure envelope surface. Thus, the shape of the yield surfaces described above remains unchanged, but they may translate in a plane orthogonal to the J_1 axis.

Translation of the yield surfaces is permitted through the introduction of a "back stress" tensor, $\boldsymbol{\alpha}$. The formulation including kinematic hardening is obtained by replacing the stress $\boldsymbol{s}$ with the translated stress tensor $\boldsymbol{\eta} \equiv \boldsymbol{s} - \boldsymbol{\alpha}$ in all of the above equations. The history tensor $\boldsymbol{\alpha}$ is assumed deviatoric, and therefore has only 5 unique components. The evolution of the back stress tensor is governed by the nonlinear hardening law

$$\dot{\boldsymbol{\alpha}} = \bar{c}\bar{F}(\boldsymbol{s}, \boldsymbol{\alpha})\dot{\boldsymbol{e}}^p \quad , \tag{149}$$

where $\bar{c}$ is a constant, $\bar{F}$ is a scalar function of $\boldsymbol{s}$ and $\boldsymbol{\alpha}$, and $\dot{\boldsymbol{e}}^p$ is the rate of deviatoric plastic strain. The constant $\bar{c}$ may be estimated from the slope of the shear stress - plastic shear strain curve at low levels of shear stress.

The function $\bar{F}$ is defined as

$$\bar{F} \equiv max\left(0, 1 - \frac{(\boldsymbol{s} - \boldsymbol{\alpha}) \bullet \boldsymbol{\alpha}}{2NF_e(J_1)}\right) \quad , \tag{150}$$

where N is a constant defining the size of the yield surface. The value of N may be interpreted as the radial distance between the outside of the initial yield surface and the inside of the limit surface. In order for the limit surface of the kinematic hardening cap model to correspond with the failure envelope surface of the standard cap model, the scalar parameter α must be replaced with $\alpha - N$ in the definition of F_e.

Each of the material parameters K, G, R, and T may be functions of relative volume V/V_0. Load curves are used to describe the variation of each parameter with relative volume, and these curves must pass through the point (1.0,1.0). If a load curve number is specified as 0.0, that material parameter is held constant at its initial value throughout the analysis.

The cap model contains a number of parameters which must be chosen to represent a particular material, and are generally based on experimental data. The parameters α, β, θ, and γ are usually evaluated by fitting a curve through failure data taken from a set of triaxial compression tests. The parameters W, D, and X_0 define the cap hardening law. The value of W represents the void fraction of the uncompressed sample and D governs the slope of the initial loading curve in hydrostatic compression. The value of R is the ratio of major to minor axes of the quarter ellipse defining the cap surface. Additional details and guidelines for fitting the cap model to experimental data are found in Chen and Baladi (1985).

Material Type 16 (Ramberg-Osgood Elastoplasticity)

Columns		Quantity	Format
1-10	Card 3	Reference shear strain γ_y	E10.0
1-10	Card 4	Reference shear stress τ_y	E10.0
1-10	Card 5	Stress coefficient α	E10.0
1-10	Card 6	Stress exponent r	E10.0
1-10	Card 7	Bulk modulus K	E10.0
	Card 8	Blank	

The Ramberg-Osgood equation is an empirical constitutive relation to represent the one-dimensional elastic-plastic behavior of many materials. This implementation of the model was developed by Whirley and Engelmann (1991b), and allows a simple rate independent representation of the hysteretic energy dissipation observed in materials subjected to cyclic shear deformation. For monotonic loading, the stress-strain relationship is given by

$$\frac{\gamma}{\gamma_y} = \frac{\tau}{\tau_y} + \alpha\left|\frac{\tau}{\tau_y}\right|^r \quad \text{if } \gamma > 0\,, \tag{151}$$

$$\frac{\gamma}{\gamma_y} = \frac{\tau}{\tau_y} - \alpha\left|\frac{\tau}{\tau_y}\right|^r \quad \text{if } \gamma < 0\,, \tag{152}$$

where γ is the shear strain and τ is the shear stress. The model approaches perfect plasticity as the stress exponent $r \to \infty$. These equations must be augmented to correctly model unloading and reloading material behavior. The first load reversal is detected by $\gamma\dot{\gamma} < 0$. After the first reversal, the stress-strain relationship is modified to

$$\frac{\gamma - \gamma_0}{2\gamma_y} = \frac{\tau - \tau_0}{2\tau_y} + \alpha\left|\frac{\tau - \tau_0}{2\tau_y}\right|^r \quad \text{if } \gamma > 0\,, \tag{153}$$

$$\frac{\gamma - \gamma_0}{2\gamma_y} = \frac{\tau - \tau_0}{2\tau_y} - \alpha\left|\frac{\tau_0 - \tau}{2\tau_y}\right|^r \quad \text{if } \gamma < 0\,, \tag{154}$$

where γ_0 and τ_0 represent the values of strain and stress at the point of load reversal. Subsequent load reversals are detected by $(\gamma - \gamma_0)\dot{\gamma} < 0$.

The Ramberg-Osgood equations are inherently one-dimensional, and are assumed to apply to shear components. To generalize this theory to the multidimensional case, it is assumed that each component of the deviatoric stress and deviatoric tensorial strain is independently related by the one-dimensional stress-strain equations. The computed stress is projected onto the deviatoric stress space. The volumetric behavior is elastic, and therefore the pressure p is found by

$$p = -K\varepsilon^v, \tag{155}$$

where ε^v is the volumetric strain.

Material Type 17 (Thermal-Elastoplasticity with 8-Curves)

Columns		Quantity	Format
1-10	Card 3	Temperature T_1	E10.0
11-20		Temperature T_2	E10.0
.		.	.
.		.	.
.		.	.
71-80		Temperature T_8	E10.0
1-10	Card 4	Young's modulusE_1 at T_1	E10.0
11-20		Young's modulus E_2 at T_2	E10.0
.		.	.
.		.	.
.		.	.
71-80		Young's modulus E_8 at T_8	E10.0
1-10	Card 5	Poisson's ratioν_1 at T_1	E10.0
11-20		Poisson's ratio ν_2 at T_2	E10.0
.		.	.
.		.	.
.		.	.
71-80		Poisson's ratioν_8 at T_8	E10.0
1-10	Card 6	Secant coefficient of thermal expansion $\bar{\alpha}_1$ to T_1	E10.0
11-20		Secant coefficient of thermal expansion $\bar{\alpha}_2$ to T_2	E10.0
.		.	.
.		.	.
.		.	.
71-80		Secant coefficient of thermal expansion $\bar{\alpha}_8$ to T_8	E10.0
1-10	Card 7	Load curve number for yield stress σ_{y1} vs. effective plastic strain $\bar{\varepsilon}_1^p$ at T_1	E10.0

Columns		Quantity	Format
11-20		Load curve number for yield stress σ_{y2} vs. effective plastic strain $\bar{\varepsilon}_2^p$ at T_2	E10.0
.		.	.
.		.	.
.		.	.
71-80		Load curve number for yield stress σ_{y8} vs. effective plastic strain $\bar{\varepsilon}_8^p$ at T_8	E10.0
	Card 8	Blank	

This model is similar to material type 4, except that a nonlinear strain hardening law is used in place of linear hardening. Material parameters E and ν, as well as the nonlinear hardening law, are functions of temperature. Load curves are used to specify the nonlinear hardening law by defining yield stress σ_y vs. effective plastic strain $\bar{\varepsilon}_p$, for each temperature. The effective hardening law used for the stress update procedure is found by a suitable interpolation. Note that the first point on each $\sigma_y - \bar{\varepsilon}^p$ load curve must be $\bar{\varepsilon}^p = 0$.

Thermal expansion due to temperature change is included when nonzero values of $\bar{\alpha}$ are specified. The secant coefficient of thermal expansion $\bar{\alpha}$ can also be a function of temperature. Total thermal strain ε_{ij}^T is defined in terms of the secant coefficient α as

$$\varepsilon_{ij}^T = \bar{\alpha}(T - T_{ref})\delta_{ij} , \tag{156}$$

where T is the current temperature and T_{ref} is the material reference temperature. Therefore, temperature dependent, secant coefficients of thermal expansion $\bar{\alpha}$ should be defined as the value **to** that temperature, not the value **at** that temperature. The secant coefficient $\bar{\alpha}$ is related to the tangent coefficient of thermal expansion at a temperature T by

$$\bar{\alpha}(T) = \frac{1}{T - T_{ref}} \int_{T_{ref}}^{T} \alpha(T) dT . \tag{157}$$

For temperature **independent** coefficients of thermal expansion, $\bar{\alpha}$ is identical to $\bar{\alpha}$, and the classical definition of thermal expansion is valid.

At least two temperatures, and their corresponding material parameters and load curve numbers, must be specified. The analysis will be terminated if a material temperature falls outside the defined range.

Material Type 18 (Thermal-Elastoplastic Quench)

Columns		Quantity	Format
1-10	Card 3	Bulk modulus K	E10.0
11-20		Load curve option flag, LFLAG EQ.0.0: for each phase, identical temperature points are used for each material parameter load curve EQ.1.0: temperature points across load curves are different.	
21-30		Load curve number defining the fraction of phase 1 vs. temperature, LPHS1. EQ.0.0: only one phase. Fraction of phase 1 is 1.0	
31-40		Load curve number defining the fraction of phase 2 vs. temperature, LPHS2. EQ.0.0: only one or two phases.	
1-10	Card 4	Load curve number for Young's modulus E in phase 1	E10.0
11-20		Load curve number for Poisson's ratio ν in phase 1	E10.0
21-30		Load curve number for secant coefficient of thermal expansion $\bar{\alpha}$ in phase 1	E10.0
31-40		Load curve number for yield stress σ_0 in phase 1	E10.0
41-50		Load curve number for hardening modulus E_p in phase 1	E10.0
1-10	Card 5	Load curve number for Young's modulus E in phase 2	E10.0
11-20		Load curve number for Poisson's ratio ν in phase 2	E10.0
21-30		Load curve number for secant coefficient of thermal expansion $\bar{\alpha}$ in phase 2	E10.0
31-40		Load curve number for yield stress σ_0 in phase 2	E10.0
41-50		Load curve number for hardening modulus E_p in phase 2	E10.0
1-10	Card 6	Load curve number for Young's modulus E in phase 3	E10.0
11-20		Load curve number for Poisson's ratio ν in phase 3	E10.0
21-30		Load curve number for secant coefficient of thermal expansion $\bar{\alpha}$ in phase 3	E10.0
31-40		Load curve number for yield stress σ_0 in phase 3	E10.0
41-50		Load curve number for hardening modulus E_p in phase 3	E10.0

Columns	Quantity	Format
Card 7	Blank	
Card 8	Blank	

This model is similar to material type 4, except that it allows properties to be defined for up to three different phases. The number of phases and the fractional amounts of each phase are determined from load curves LPHS1 and LPHS2, and the current temperature T as follows:

- For a three phase material, load curve LPHS1 defines the fraction of phase one vs. temperature and load curve LPHS2 defines the fraction of phase two vs. temperature. The fraction of phase three, at any temperature, is 1.0 minus the sum of the fractions of phase one and phase two, at that temperature.
- For a two phase material, load curve LPHS1 defines the fraction of phase 1 vs. temperature and LPHS2 should be set to zero. The fraction of phase two is 1.0 minus the fraction of phase one.
- For a one phase material, LPHS1 and LPHS2 should be set to zero. The fraction of phase one is 1.0.

Material parameter load curves specify the material parameters E, ν, σ_0, and E_p as a function of temperature, for each phase. For the stress update and thermal expansion computation, material properties are first determined for each phase at the current temperature. Properties are then averaged according to the fractional amounts of each phase. The bulk modulus K is only a characteristic modulus and is not used for the stress update calculation.

Thermal expansion due to temperature change is included when nonzero values of $\bar{\alpha}$ are specified for any active phase. The "phase weighted" average of the temperature dependent secant coefficients of thermal expansion $\bar{\alpha}$ may be denoted $\bar{\alpha}$. Total thermal strain ε_{ij}^{T} is then defined in terms of the averaged secant coefficient $\bar{\alpha}_{\mathrm{A}}$ as

$$\varepsilon_{ij}^{T} = \bar{\alpha}_{A}(T - T_{ref})\delta_{ij} , \tag{158}$$

where T is the current temperature and T_{ref} is the material reference temperature. Therefore temperature dependent secant coefficients of thermal expansion $\bar{\alpha}$ should be defined as the value **to** that temperature, not the value **at** that temperature.

Material parameter load curve numbers must be specified for each material parameter of each of the phases considered. Each load curve must contain at least two temperatures and their corresponding material parameter values. The analysis will be terminated if a material temperature falls outside the defined range.

Material Type 19 (Strain Rate Sensitive Power Law Plasticity)

Columns		Quantity	Format
1-10	Card 3	Young's modulus E	E10.0
11-20		Poisson's ratio ν	E10.0
21-30		Strength coefficient k. If $k < 0$, the absolute value of k is the number of the load curve defining k as a function of effective plastic strain $\bar{\varepsilon}^p$	E10.0
31-40		Hardening exponent n. If $n < 0$, the absolute value of n is the number of the load curve defining n as a function of effective plastic strain $\bar{\varepsilon}^p$	E10.0
41-50		Strain rate sensitivity exponent m. If $m < 0$, the absolute value of m is the number of the load curve defining m as a function of effective plastic strain $\bar{\varepsilon}^p$	E10.0
51-60		Initial strain rate (.0002)	E10.0
	Card 4	Blank	
.		.	.
.		.	.
.		.	.
	Card 8	Blank	

This model differs from material type 10 in that the hardening law is strain rate sensitive, and the hardening parameters may be a function of effective plastic strain. The material behavior is elasto-plastic with isotropic hardening. The nonlinear hardening law is given by

$$\sigma_y = k\dot{\varepsilon}^m(\varepsilon_0 + \bar{\varepsilon}^p) \ , \tag{159}$$

where $\dot{\varepsilon}$ is the effective strain rate and ε_0 is the initial yield strain given by

$$\varepsilon_0 = \left(\frac{E}{k\dot{\varepsilon}^m}\right)^{\frac{1}{n-1}} \ . \tag{160}$$

Absence of strain hardening can be modeled by setting the hardening exponent to a very small positive value, i.e. 0.0001.

Material Type 20 (Power Law Thermoplasticity with Failure)

Columns		Quantity	Format
1-10	Card 3	Temperature T_1	E10.0
11-20		Temperature T_2	E10.0
.		.	.
.		.	.
.		.	.
71-80		Temperature T_8	E10.0
1-10	Card 4	Young's modulus E_1 at T_1	E10.0
11-20		Young's modulus E_2 at T_2	E10.0
.		.	.
.		.	.
.		.	.
71-80		Young's modulus E_8 at T_8	E10.0
1-10	Card 5	Poisson's ratio ν_1 at T_1	E10.0
11-20		Poisson's ratio ν_2 at T_2	E10.0
.		.	.
.		.	.
.		.	.
71-80		Poisson's ratio ν_8 at T_8	E10.0
1-10	Card 6	Coefficient of thermal expansion α_1 at T_1	E10.0
11-20		Coefficient of thermal expansion α_2 at T_2	E10.0
.		.	.
.		.	.
.		.	.
71-80		Coefficient of thermal expansion α_8 at T_8	E10.0

Columns		Quantity	Format
1-10	Card 7	Strength coefficient k_1 at T_1	E10.0
11-20		Strength coefficient k_2 at T_2	E10.0
.		.	.
.		.	.
.		.	.
71-80		Strength coefficient k_8 at T_8	E10.0
1-10	Card 8	Hardening exponent n_1 at T_1	E10.0
11-20		Hardening exponent n_2 at T_2	E10.0
.		.	.
.		.	.
.		.	.
71-80		Hardening exponent n_8 at T_8	E10.0
1-10	Card 9	Strength to failure from tensile test σ_{tf1} at T_1	E10.0
11-20		Strength to failure from tensile test σ_{tf2} at T_2	E10.0
.		.	.
.		.	.
.		.	.
71-80		Strength to failure from tensile test σ_{tf8} at T_8	E10.0
1-10	Card 10	Strength to failure from shear test σ_{sf1} at T_1	E10.0
11-20		Strength to failure from shear test σ_{sf2} at T_2	E10.0
.		.	.
.		.	.
.		.	.
71-80		Strength to failure from shear test σ_{sf8} at T_8	E10.0
1-10	Card 11	Failure option flag, IFAIL LE.1.0: Mohr-Coulomb EQ.2.0: Drucker-Prager EQ.3.0: both Mohr Coulomb and Drucker Prager	

This model is identical to material type 12, except that simulation of material failure is included. Prior to failure, the material behavior is elastoplastic with isotropic power law hardening. Material parameters E, ν, k, and n can all be functions of temperature. Thermal expansion due to temperature change is included when nonzero values of α are specified. The coefficient of thermal expansion α can also be a function of temperature and, for this model, represents a tangent value. Thermal strain rate $\dot{\varepsilon}_{ij}^{T}$ is defined in terms of the tangent coefficient of thermal expansion α as

$$\dot{\varepsilon}_{ij}^{T} = \alpha(T)\dot{T}\delta_{ij} , \tag{161}$$

where T is the current temperature.

Failure is initiated when material state variables exceed the specified criterion. When failure is reached at all Gauss points in an element, the strength of the element is reduced to nearly zero, and that element is deleted from the plot database. The specified tensile and shear strengths at failure may be functions of temperature. In this case, effective values for σ_{tf} and σ_{sf} are found for the current temperature by interpolation. Several failure options are available and are defined as follows:

- If IFAIL = 1.0, the Mohr-Coulomb failure criterion is invoked. Failure is initiated when stress values exceed the Mohr-Coulomb criterion

  $$\sigma_{sf} = m\sigma_{tf} + b . \tag{162}$$

  The slope m and intercept b are determined from interpolated tensile and shear test values σ_{tf} and σ_{sf} by

  $$m = \frac{\frac{1}{2}\sigma_{tf} - \sigma_{sf}}{\sqrt{\sigma_{tf}\sigma_{sf} - \sigma_{sf}^2}} , \tag{163}$$

  $$b = \frac{\sigma_{tf}\sigma_{sf}}{2\sqrt{\sigma_{tf}\sigma_{sf} - \sigma_{sf}^2}} = m\frac{\sigma_{tf}\sigma_{sf}}{\sigma_{tf} - 2\sigma_{sf}} . \tag{164}$$

  The values of σ_{tf} and σ_{sf} are restricted to

  $$\sigma_{sf} > 0 , \tag{165}$$

  $$\sigma_{tf} > \sigma_{sf} . \tag{166}$$

and therefore specified values at each temperature are also restricted.

- If IFAIL = 2.0, the Drucker-Prager failure criterion is invoked. The Drucker-Prager surface is constructed from tensile and shear strengths at failure σ_{tf} and σ_{sf}.
- If IFAIL = 3.0, both the Mohr-Coulomb and Drucker-Prager failure criteria are invoked.

If all material parameters (including failure parameters), are temperature independent, one set of parameters may be defined with T_1 set to zero. This case commonly occurs when thermal expansion is the only temperature effect of interest. In all other cases, at least two temperatures and their corresponding material and failure parameters must be specified. The analysis will be terminated if a material temperature falls outside the defined range. A purely thermoelastic material with failure simulation is obtained by leaving cards 7 and 8 blank.

Material Type 21 (Nonlinear Elastoplasticity)

Columns		Quantity	Format
1-10	Card 3	Constant bulk modulus K_0	E10.0
11-20		Bulk modulus coefficient K_1	E10.0
21-30		Constant shear modulus G_0	E10.0
31-40		Shear modulus coefficient G_1	E10.0
41-50		Constant yield stress Y_0	E10.0
51-60		Yield stress coefficient Y_1	E10.0
61-70		Minimum pressure p_c, $(p_c < 0)$	E10.0
	Card 4	Blank	
.		.	.
.		.	.
.		.	.
	Card 8	Blank	

This model incorporates a pressure-volume relationship of the form

$$p = \frac{K_0}{K_1}\left[\left(\frac{V_0}{V}\right)^{K_1} - 1\right] \tag{167}$$

for hydrostatic compression ($p > 0$), and

$$p = K_0 ln\left(\frac{V_0}{V}\right) \tag{168}$$

for hydrostatic tension ($p \geq 0$). Equivalently, the volumetric response may be written as

$$p = -K\varepsilon^v, \tag{169}$$

where the effective bulk modulus K is

$$K = K_0 + K_1 p \tag{170}$$

for hydrostatic compression and

$$K = K_0, \tag{171}$$

for hydrostatic tension. A minimum pressure p_c, $(p_c < 0)$ may be specified. If the drops below this cutoff value, it is reset to the cutoff value.

The deviatoric response is elastic, perfectly plastic. The effective shear modulus G and yield stress σ_y are defined as

$$G = G_0 + G_1 p, \tag{172}$$

$$\sigma_y = Y_0 + Y_1 p, \tag{173}$$

for hydrostatic compression and

$$G = G_0, \tag{174}$$

$$\sigma_y = Y_0, \tag{175}$$

for hydrostatic tension.

Material Type 22 (Polynomial Hyperelastic Rubber)

Columns		Quantity	Format
1-10	Card 3	Strain energy density coefficient C_{001}	E10.0
11-20		Strain energy density coefficient C_{010}	E10.0
21-30		Strain energy density coefficient C_{020}	E10.0
31-40		Strain energy density coefficient C_{100}	E10.0
41-50		Strain energy density coefficient C_{101}	E10.0
1-10	Card 4	Strain energy density coefficient C_{110}	E10.0
11-20		Strain energy density coefficient C_{200}	E10.0
21-30		Strain energy density coefficient C_{210}	E10.0
31-40		Strain energy density coefficient C_{300}	E10.0
41-50		Strain energy density coefficient C_{400}	E10.0
	Card 5	Blank	
	Card 6	Blank	
	Card 7	Blank	
	Card 8	Blank	

The implementation of this model was developed by Kenchington (1988), and is defined in a total Lagrangian context. The strain energy density function W is a polynomial form of Green-Lagrange strain E_{ij}. It is defined as

$$W = C_{100}I_1 + C_{200}I_1^2 + C_{300}I_1^3 + C_{400}I_1^4 + C_{010}I_2 + C_{020}I_2^2 + C_{110}I_1I_2 + C_{210}I_1^2I_2 + C_{001}I_3 + C_{101}I_1 \quad (176)$$

where I_1, I_2, and I_3 are the first, second, and third principal invariants of the Green-Lagrange strain tensor E_{ij}. The second Piola-Kirchhoff stress S_{ij} is found by differentiating the strain energy density W with respect to E_{ij},

$$S_{ij} = \frac{\partial W}{\partial E_{ij}}. \quad (177)$$

The Cauchy stress τ_{ij} is determined from the second Piola-Kirchhoff stress S_{ij} by

$$\tau_{ij} = \frac{1}{V_r} F_{ik} F_{jl} S_{kl}, \tag{178}$$

where V_r is the relative volume and F_{ij} is the deformation gradient.

Material Type 23 (Primary, Secondary, Tertiary Creep)

Columns		Quantity	Format
1-10	Card 3	Young's modulus E	E10.0
1-10	Card 4	Poisson's ratio ν	E10.0
	Card 5	Stress coefficient A	E10.0
	Card 6	Stress exponent n	E10.0
	Card 7	Time exponent m	E10.0
	Card 8	Blank	

The implementation of this model was developed by Whirley and Henshall (1990). The effective creep strain ε^c is defined as

$$\varepsilon^c = A\sigma^n \bar{t}^m, \tag{179}$$

where $\bar{t}$ is the effective time, and the effective stress σ is defined as

$$\sigma = \sqrt{\frac{3}{2}\sigma_{ij}\sigma_{ij}}\ . \tag{180}$$

The effective creep strain evolves in the direction of current deviatoric stress and the volumetric behavior is assumed elastic. By varying the value of the time exponent m, the three classical creep regimes may be simulated:

- $m < 1$ Primary creep
- $m = 1$ Secondary (steady-state) creep
- $m > 1$ Tertiary creep

Material Type 24 (Deformation Mechanism)

Columns		Quantity	Format
1-10	Card 3	Temperature T_1	E10.0
11-20		Temperature T_2	E10.0
.		.	.
.		.	.
.		.	.
71-80		Temperature T_8	E10.0
1-10	Card 4	Young's modulusE_1 at T_1	E10.0
11-20		Young's modulus E_2 at T_2	E10.0
.		.	.
.		.	.
.		.	.
71-80		Young's modulus E_8 at T_8	E10.0
1-10	Card 5	Poisson's ratioν_1 at T_1	E10.0
11-20		Poisson's ratio ν_2 at T_2	E10.0
.		.	.
.		.	.
.		.	.
71-80		Poisson's ratioν_8 at T_8	E10.0
1-10	Card 6	Secant coefficient of thermal expansion $\bar{\alpha}_1$ to T_1	E10.0
11-20		Secant coefficient of thermal expansion $\bar{\alpha}_2$ to T_2	E10.0
.		.	.
.		.	.
.		.	.
71-80		Secant coefficient of thermal expansion $\bar{\alpha}_8$ at T_8	E10.0
1-10	Card 7	Deformation mechanism ID number, DMID EQ.1: obstacle controlled plasticity EQ.2: power law creep EQ.3: power law breakdown EQ.4: diffusional flow	E10.0

Columns		Quantity	Format
1-10	Card 8	Plot database flag, IPLOT EQ.0.0: Effective plastic strain $\bar{\varepsilon}^p$ EQ.1.0: Thermal Strain ε^T EQ.2.0: Effective plastic strain rate $\dot{\bar{\varepsilon}}^p$ EQ.1.0: Strength S EQ.2.0: Grain size d	E10.0
11-20		Constitutive convergence tolerance	E10.0
21-30		Maximum number of constitutive iterations	E10.0
1-5	Card 9	Number of kinetic equation temperatures, NKET	I5
6-10		Number of strength parameter temperatures, NSPT	I5
11-15		Number of grain size temperatures, NGST	I5

For obstacle controlled plasticity, DMID = 1, define kinetic equation cards 10,...,9+NKET.

Columns	Quantity	Format
1-10	Temperature T	E10.0
11-20	Stress coefficient A	E10.0
21-30	Strain rate sensitivity m	E10.0
31-40	Stress constant τ	E10.0
41-50	Stress exponent p	E10.0
51-60	Stress factor exponent q	E10.0
61-70	Normalized activation energy $\tilde{Q} = Q/R$	E10.0

For power law creep, DMID = 2, define kinetic equation cards 10,...,9+NKET.

Columns	Quantity	Format
1-10	Temperature T	E10.0
11-20	Temperature coefficient T_0	E10.0
21-30	Stress coefficient A	E10.0
31-40	Strain rate sensitivity m	E10.0
41-50	Normalized activation energy $\tilde{Q} = Q/R$	E10.0

For power law breakdown, DMID = 3, define kinetic equation cards 10,...,9+NKET.

Columns	Quantity	Format
1-10	Temperature T	E10.0
11-20	Temperature coefficient T_0	E10.0
21-30	Stress coefficient A	E10.0
31-40	Strain rate sensitivity n'	E10.0
41-50	Normalized activation energy $\tilde{Q} = Q/R$	E10.0

For diffusional flow, DMID = 4, define kinetic equation cards 10,...,9+NKET.

Columns	Quantity	Format
1-10	Temperature T	E10.0
21-30	Stress coefficient A	E10.0
31-40	Strain rate sensitivity m	E10.0
41-50	Normalized activation energy $\tilde{Q} = Q/R$	E10.0

Define strength parameter cards 10+NKET,...,9+NKET+NSPT.

Columns	Quantity	Format
1-10	Temperature T	E10.0
11-20	Initial strength S_0	E10.0
21-30	1st strain hardening coefficient k_1	E10.0
31-40	1st strain hardening exponent n_1	E10.0
41-50	2nd strain hardening coefficient k_2	E10.0
51-60	2nd strain hardening exponent n_2	E10.0
61-70	Strength exponent n_3	E10.0

For diffusional flow, DMID = 4, define grain size cards 10+NKET+NSPT,... ,9+NKET+NSPT +NGST.

Columns	Quantity	Format
1-10	Temperature T	E10.0
11-20	Initial grain size d_0	E10.0
21-30	Grain size parameter b	E10.0
31-40	Grain size exponent r	E10.0
41-50	Grain size growth coefficient c	E10.0
51-60	Grain size growth exponent s	E10.0
61-70	Normalized activation energy $\tilde{F} = F/R$	E10.0

This deformation mechanism model predicts plastic strain rate and temperature dependent plasticity with isotropic hardening and grain size effects. The implementation of this model was developed by Raboin (1990). Four kinetic equations are available to predict the rate of plastic straining: obstacle controlled plasticity, power law creep, power law breakdown, and diffusional flow. A strength parameter S describes the isotropic hardening, and for diffusional flow, a grain size parameter d models grain size effects.

Data for this material model is grouped into 4 sets. Elastic and thermal expansion properties are in the first set. Then, data for the kinetic equation, the strength evolution equation and the grain size evolution equation comprise the second, third and fourth data sets. The fourth set is needed for diffusional flow only.

In the first set of data, the Young's modulus E, Poisson's ratio ν, and secant coefficient of thermal expansion $\bar{\alpha}$ are defined for up to 8 temperatures. Thermal expansion due to temperature change is included when nonzero values of $\bar{\alpha}$ are specified. The secant coefficient of thermal expansion $\bar{\alpha}$ can also be a function of temperature. Total thermal strain ε_{ij}^{T} is defined in terms of the secant coefficient $\bar{\alpha}$ as

$$\varepsilon_{ij}^{T} = \bar{\alpha}(T - T_{ref})\delta_{ij} , \tag{181}$$

where T is the current temperature and T_{ref} is the material reference temperature. Therefore, temperature dependent, secant coefficients of thermal expansion $\bar{\alpha}$ should be defined as the value **to** that temperature, not the value **at** that temperature. The secant coefficient $\bar{\alpha}$ is related to the tangent coefficient of thermal expansion α at a temperature T by

$$\bar{\alpha}(T) = \frac{1}{T - T_{ref}} \int_{T_{ref}}^{T} \alpha(T) dT . \tag{182}$$

For temperature **independent** coefficients of thermal expansion, $\bar{\alpha}$ is identical to α, and the classical definition of thermal expansion is valid.

For the kinetic equations, the state variables are effective stress σ and temperature T. The history variables are the strength parameter S and grain size d. The shear modulus G is defined as $G = E/(2(1+\nu))$. The four kinetic equations are defined below.

- Obstacle controlled plasticity (DMID = 1)

$$\dot{\bar{\varepsilon}}^{p} = \left(\frac{A\sigma}{SG}\right)^{\frac{1}{m}} exp\left\{-\frac{\tilde{Q}}{T}\left[1 - \left(\frac{\sigma}{\tau}\right)^{p}\right]^{q}\right\} , \tag{183}$$

- Power-law creep (DMID = 2)

$$\dot{\bar{\varepsilon}}^{p} = \frac{T_0}{T}\left(\frac{A\sigma}{SG}\right)^{\frac{1}{m}} exp\left(-\frac{\tilde{Q}}{T}\right) , \tag{184}$$

- Power-law breakdown (DMID = 3)

$$\dot{\bar{\varepsilon}}^p = \frac{T_0}{T}\left[\sinh\left(\frac{A\sigma}{SG}\right)\right]^{n'} exp\left(-\frac{\tilde{Q}}{T}\right) \quad , \tag{185}$$

- Diffusional flow (DMID = 4)

$$\dot{\bar{\varepsilon}}^p = \left(\frac{A\sigma}{SG}\right)^{\frac{1}{m}}\left(\frac{b}{d}\right)^r exp\left(-\frac{\tilde{Q}}{T}\right) \quad . \tag{186}$$

By specifying the type of deformation-mechanism (DMID), the appropriate kinetic equation is used to predict the rate of plastic deformation.

The evolution of the strength parameter S depends on the rate of plastic straining, the current strength, and the temperature,

$$\dot{S} = k_1(\dot{\bar{\varepsilon}}^p)^{n_1} + k_2(\dot{\bar{\varepsilon}}^p)^{n_2} S^{n_3} \; . \tag{187}$$

Setting S constant results in linear hardening. By using both terms in the S evolution equation, dynamic recovery effects can be modeled.

A static grain growth equation describes the evolution of the grain size d,

$$\dot{d} = cd^s exp\left(-\frac{\tilde{F}}{T}\right) \; . \tag{188}$$

Grain growth depends on the current grain size, and temperature. Grain size effects are included in the diffusional flow kinetic equation only.

An extended data base format is used for the kinetic equation, strength parameter and grain size data sets. It is different in two ways from the other temperature dependent material arrays used in NIKE2D. First, any number of temperature data points can be defined. Secondly, not all of the material properties have to be specified for each input temperature. Undefined material properties are interpolated when the temperature of the desired material property is within the temperature range of defined values. Outside a defined temperature range, the value of the material property closest to a defined temperature is used.

Material Type 25 (Gurson-Tvergaard Void Growth Plasticity)

Columns		Quantity	Format
1-10	Card 3	Young's modulus E	E10.0
1-10	Card 4	Poisson's ratio ν	E10.0
1-10	Card 5	Yield stress σ_0	E10.0
1-10	Card 6	Hardening modulus E_p	E10.0
1-10	Card 7	First Gurson parameter q_1	E10.0
		Second Gurson parameter q_2	E10.0
		Initial void fraction f_0	E10.0
	Card 8	Blank	

The material behavior is elastoplastic with modifications to include void growth under hydrostatic tension. The development and implementation of this model is discussed in Whirley and Engelmann (1991), and is based on a unification of the Gurson and Tvergaard formulations described in Hom and McMeeking (1989). Studies have shown that ductile fracture in metals may be proceeded by the generation of considerable porosity, and thus the presence of voids lead to yield behavior dependent on the hydrostatic component of stress. The observed behavior is usually attributed to void growth, and the matrix material is believed essentially incompressible. The Gurson and Tvergaard theories macroscopically model the void growth phenomenon, and may be useful for problems with regions of large hydrostatic tensile stresses, such as at the base of notches and in the constrained tensile loading of bars and plates.

The Gurson and Tvergaard yield surfaces are members of the family defined by the function

$$\phi = \frac{\sigma^2}{\sigma_y^2} + 2 f q_1 \cosh\left(\frac{\sigma_{kk}}{2\sigma_y}\right) - (1 + q_2 f^2) \ , \tag{189}$$

where $q_1 = q_2 = 1.0$ for the Gurson model, and $q_1 = 1.5$ and $q_2 = q_1^2$ for the Tvergaard model. The von Mises yield surface of material type 3 may be recovered by setting $q_1 = q_2 = 0$. The effective stress σ is defined as the norm of the deviatoric stress tensor s_{ij},

$$\sigma = \left(\frac{3}{2} s_{ij} s_{ij}\right)^{\frac{1}{2}} \ . \tag{190}$$

Linear isotropic hardening is assumed so the current yield stress σ_y is given by

$$\sigma_y = \sigma_0 + E_p \bar{\varepsilon}^p , \tag{191}$$

where $\bar{\varepsilon}^p$ is the effective plastic strain. Associated flow is considered, and therefore the rate of plastic strain is in the direction normal to the yield surface,

$$\dot{\varepsilon}_{ij}^p = \dot{\lambda} \frac{\partial \phi}{\partial \sigma_{ij}} . \tag{192}$$

The evolution of the void fraction f is given by

$$\dot{f} = (1 - f)\varepsilon_{kk}. \tag{193}$$

Typical initial void fractions are in the range of $0.001 \le f_0 \le 0.1$.

Material Type 26 (Mooney-Rivlin Rubber)

Columns		Quantity	Format
1-10	Card 3	Strain energy density coefficient a	E10.0
1-10	Card 4	Strain energy density coefficient b	E10.0
1-10	Card 5	Poisson's ratio ν	E10.0
	Card 6	Blank	
	Card 7	Blank	
	Card 8	Blank	

The development and implementation of this slightly compressible, Mooney Rivlin hyperelastic model is disused in Whirley, Engelmann, and Maker (1990). This model is useful for describing the mechanical behavior of natural rubber and is defined in a total Lagrangian context. The strain energy density function is given by

$$W = a(I_1 - 3) + b(I_2 - 3) + c(I_3^{-2} - 1) + d(I_3 - 1)^2 \quad , \tag{194}$$

where

$$I_1 = C_{kk}, \tag{195}$$

$$I_2 = \frac{1}{2}[C_{ii}C_{jj} - C_{ij}C_{ij}] , \tag{196}$$

$$I_3 = V_r^2, \tag{197}$$

V_r is the relative volume (or equivalently $V_r = J = det(F_{ij})$ is the Jacobian of the deformation), F_{ij} is the deformation gradient, $C_{ij} = F_{ki}F_{kj}$ is the right Cauchy-Green tensor, and a, b, c, d are material constants. The second Piola-Kirchhoff stress S_{ij} is found by differentiating the strain energy density function with respect to the Green-Lagrange strain,

$$E_{ij} = \frac{1}{2}(C_{ij} - \delta_{ij}) \ . \tag{198}$$

Thus

$$S_{ij} = 2a\delta_{ij} + 2b(\delta_{ij}C_{kk} - C_{ij}) + 4[cI_{\bar{3}}^{-2} + d(I_{\bar{3}}^{2} - I_3)]C_{ij}^{-1} \tag{199}$$

The Cauchy stress τ_{ij} is related to the second Piola-Kirchhoff stress by

$$\tau_{ij} = \frac{1}{V_r}F_{ik}F_{jl}S_{kl}. \tag{200}$$

The material constants c and d are defined in terms of material parameters a, b, and Poisson's ratio ν by

$$c = \frac{a}{2} + b, \tag{201}$$

$$d = \frac{a(5\nu - 2) + b(11\nu - 5)}{2(1 - 2\nu)} \quad . \tag{202}$$

Poisson's ratio should be chosen such that $0.48 \le \nu < 0.5$.

4.4 NODES

Define a card for each node.

Cards 1,2,...,NUMNP

Columns	Quantity	Format
1-5	Node number, n^i	I5
6-10	Boundary condition code, BCC^i [NBC, NBCS] EQ.0.0: no constraint EQ.1.0: r-constraint EQ.2.0: z-constraint EQ.3.0: r- and z-constraints If BCC^i is not any of the above, it is assumed to be the angle in degrees between the positive r-axis and the direction of the motion along a sliding boundary (Figure 9)	F5.0
11-20	r^i-coordinate	E10.0
21-30	z^i-coordinate	E10.0
31-35	Generation interval KN EQ.0: default set to 1	I5
36-45	Nodal reference temperature if ITREF = 1 or TEO = -3	E10.0

Node cards do not need to be in order. However, the first card must contain the first node, and the last card must contain the highest node number. Cards containing intermediate node numbers may be omitted (in this case, fewer than NUMNP nodes are specified) and their data is internally generated as follows. Node numbers are generated according to the sequence

$$n^i,\ n^i + \mathrm{KN},\ n^i + 2\mathrm{KN},\ldots,\ n^j \tag{203}$$

where n^i and n^j are the nodal numbers defined on the two consecutive cards, and KN is taken from the first consecutive card. Linear interpolation is used to obtain the coordinate of the generated nodes and the nodal temperatures. The boundary condition code of generated data is set to zero whenever $BCC^i \neq BCC^j$; otherwise, it is assumed to be the same. Unconstrained nodes can be generated between constrained nodes that have the same boundary condition by making the code on the second card (node n^j) negative. After the data is generated the code is reset.

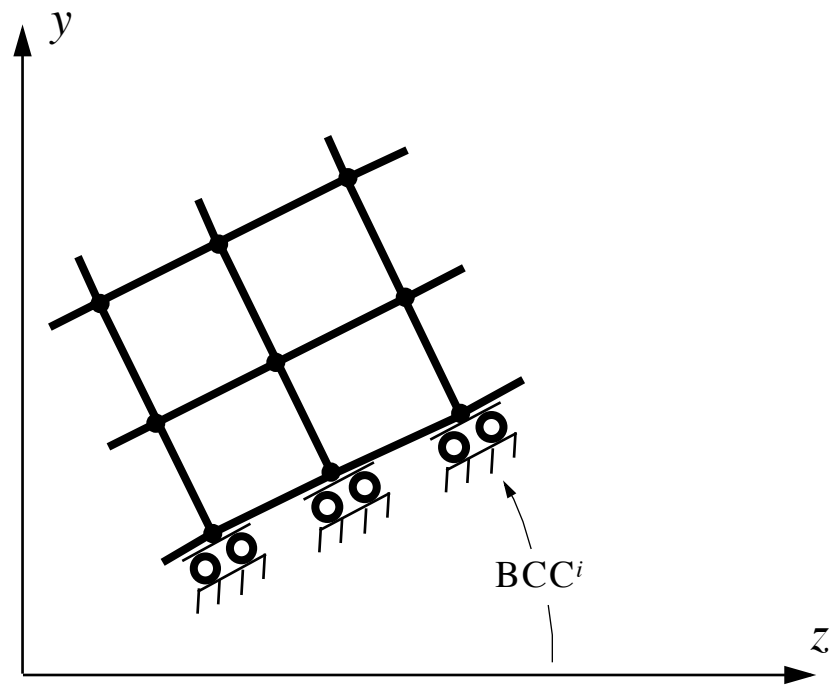

Figure 9
Roller boundary condition that is obtained if BCC^i is not equal to 0, 1, 2, or 3.

4.5 ELEMENTS

Define a card for each element.

Cards 1,2,...,NUMEL

Columns	Quantity	Format
1-5	Element number	I5
6-10	Node n_1	I5
11-15	Node n_2	I5
16-20	Node n_3	I5
21-25	Node n_4	I5
26-30	Material number EQ.0: element is deleted	I5
31-35	Generation increment, KN	I5
36-45	Material dependent parameter: Angle ψ in radians for orthotropic materials (default = 0.0), and initial relative volume for material models 5, 14 and 22 (default = 1.0)	E10.0
46-55	Element birth time	E10.0
56-65	Element death time (the time removal begins) EQ.0.0: default set to 1.e20	E10.0
66-75	Element burial time (the time removal is complete) EQ.0.0: default set to 1.e20	E10.0

Element cards must be in order. The first set of cards must contain data for the first element and the last set of cards must contain the data for the highest element number. Cards containing intermediate element data may be omitted (in this case, fewer than NUMEL sets of cards are specified), and these elements will be generated internally. Connecting node numbers n_j are generated with respect to the first card prior to omitted data by

$$n_j^{i+1} = n_j^i + \mathrm{KN} \tag{204}$$

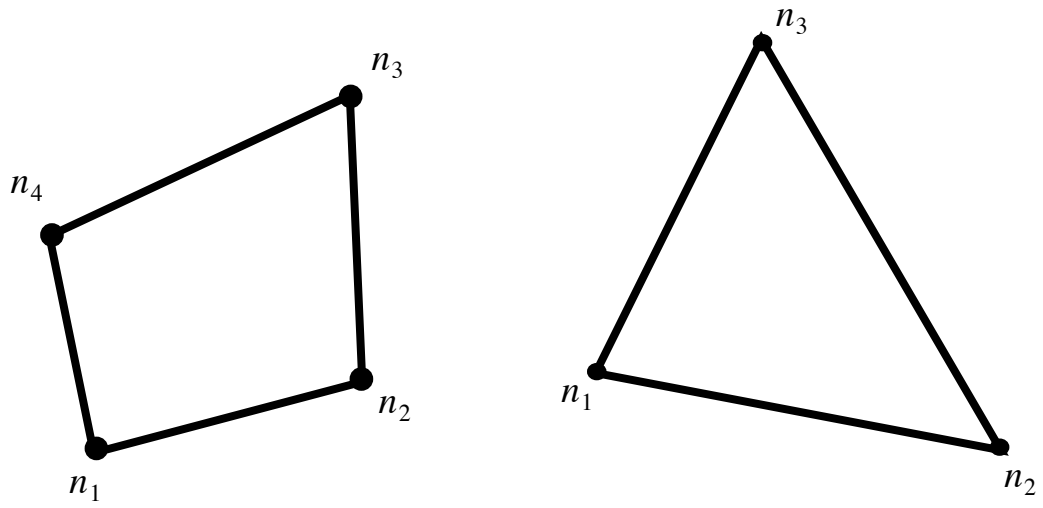

Figure 10
Two-dimensional plane strain, plane stress, and axisymmetric elements available in NIKE2D.

Element attributes, such as material number, are taken from this first card. The convention for numbering nodes is shown in Figure 10, where n_1, n_2, n_3, and n_4 are global node numbers. Triangular elements are defined by replacing n_4 by n_3. Element stress and history data is computed and printed at Gauss integration points.

4.6 SLIDELINE CONTROL

Skip this section if NSL = 0. Otherwise, define a control card for each slideline.

Cards 1,2,...,NSL

Columns	Quantity	Format
1-5	Number of slave nodes in slideline, NSN	I5
6-10	Number of master nodes in slideline, NMN	I5
11-15	Slideline type number, ISLT EQ.1: sliding only EQ.2: tied EQ.3: sliding with separation EQ.4: sliding with separation and interface friction EQ.5: sliding with separation and tie break EQ.6: single surface contact EQ.7: eroding pressure contact with separation EQ.8: merge/release and sliding with separation	I5
16-25	Penalty Function Scale Factor EQ.0.0: default set to 1.0	E10.0
26-30	Lagrange augmentation flag EQ.0: none EQ.1: augmentations (convergence based on penalty) EQ.2: augmentations (convergence based on gap)	I5
31-40	Augmentation tolerance (normal direction)	E10.0
41-50	Augmentation tolerance (tangential direction)	E10.0
51-55	Small penetration flag EQ.0: all penetrations considered EQ.1: only small penetrations considered	I5

4.7 SLIDELINE DEFINITIONS

Skip this section if NSL = 0. Otherwise, define the following set of cards for each slideline.

Card 1

Columns	Quantity	Format
1-10	Friction coefficient EQ.0.0: if ISLT.LT.4 GT.0.0: if ISLT.EQ.4	E10.0
11-20	Plastic strain to fail tiebreak if ISLT = 5 or Erosion pressure if ISLT = **7** Merge/release load curve number if ISLT = **8**	E10.0
21-26	Slave surface description flag EQ.0: as is EQ.1: smoothed	I5
26-30	Master surface description flag EQ.0: as is EQ.1: smoothed	I5
31-35	Interface penetration flag if ISLT **= 3, 4** EQ.0: none EQ.#: Interference load curve number	I5

Cards 2,3,...,NSN+1

Columns	Quantity	Format
1-5	Slave number EQ.0: the preceding slave number is incremented by one	I5
6-10	Node number	I5
11-20	Plastic strain to fail tiebreak. If zero, the value on Card 1 is used (ISLT = 5 only)	E10.0

Omitted data is automatically generated by incrementing the nodal point numbers by

$$(n_i - n_j) / (sn_i - sn_j) \tag{205}$$

where sn_i, sn_j are the slave numbers on two successive cards and n_i and n_j are their corresponding node numbers.

Omit the following cards if ISLT = 6. A master surface is not defined for single surface contact.

Cards NSN+2,...,NSN+NMN+1

Columns	Quantity	Format
1-5	Master number EQ.0: the preceding master number is incremented by one	I5
6-10	Node number	I5
11-20	Plastic strain to fail tiebreak. If zero, the value on Card 1 is used (ISLT = 5 only)	E10.0

Omitted data is generated as described above. The slave surface must lie to the left of the master surface as one moves along the master surface, encountering the master nodes in the order they are defined.

SLIDING INTERFACE NOTES

The **sliding only** (Type 1) slideline is a two surface method where arbitrary, frictionless sliding is allowed with the constraints of neither penetration nor separation of nodes in a direction normal to the interface. Nodes may slide tangentially out of contact from the ends of the slide line, but not normally from the slideline.

The **tied** (Type 2) slideline prevents the relative tangental and normal displacements between two adjacent surfaces. It provides a means of joining two dissimilarly meshed parts.

The **sliding with separation** (type 3) and the **sliding with separation and interface friction** (type 4) slidelines are the most generally applicable forms of contact. Parts may initially be separated or in contact, and large relative motions between the surfaces is permitted. A constant Coulomb friction is modeled with type 4.

The **sliding with separation and tie break** (type 5) slideline is a nodal constraint methodology for having an initially tied slideline separate and slide apart when the element plastic strains on either side of the interface exceeds an input parameter. The plastic strain to fail tiebreak may be entered once for all nodes of a slideline definition or for each node individually.

The **single surface contact** (type 6) slideline prevents interpenetration between two portions of the same body (e.g. buckling problems). Frictional effects are allowed. There is no need for a master surface description.

The **eroding pressure contact with separation** (type 7) slideline is a unique form of contact. It is a part of a larger methodology to model the effects of material removal on part distortion. This slide type is used in conjunction with the rezoning **"sc"** option to project slave nodes that have penetrated the master surface back onto the master surface. Thus, the master surface maintains its shape and material is removed from the slave surface (equal to the area of penetration). Rezoning should be automatically invoked every time step (SIAR=1 on Solution Definition Card 1). During equilibrium iterations, penetration between the slide surfaces is allowed, and wherever this penetration occurs, a contact pressure is applied to both surfaces.

The **merge/release with sliding and separation** (type 8) slideline is a combination of merged nodal constraints and a type 3,4 penalty contact, and is designed for simulating progressive separation between two parts, e.g. fracture. A user specified load curve gives the number of nodes released as a function of time. Node release occurs in the same order as the slideline definition; the first slave and master nodes defined are the first pair released. Master and slave nodes must be initially coincidental for release.

Lagrange augmentation is an enhancement to the penalty formulation of enforced contact. Through the use of an iterative scheme of evolving interface penalties and gaps, the accuracy of the slideline contact enforcement is tested until slideline convergence criteria (penalty or gap) are satisfied.

Deliberate interface penetration between surfaces is allowed for slideline types 3 and 4 by specifying an interference penetration load curve on the slideline definition card. This load curve should define a time versus penetration factor curve, where a function value of 0.0 represents no contact forces and a 1.0 provides for full contact. When using this option, the initialization phase of NIKE2D will not reposition slideline nodes to prevent interpenetration.

4.8 NODAL PRINTOUT BLOCKS

Skip this section if NNPB = 0. Otherwise, define one card with the following information [NPBK]. Up to eight nodal printout blocks may be defined.

Card 1

Columns	Quantity	Format
1-5	First node of first printout block	I5
6-10	Last node of first printout block	I5
11-15	First node of second printout block	I5
16-20	Last node of second printout block	I5
.	.	.
.	.	.
.	.	.
71-75	First node of eighth printout block	I5
76-80	Last node of eighth printout block	I5

4.9 ELEMENT PRINTOUT BLOCKS

Skip this section if NEPB = 0. Otherwise, define one card with the following information [EPBK]. Up to eight element printout blocks may be defined.

Card 1

Columns	Quantity	Format
1-5	First element of first printout block	I5
6-10	Last element of first printout block	I5
11-15	First element of second printout block	I5
16-20	Last element of second printout block	I5
.	.	.
.	.	.
.	.	.
71-75	First element of eighth printout block	I5
76-80	Last element of eighth printout block	I5

4.10 CONSTRAINED NODAL PAIRS

Skip this section if NCNP = 0. Otherwise, define a card for each constrained nodal pair [CNPR].

Cards 1,2,...,NCNP

Columns	Quantity	Format
1-5	First node of pair	I5
6-10	Second node of pair	I5
11-15	Constrained degrees of freedom EQ.1: *r* EQ.2: *z* EQ.3: *r* and *z*	I5

The nodal pairs are constrained to move together. One or two degrees-of-freedom are eliminated from the solution for each pair listed.

4.11 LOAD CURVES

Skip this section if NLC = 0. Otherwise, define the following set of cards for each load curve [LCD].

Card 1

Columns	Quantity	Format
1-5	Load curve number	I5
6-10	Number points in load curve, NPTS	I5

Cards 2,3,...,NPTS+1

Columns	Quantity	Format
1-10	Time, temperature, or independent variable x	E10.0
11-20	Function value	E10.0

Various options in NIKE2D utilize load curves to define functional relationships. Many loads and boundary conditions are functions of time, and for these options, the specified load curve should relate load (or boundary condition) value $f(x)$ to time x. Certain material models require the specification of load curves defining various material parameters $f(x)$ vs. temperature x. Others require the specification of load curves defining effective stress $f(x)$ as a function of effective plastic strain x, etc. For options in which load curve multipliers exist, load curves that have the same shape and x values need not be defined. When arc length methods are used, load curves associated with loads and boundary conditions should only have two points, and NIKE2D will extrapolate as necessary.

4.12 CONCENTRATED NODAL LOADS AND FOLLOWER FORCES

Skip this section if NCNL = 0. Otherwise, define a card for each concentrated nodal load or follower force [CNL,CNLS].

Cards 1,2,...,NCNL

Columns	Quantity	Format
1-5	Nodal point number *m* to which this load is applied	I5
6-10	Direction in which load acts EQ.1: and IFW.EQ.0: *r*-direction EQ.2: and IFW.EQ.0: *z*-direction EQ.*n*: and IFW.EQ.1: *n* is a node number that defines a line beginning at *m* and ending at *n*. The force is perpendicular to the line, and points to the right as one moves along the surface from *n* to *m*.	I5
11-15	Load curve number for force vs. time	I5
16-25	Load curve multiplier EQ.0.0: default set to 1.0	E10.0
26-30	Follower force flag, IFW EQ.0: concentrated force acts in either *r*- or *z*-direction EQ.1: follower force is defined	I5

For axisymmetric geometries, the force is defined per unit radian; in plane strain, per unit thickness; and in plane stress, the actual force is applied.

4.13 PRESSURE AND SHEAR LOADS

Skip this section if NPSL = 0. Otherwise, define a card for each pressure and shear load segment [PBC, PBCS].

Cards 1,2,...,NPSL

Columns	Quantity	Format
1-5	Card number EQ.0: the preceding card number is incremented by one	I5
6-10	Load curve number for pressure or shear vs. time	I5
11-15	Node n_1	I5
16-20	Node n_2	I5
21-30	Multiplier of load curve at n_1 EQ.0.0: default set to 1.0	E10.0
31-40	Multiplier of load curve at n_2 EQ.0.0: default set to 1.0	E10.0
41-50	Arrival time of load on the surface	E10.0
51-55	Generation interval, KN EQ.0: default set to 1	I5
56-60	Loading type flag EQ.0: pressure EQ.1: shear	I5
61-70	r-maximum (default = 10^{20}) when the r-coordinate of the pressure segment exceeds this value the pressure is removed from the segment	E10.0
71-80	z-maximum (default = 10^{20}). As above but for the z-coordinate of segment	E10.0

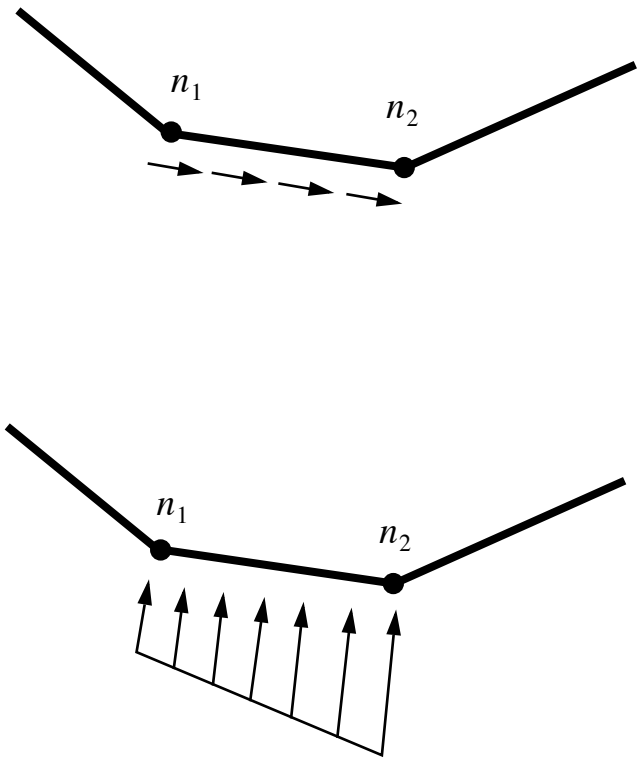

Figure 11
Definition of n_1 and n_2 for the application of traction boundary conditions.

Each card defines a segment (element side) in which a pressure or shear load (traction) is applied. Each segment is specified by nodes n_1 and n_2 as shown in Figure 11. These nodes should be defined in counterclockwise order. Pressure and shear cards must be defined in sequence. Nodes n_j for omitted cards (in this case, fewer than NPSL cards are specified) are generated with respect to the first card prior to the omitted data as

$$n_j^{i+1} = n_j^i + \mathrm{KN} \tag{206}$$

The start times and multipliers are taken from this first card. Equivalent nodal loads are calculated by numerically integrating the tractions along the surface. Traction loads are always evaluated in the current geometry.

4.14 PRESCRIBED DISPLACEMENT BOUNDARY CONDITIONS

Skip this section if NDBC = 0. Otherwise, define a card for each prescribed displacement degree-of-freedom [DBC, DBCS].

Cards 1,2,...,NDBC

Columns	Quantity	Format
1-5	Node number to which this displacement is applied	I5
6-10	Direction in which the node is displaced EQ.1: *r*-direction EQ.2: *z*-direction	I5
11-15	Load curve number for prescribed displacement vs. time	I5
16-25	Load curve multiplier EQ.0.0: default set to 1.0	E10.0
26-35	Removal time. At this time the displaced nodes are treated as free surface nodes. EQ.0.0: default set to 10^{20}	E10.0

4.15 BODY FORCE LOADS DUE TO R-BASE ACCELERATION

Skip this section if IBFR = 0. Otherwise, define the following card [BFGR].

Card 1

Columns	Quantity	Format
1-5	Load curve number for *r*-acceleration vs. time	I5
6-15	Load curve multiplier EQ.0.0: default set to 1.0	E10.0

This card applies only to plane strain and plane stress geometries.

4.16 BODY FORCE LOADS DUE TO Z-BASE ACCELERATION

Skip this section if IBFZ = 0. Otherwise, define the following card [BFGZ].

Card 1

Columns	Quantity	Format
1-5	Load curve number for z-acceleration vs. time	I5
6-15	Load curve multiplier EQ.0.0: default set to 1.0	E10.0

4.17 BODY FORCE LOADS DUE TO ANGULAR VELOCITY

Skip this section if IBFA = 0. Otherwise, define the following card [BFSZ].

Card 1

Columns	Quantity	Format
1-5	Load curve number for angular acceleration vs. time	I5
6-15	Load curve multiplier EQ.0.0: default set to 1.0	E10.0

Nodal loads due to the angular velocity are always calculated with respect to the deformed configuration. Angular velocity is assumed to have the units of radians per unit time.

4.18 CONCENTRATED NODAL MASSES

Skip this card if NCNM = 0. Otherwise, define a card for each concentrated nodal mass [CNMS].

Cards 1,2,...,NCNM

Columns	Quantity	Format
1-5	Node number	I5
6-15	Mass in *r*-direction	E10.0
16-25	Mass in *z*-direction	E10.0

4.19 CONCENTRATED NODAL DAMPERS

Skip this card if NCND = 0. Otherwise, define a card for each concentrated nodal damper [CNDP].

Cards 1,2,...,NCND

Columns	Quantity	Format
1-5	Node number	I5
6-15	Damping in *r*-direction	E10.0
16-25	Damping in *z*-direction	E10.0

4.20 INITIAL VELOCITY

Skip this section if INC ≠ 1. Otherwise, define an initial velocity card for each node [IV, IVP].

Cards 1,2,...,NUMNP

Columns	Quantity	Format
1-5	Node number	I5
6-15	Initial velocity in *r*-direction	E10.0
16-25	Initial velocity in *z*-direction	E10.0
26-30	Generation interval EQ.0: default set to 1	I5

These cards do not need to be in order. However, the highest node number must terminate the data. Omitted data is generated as described in Section 4.4 on page 113 (in this case, fewer than NUMNP cards are specified).

4.21 INITIAL ANGULAR VELOCITY

Skip this section if INC ≠ -1. Otherwise, define the following card [IAV].

Card 1

Columns	Quantity	Format
1-10	Angular velocity in radians per unit time	E10.0
11-20	*r*-coordinate of spin axis	E10.0
21-30	*z*-coordinate of spin axis	E10.0

This card applies only to plane strain or plane stress geometries.

4.22 ELEMENT BODY FORCE LOADS

Skip this section if NBFL=0. Otherwise, define a card for each element body force.

Cards 1,2,...,NBFL

Columns	Quantity	Format
1-5	Element number n^i	I5
6-15	Scale factor for y-component of element body force (per unit volume)	E10.0
16-25	Scale factor for z-component of element body force (per unit volume)	E10.0
26-30	Generation increment KN	I5

These cards do not need to be in element order. For nonzero generation increments KN, element body force loads are generated as follows. Element numbers are generated according to the sequence

$$n^i, n^i + \mathrm{KN}, n^i + 2\mathrm{KN}, \ldots, n^j \tag{207}$$

where n^i and n^j are the element numbers defined on the two consecutive cards, and KN is taken from the first card. Linear interpolation is used to obtain the scale factors of the generated element body force loads. The total number of defined and generated element body force loads should be equal to NBFL.

4.23 NODAL TEMPERATURES

Skip this section if unless TEO=2. Otherwise, define a temperature card for each node.

Cards 1,2,...,NUMNP

Columns	Quantity	Format
1-5	Node number	I5
6-15	Base temperature T^B	E10.0
16-25	Load curve multiplier temperature T^M	E10.0
26-30	Generation increment EQ.0: default set to 1	I5

Nodal temperatures at time *t* are computed by Eq. (34), load curve ITCURV and temperatures T^B and T^M. These cards do not need to be in order. However, the highest node number must terminate the data. Omitted data is generated as described in Section 4.4 on page 113 (in this case, fewer than NUMNP cards are specified).

5.0 RESTART INPUT FILE FORMAT

The following sections describe the format of the NIKE2D restart input file. The specification of a restart input file is optional when restarting a NIKE2D analysis, and may be used only when fixed step solution strategies are employed. For an adaptive solution strategy, a restart ISLAND solution template should be used in place of a restart input file to modify solution and algorithmic parameters. For fixed step strategies, a restart input file may be used to add or modify:

- analysis type (quasistatic or dynamic),
- number of additional time steps,
- time step size,
- output printing interval,
- output plotting interval,
- integration constants,
- equilibrium iteration parameters,
- load curves,
- material properties.

All changes included in the restart input file are incorporated in the restarted analysis, and will be reflected in subsequent binary regular and running dump files.

5.1 CONTROL SECTION

Card 1

Columns	Quantity	Format
1-72	Identification	12A6

Card 2

Columns	Quantity	Format
1-5	Number of additional time steps, NATS EQ.0: number of time steps remains unchanged	I5
6-15	Time step size EQ.0: time step size remains unchanged	E10.0
16-20	Output printing interval EQ.0: step interval for printing remains unchanged	I5
21-25	Output plotting interval EQ.0: step interval for plotting remains unchanged	I5
26-35	Newmark parameter γ (ignored if columns 6-15 are blank; otherwise, defaults to 0.5)	E10.0
36-45	Newmark parameter β (ignored if columns 6-15 are blank; otherwise, defaults to 0.25)	E10.0

The number of additional time steps, NATS, is added to the previously defined total number of time steps to be taken. It may be set to a negative number to reduce the total number of steps to be taken.

Card 3

Columns	Quantity	Format
1-5	Analysis type change flag, IACF EQ.0: no change EQ.1: changed as specified below	I5
6-10	Number of load curves to be redefined, NTHRD	I5
11-15	Number of materials to be redefined, NMRDF	I5

Card 4

Columns	Quantity	Format
1-5	Number of time steps between stiffness reformations EQ.0: this parameter remains unchanged	I5
6-10	Number of time steps between equilibrium iterations EQ.0: this parameter remains unchanged	I5
11-15	Maximum number of equilibrium iterations between stiffness matrix reformations EQ.0: this parameter remains unchanged	I5
16-20	Maximum number of stiffness matrix reformations per time step EQ.0: this parameter remains unchanged	I5
21-30	Convergence tolerance on displacements EQ.0.0: this parameter remains unchanged	E10.0
31-40	Convergence tolerance on energy EQ.0.0: this parameter remains unchanged	E10.0
41-45	Number of time steps between restart dumps	I5
46-50	Number of slidelines of type 2 and 4 to be tied, NTSL	I5

5.2 ANALYSIS TYPE CHANGE

Skip this section if IACF = 0. Otherwise, define the following analysis type change card.

Card 1

Columns	Quantity	Format
1-5	Analysis flag EQ.0: quasistatic analysis EQ.1: dynamic analysis	I5

In changing from a quasistatic to a dynamic analysis, the densities that were defined in the original input file are used.

5.3 LOAD CURVES

Skip this section if NTHRD = 0. Otherwise, define NTHRD sets of cards.

Card 1

Columns	Quantity	Format
1-5	Load curve number of load curve to be redefined	I5

Cards 2,3,...,NPTS+1

Columns	Quantity	Format
1-10	Time, temperature or independent variable x	E10.0
11-20	Function value $f(x)$	E10.0

The number of points in each load curve, NPTS, may not change from that defined in the original input file.

5.4 MATERIAL PROPERTY CHANGE

Skip this section if NMRDF = 0. Otherwise, enter data for NMRDF materials as described in section 4.3 on page 46. The number of materials redefined (NMRFD) cannot exceed the number of materials specified in the original input file.

5.5 SLIDELINE TYPE CHANGE

Skip this section if NTSL = 0. Otherwise, define a card for each type 3 or type 4 slideline to be tied.

Cards 1,2,...,NTSL

Columns	Quantity	Format
1-5	Number of slideline to be tied	I5

6.0 REZONING

The following sections describe the commands used for both interactive rezoning and automatic rezoning via a command file. Interactive rezoning is initiated by typing the `SW5.` sense switch control during program execution. The analyst is next prompted for a TMDS monitor or graphics device number. Commands can then be typed to study current results and rezone the mesh. Automatic rezoning command files should contain similar command sequences. The TMDS monitor or graphics device number should not be included in the rezone command file.

6.1 LIST OF COMMANDS BY FUNCTION

Rezoning is performed by material. The following commands are useful, but do not in themselves rezone a material:

A, DEB, DMB, DSL, ELPLT, END, F, FR, FRAME, FSET, G, GRID, GSET, IP, MC, MD, MN, NDPLT, NOFRAME, NOGRID, PLOTS, PLTI, PRIT,R ,SC, SD, SETF, SN, T, TERM, TR, TV, Z

Materials for which boundaries have been changed by the SC, SD, MC, and MD commands must still be rezoned. Commands for rezoning a material (may be used with above commands) are:

B, CN, M, S, TN, V

Commands that are available for adjusting boundary nodes following the "B" command are:

BD, BDS, ES, ESS, ER, ERS, EZ, EZS, SLN, SLNS, VS, VSS

The "B" command should be used only if a material has been designated for rezoning with the "M" command.

6.2 COMMAND DEFINITIONS

HELP	Enter HELP package and display all available commands. Description of each command is available in the HELP package.
HELP/commandname	Do not enter HELP package but print out the description on the terminal of the command following the slash
PHP ans	Print help package - If answer equals 'y' the package is printed in the high speed printer file.
TV n	Use TMDS with monitor number n. If n is the red channel of a color TMDS, ORION will automatically grab the green and blue channel. (The author must be aware of the TMDS channel numbers for this to occur, however.)
TV -n_1 n_2 n_3	Use color TMDS with monitor numbers n_1, n_2, and n_3 for the red, green, and blue channels, respectively.
T or END	Terminate.
F	Terminate interactive phase, remap, continue in execution phase.
FR	Terminate interactive phase, remap, write restart dump, and call exit.
Z r z ΔL	Zoom in at point (r,z) with window ΔL
UZ a b ΔL	Zoom in at point (a,b) with window ΔL where a, b, and ΔL are numbers between 0 and 1. The picture is assumed to lie in a unit square.
UZG	Cover currently displayed picture with a 10 by 10 square grid to aid in zooming with the unity zoom, "UZ", command.
FIX	Set TMDS picture to its current window. This window is set until it is reset by the "GSET, "FSET," or "SETF" commands or released by the "UNFIX" command.
UNFIX	Release current TMDS window set by the "FIX," "GSET," "FSET" or "SETF" commands.
GSET r z ΔL	Center TMDS pictures at point (r,z) with square window of width ΔL. This window is set until it is reset or the "UNFIX" command is typed.
FSET n Δr Δz	Center TMDS pictures at node n with a rectangular Δr x Δz window. This window is set until it is reset with or the "UNFIX" command is typed.

SETF r z Δr Δz	Center TMDS pictures at point (r,z) with a rectangular Δr x Δz window. This window is set until it is reset or the "UNFIX" command is typed.
FR80 filmtype	Select FR80 camera. FR80 default filmtype is FICHE48. Other options include: FICH48D, FICHE24, FICH24D, 35mm, COLOR35, DICO35, P16mm, COLOR16, DICO16, CSLIDE35, HARDCOPY, REPORT, VUGRAPH, and VUGRAF11. This command, if used, must precede the "PLOTS" command.
CLASS level	Set classification level of FR80 output. The default is UNCLASS. Other levels include: PROGLEV, PARD, ADP, CONFIDNT, SRD, and SYSTEM. This command, if used, must precede the "PLOTS" command.
GIVE	Give the FR80 file to the system for plotting upon termination. This command, if used, must precede the "PLOTS" command.
PLOTS	Create FR80 plotfile containing a record of the TMDS display.
C	Comment - proceed to next line.
GRID	Overlay TMDS displays with a grid of orthogonal lines.
NOGRID	Do not overlay TMDS displays with a grid of orthogonal lines (default).
G	View mesh.
GS	View mesh and solid fill elements to identify materials by color
GO	View mesh right of centerline and outline left of centerline.
UG	Display undeformed mesh.
RPVA	Reflect mesh, contour, fringe, etc., plots about vertical axis. Retyping "RPVA" turns this option off.
RPHA	Reflect mesh, contour, fringe, etc., plots about horizontal axis. Retyping "RPHA" turns this option off.
FRAME	Frame plots with a reference grid (default).
NOFRAME	Do not plot a reference grid.
RJET n i	Send a copy of the FR8o(0,/) file to rjet n using plot format i where i=1 gives a 5" plot

	i=2 gives a 8" plot i=3 gives a 10.5" plot i=4 gives the largest possible plot. If i is negative, the plot is sideways, rotated 90 degrees clockwise on the paper. Plots may be sent to either the 11 or 22 inch plotters.
RESO n_x n_y	Set the x and y resolutions of NIKE2D plots to nx and ny, respectively. We default both nx and ny to 1024.
LOGO	Put LLNL logo on all plots (default). Retyping this command removes the logo.
O	Plot outlines of all material.
FSON	Plot only free surfaces and slideline interfaces with "O" command. [Must be used before "O" command.]
FSOFF	Turn off the "FSON" command.
MNOFF	Do not plot material numbers with the "0", "G", and "GO" commands (default).
MNON	Plot material numbers with "0", "G", and "GO" commands.
CONTOUR c n m_1 m_2... m_n	Contour component number c on n materials including materials m_1, m_2,..., m_n. If n is zero, only the outline of material m_1 with contours is plotted. Component numbers are given in Table 6.1.
PRIN c n m_1 m_2... m_n	Plot lines of principal stress and strain in the yz plane on n materials including materials m_1, m_2,..., m_n. If n is zero, only the outline of material m1 is plotted. The lines are plotted in the principal stress and strain directions. Permissible component numbers in Table 6.1 include 0, 5, 6, 100, 105, 106,...,etc. Orthogonal lines of both maximum and minimum stress are plotted if components 0, 100, 200, etc. are specified.
FRINGE c n m_1 m_2... m_n	Fringe component number c on n materials including m_1, m_2,..., m_n. If n is zero, only the outline of material m1 with contours is plotted. Component numbers are given in Table 1.
NCOL n	Number of colors in fringe plots is n. The default value for n is 6 which includes colors magenta, blue, cyan, green, yellow, and red. An alternative value for n is 5 which eliminates the minimum value magenta.

PROFILE c n m_1 m_2...m_n	Plot component c versus element number for n materials including materials m_1, m_2,..., m_n. If n is o(0,/), then component c is plotted for all elements. Component numbers are given in Table 1.
VECTOR c n m_1 m_2...m_n	Make a vector plot of component c on n materials including materials m_1, m_2,..., m_n. If n is zero, only the outline of material m_1 with vectors is plotted. Component c may be set to "D" and "V" for vector plots of displacement and velocity, respectively.
LINE c n m_1 m_2...m_n	Plot variation of component c along line defined with the "NLDF", "PLDF", "NSDF", or the "NSSDF" commands given below. In determining variation, consider n materials including material number m_1, m_2,..., m_n.
NLDF n n_1 n_2...n_3	Define line for "LINE" command using n nodes including node numbers n_1, n_2,...n_n. This line moves with the nodes.
PLDF n r_1 z_1...r_n z_n	Define line for "LINE" command using n coordinate pairs (r_1,z_1), (r_2,z_2),...(r_n,z_n). This line is fixed in space.
NSDF m	Define line for "LINE" command as side m. Side m is defined for material n by the "B" command.
NSSDF m n	Define line for "LINE" command and that includes boundary nodes m to n (counterclockwise) in the interface definitions. This command must follow the "B" command.
RANGE r_1 r_2	Set the range of levels to be between r_1 and r_2 instead of in the range chosen automatically by ORION. To deactivate this command, type RANGE 0. 0.
MOLP	Overlay the mesh on the contour, fringe, principal stress, and principal strain plots. Retyping "MOLP" turns this option off.
NUMCON n	Plot n contour levels. The default is 9.
PLOC	Plot letters on contour lines to identify their levels (default).
NLOC	Do not plot letters on contour lines.
IFD n	Begin definition of interface n. If interface n has been previously defined, this command has the effect of destroying the old definition.
IFS m	Include side m in the interface definition. Side m is defined for material n by the "B" command.

IFN m	Include boundary nodes to m (counterclockwise) in the interface definition. This command must follow the "B" command.
IFP c m	Plot component c of interface m. Component numbers are given in Table 2.
IFVA r_c z_c	Plot the angular location of the interface based on the center point (r_c,z_c) along the abcissa. Positive angles are measured counterclockwise from the y axis.
IFVS	Plot the distance along the interface from the first interface node along the abcissa (default).
A	Display all slidelines. Slave sides are plotted as dashed lines.
SN n	Display slideline n with slave node numbers.
SC n	Check slave nodes of slideline n and put any nodes that have penetrated through the master surface back on the master surface.
SD n	Dekink slave side of slideline n - after using this command, the SC or MC command is sometimes advisable.
MN n	Display slideline n with master node numbers.
MC n	Check master nodes of slideline n and put any nodes that have penetrated through the slave surface back on the slave surface.
MD n	Dekink master side of slideline n. After using this command, the SC or MC command is sometimes advisable.
DE e_1 e_2	Delete elements e_1 to e_2.
DM n m_1 m_2... m_n	Delete n materials including m_1, m_2,..., and m_n.
R	Restore original mesh.
DEB n f_1 g_1...f_n g_n	Delete n element blocks consisting of element numbers f_1 to $_1$ f_2 to g_2..., and f_n to g_n inclusive. These elements will be inactive when the calculation resume.
DMB n m_1 m_2... m_n	Delete n material blocks consisting of all elements with material numbers m_1, m_2,...,and m_n. These materials will be inactive when the calculations resume.
DSL n g_1 g_2...g_n	Delete n slidelines including slideline numbers g_1, g_2,..., and g_n.
TERM t	Reset the termination to t.
PRTI Δt	Reset the node and element printout interval to Δt.

PLTI Δt	Reset the node and element data dump interval to Δt
TIESL n	Switch slideline n to a tied interface.
M n	Material n is to be rezoned.
NDPLT	Plot node numbers on mesh of material n.
ELPLT	Plot element numbers on mesh of material n.
V	Display material n on TMDS.
VS	Display material n on TMDS and solid fill elements
S	Smooth mesh of material n. To smooth a subset of elements, a window can be set via the "GSET", "FSET", OR "SETF" commands. Only the elements lying within the window are smoothed.
BLEN s	Smooth option where s=0 and s=1 correspond o equipotential and isoparametric smoothing, respectively. By letting $0 \le s \le 1$ a combined blending is obtained.
TN r z ΔL	Type node numbers and coordinates of all nodes within window $(r + \Delta L / 2, z + \Delta L / 2)$.
CN m r z	Node m has new coordinate (r,z).
B	Determine boundary nodes and sides of material n and display boundary with nodes and side numbers on TMDS.
ER m n	Equal space in r-direction boundary nodes m to n (counter-clockwise).
ERS s	Equal space in the r-direction boundary nodes on side s.
EZ m n	Equal space in z-direction boundary nodes m to n (counter-clockwise).
EZS s	Equal space in the z-direction boundary nodes on side s.
ES m n	Equal space along boundary, boundary nodes m to n (counter-clockwise).
ESS s	Equal space along boundary, boundary nodes on side s.
SLN m n	Equal space boundary nodes between nodes m to n on a straight line connecting node m to n.
SLNS n	Equal space boundary nodes along side n on a straight line connecting the corner nodes.

VS m n r	Vary the spacing of boundary nodes m to n such that r is the ratio of the first segment length to the last segment length.
VSS s r	Vary the spacing of boundary nodes on side s such that r is the ratio of the first segment length to the last segment length.
BD m n	Dekink boundary from boundary node m to boundary node n (counterclockwise).
BDS s	Dekink side s.
TR n	T on time step in NIKE2D will stop and enter interactive rezoning phase.

6.3 CURSOR COMMANDS

DZ a b	Use cursor to define points a and b on the diagonal of a window for zooming.
DTN a b	Use cursor to define points a and b on the diagonal of a window. The node numbers and coordinates of nodal points lying within the window are typed on the terminal.
DTE a b	Use cursor to define points a and b on the diagonal of a window. The element numbers and coordinates of elements lying within the window are typed on the terminal.
DTNC a	Use cursor to define point a. The nodal point number and nodal coordinates of the node lying closest to point a will be printed.
DCN a b	Use cursor to define points a and b. The node closest to point a will be moved to point b.
DCSN n a	Move nodal point n to point a defined by the cursor.
DER a b	Use cursor to define points a and b on boundary. Equal space nodes in r-direction along boundary starting at a, moving counterclockwise, and ending at b.
DEZ a b	Use cursor to define points a and b on boundary. Equal space nodes in z-direction along boundary starting at a, moving counterclockwise, and ending at b.
DES a b	Use cursor to define points a and b on boundary. Equal space nodes along boundary starting at a, moving counterclockwise, and ending at b.

DBD a b	Use cursor to define points a and b on boundary. Dekink boundary starting at a moving counterclockwise, and ending at b.
DZZ a	Use cursor to define point a and zoom in at this point. The new window is.15 as large as the previous window. The zoom factor can be reset by the crzf command or the.15 default.
DVS a b r	Use cursor to define points a and b on boundary. Variable space nodes along boundary starting at a, moving counterwise, and ending at b. The ratio of the first segment length to the last segment length is give by r (via terminal).
DCNM a b	Use cursor to define points a and b. The node at point a is given the coordinate at point 2.

The following commands apply to line plots, interface plots, etc.

ASET amin amax	Set minimum and maximum values on abscissa to amin and amax, respectively. If amin=amax=0.0 (default) NIKE2D determines the minimum and maximum values.
OSET omin omax	Set minimum and maximum values on ordinate to omin and omax, respectively. If omin=omax=0.0 (default) NIKE2D determines the minimum and maximum values.
ASCL f_a	Scale all abscissa data by f_a. The default is f_a=1.
OSCL f_o	Scale all ordinate data by f_o. The default is f_o=1.
SMOOTH n	Smooth a data curve by replacing each data point by the average of the 2n adjacent points. The default is n=0.

No.	Component	No.	Component
1	y	21*	ln (V/Vo) (volumetric strain)
2	z	22*	y-displacement
3	hoop	23*	z-displacement
4	yz	24*	maximum displacement
5	maximum principal	25*	y-velocity, y-heat flux
6	minimum principal	26*	z-velocity, z-heat flux
7	von Mises (Appendix A)	27*	maximum velocity, max. heat flux
8	pressure or average strain	28	ij normal
9	maximum principal-minimum principal	29	jk normal
10	y minus hoop	30	kl normal
11	maximum shear	31	li normal
12	ij and kl normal (Appendix B)	32	ij shear
13	jk and li normal	33	jk shear
14	ij and kl shear	34	kl shear
15	jk and li shear	35	li shear
16	y-deviatoric	36*	relative volume V/Vo
17	z-deviatoric	37*	Vo/V-1
18	hoop-deviatoric	38*	bulk viscosity, Q
19*	effective plastic strain	39*	P + Q
20*	temperature	40*	density

Table 1.
Component numbers for element variables. By adding 100, 200 300, 400, and 500 to the component numbers not superscripted by an asterisk, components numbers for infinitesimal strains, Green-St. Venant strains, Almansi strains, strain rates, and extensions are obtained, respectively. Maximum and minimum principal stresses and strains are in the yz plane. The corresponding hoop quantities must be examined to determine the overall extremum.

No.	Component
1	pressure
2	shear stress
3	normal force
4	tangential force
5	y-force
6	z-force

Table 2.
Component numbers for interface variables.
In axisymmetric geometries the force is per unit radian.

7.0 EXAMPLES

To illustrate the analysis capability of the NIKE2D code, five of the standard NIKE2D examples are presented. The default values for the solution parameters are used for each of these examples unless otherwise specified. An additional example illustrates the application of NIKE2D with ISLAND to simulate a superplastic forming operation. An ISLAND template is used to solve this process control problem, demonstrating a powerful use of the adaptive features of the ISLAND language.

7.1 ROTATING CYLINDER

The first example is the dynamic analysis of a rotating cylinder subject to an internal pressure. This problem was proposed by Key, Biffle, and Krieg (1976) to evaluate both the modeling of the constitutive response and the correct treatment of rigid body motions. The plane strain finite element model is shown in Figure 12. The material is assumed to be elastoplastic (material type 3), with Young's modulus $E = 71.0$ *GPa*, Poisson's ratio $v = 0.333$, yield stress $\sigma_0 = 0.286$ *GPa*, hardening modulus $E_p = 3.56$ *GPa*, hardening parameter $\beta = 0.0$, and density $\rho = 2680$ Kg/m^3. At time zero, an initial angular velocity of 4000 *rad/s* is specified and a pressure of 0.0669 *GPa* is applied. The analysis is performed with both 500 steps of 5 μs and 100 steps of 50 μs to simulate a complete revolution of the cylinder.

Using 500 steps, the cylinder expands from an initial radius of 25.4 *mm* to a radius of 32.5 *mm* and oscillates about this deformed configuration at a frequency of 2.67×104 *Hz*. Time histories of *y*-stress, *z*-stress, and maximum principal stress are shown in Figure 13 and Figure 14. These same stress components are plotted in Figure 15 and Figure 16 for the case of 100 steps. Although the overall behavior is similar in both cases, the elastic ringing is not resolved for the larger time step. The *y* and *z* displacements at node 1 for both calculations are shown in Figure 17 and Figure 18, respectively.

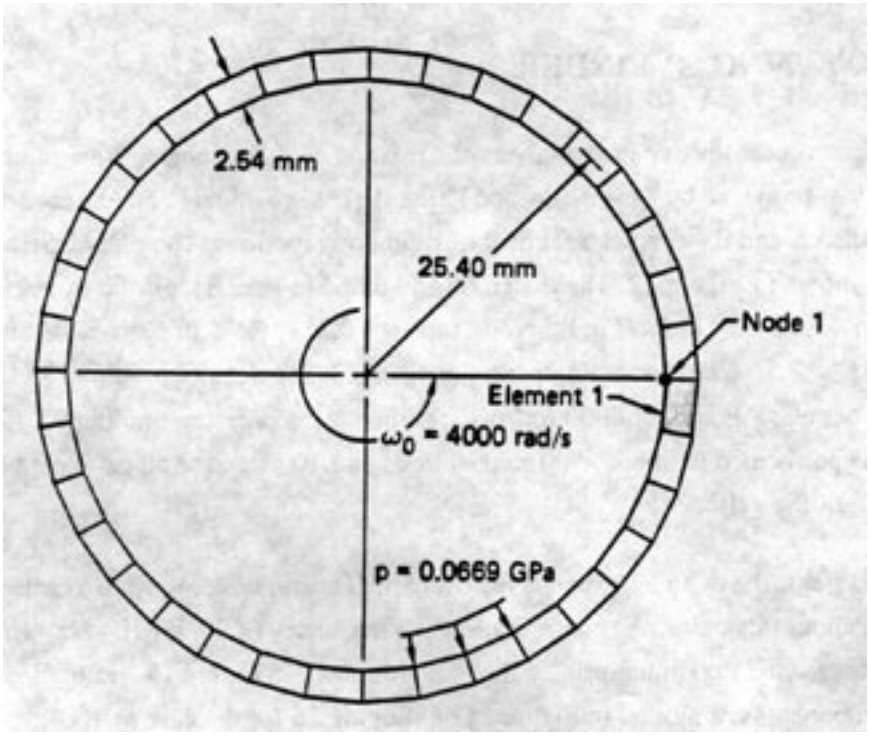

Figure 12
Plane strain finite element model of rotating cylinder.

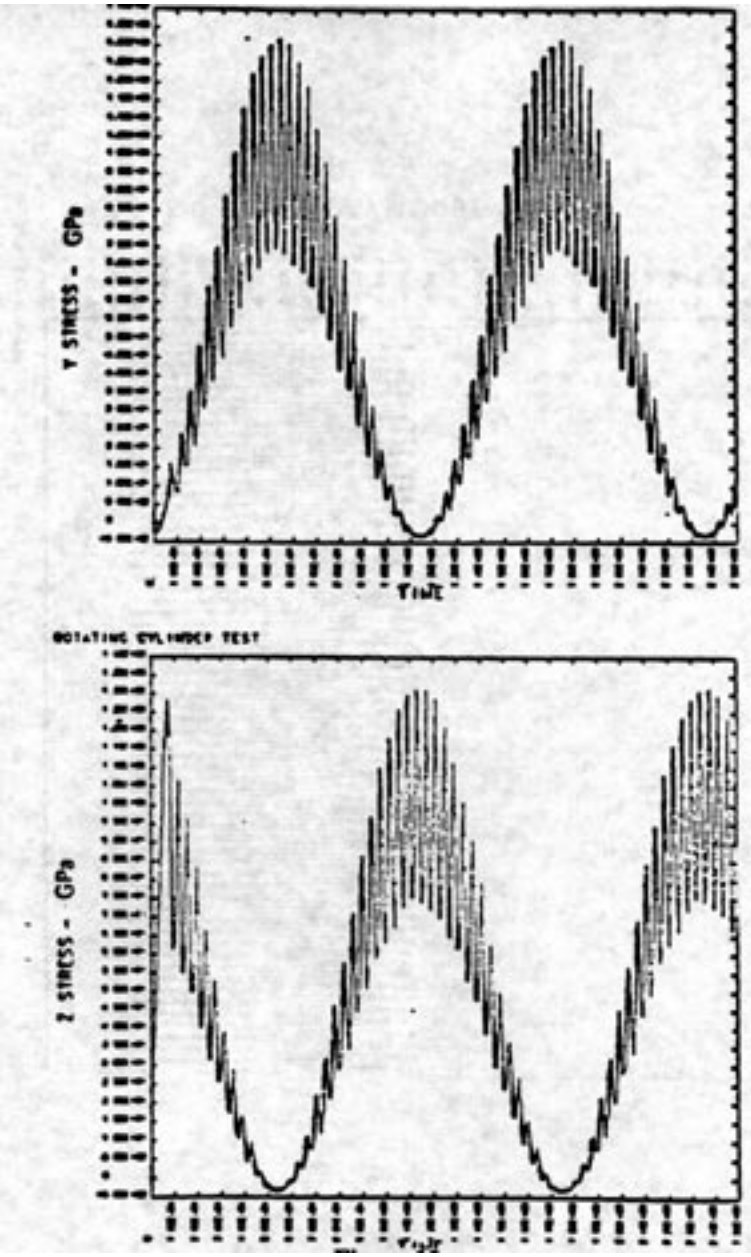

Figure 13
Stresses in element 1 ($\Delta t = 5$ μs): (a) *y*-stress, (b) *z*-stress.

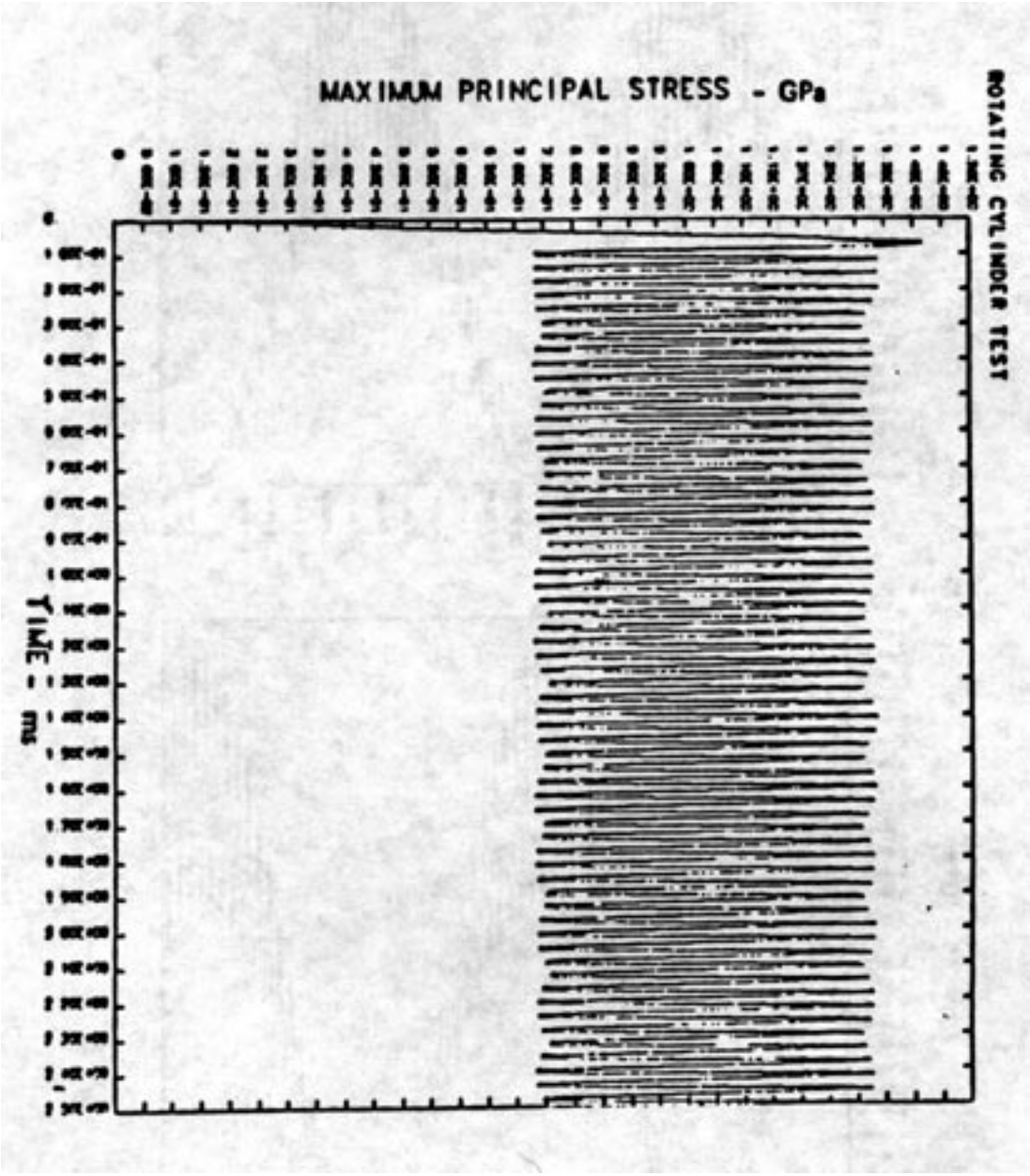

Figure 14
Maximum principal stress in element 1 (Δt = 5 μs).

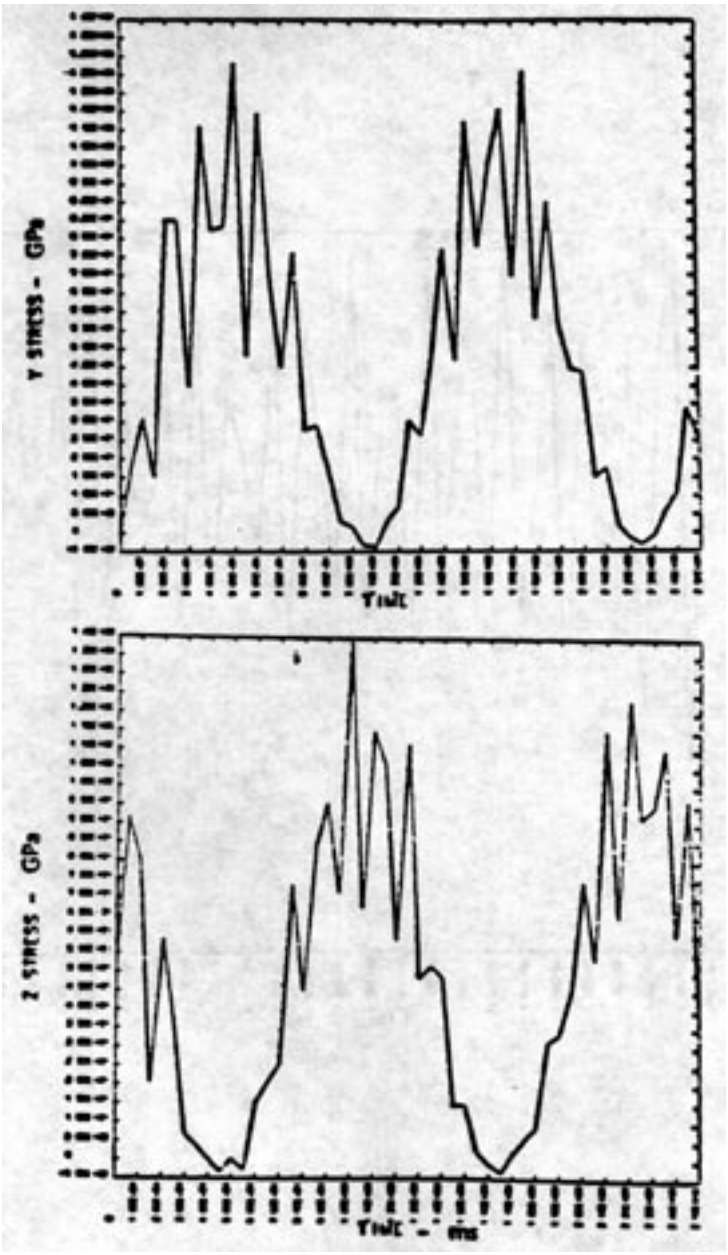

Figure 15
Stresses in element 1 (Δt = 50 μs): (a) *y*-stress, (b) *z*-stress.

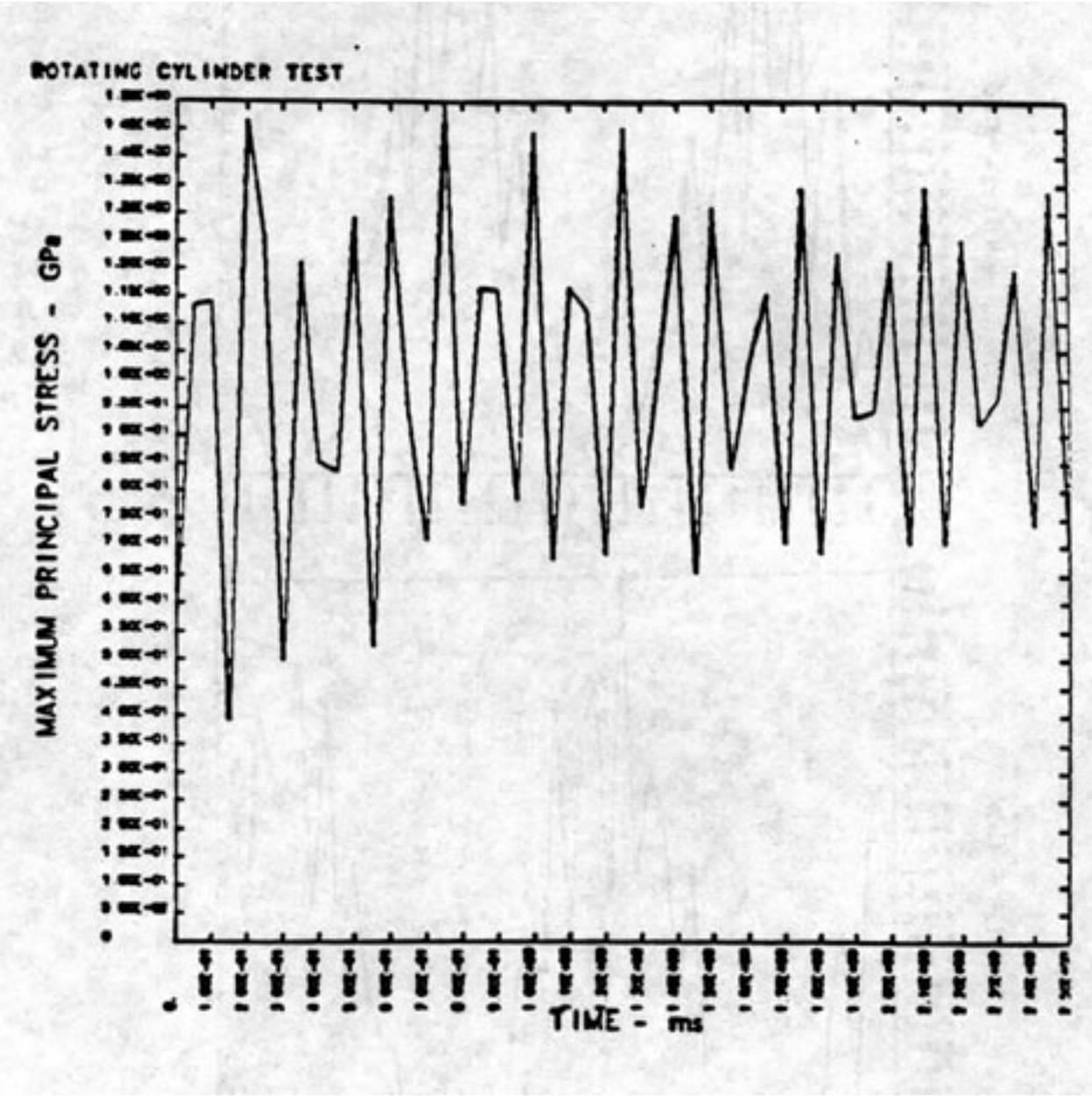

Figure 16
Maximum principal stress in element 1 (Δt = 50 μs).

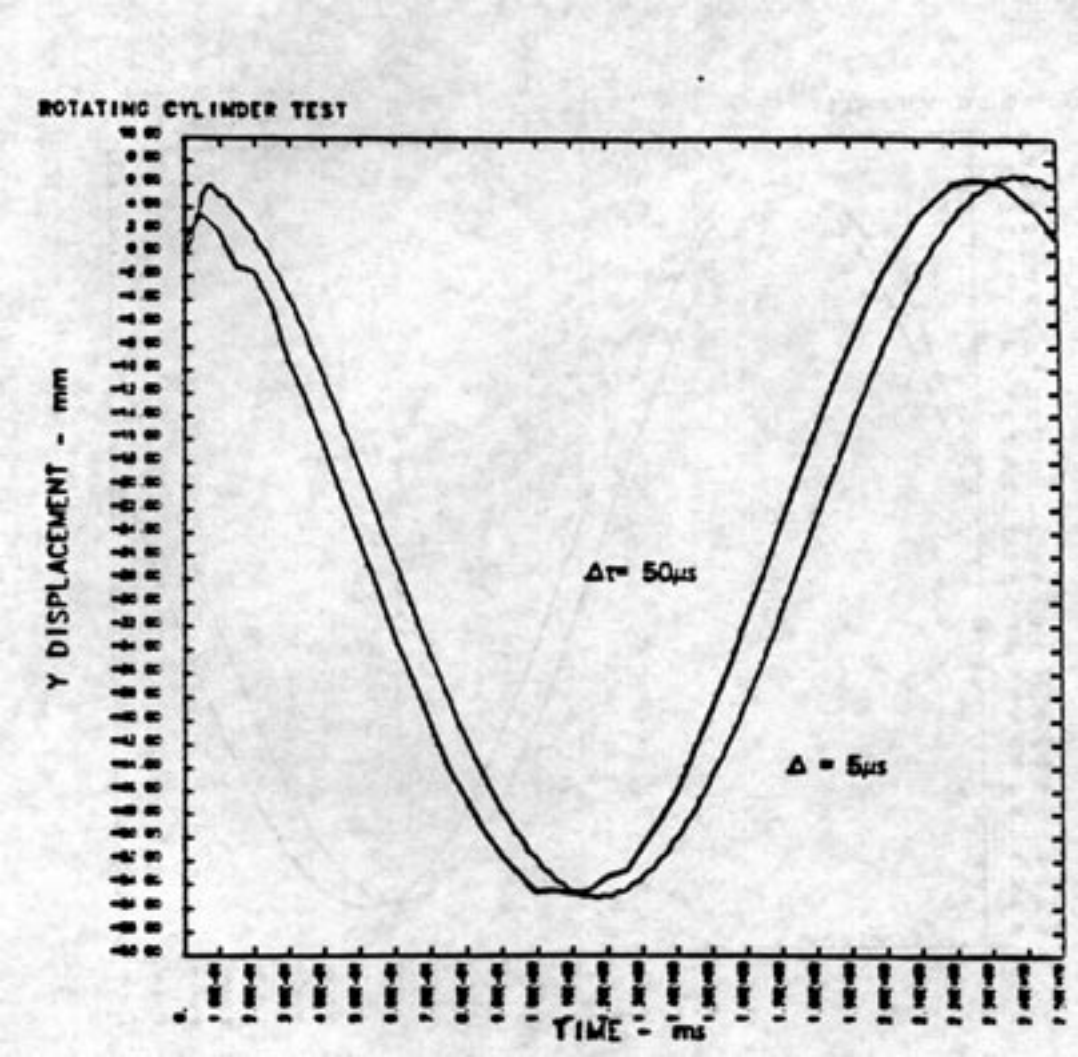

Figure 17
Effect of time step on *y*-displacement at node 1.

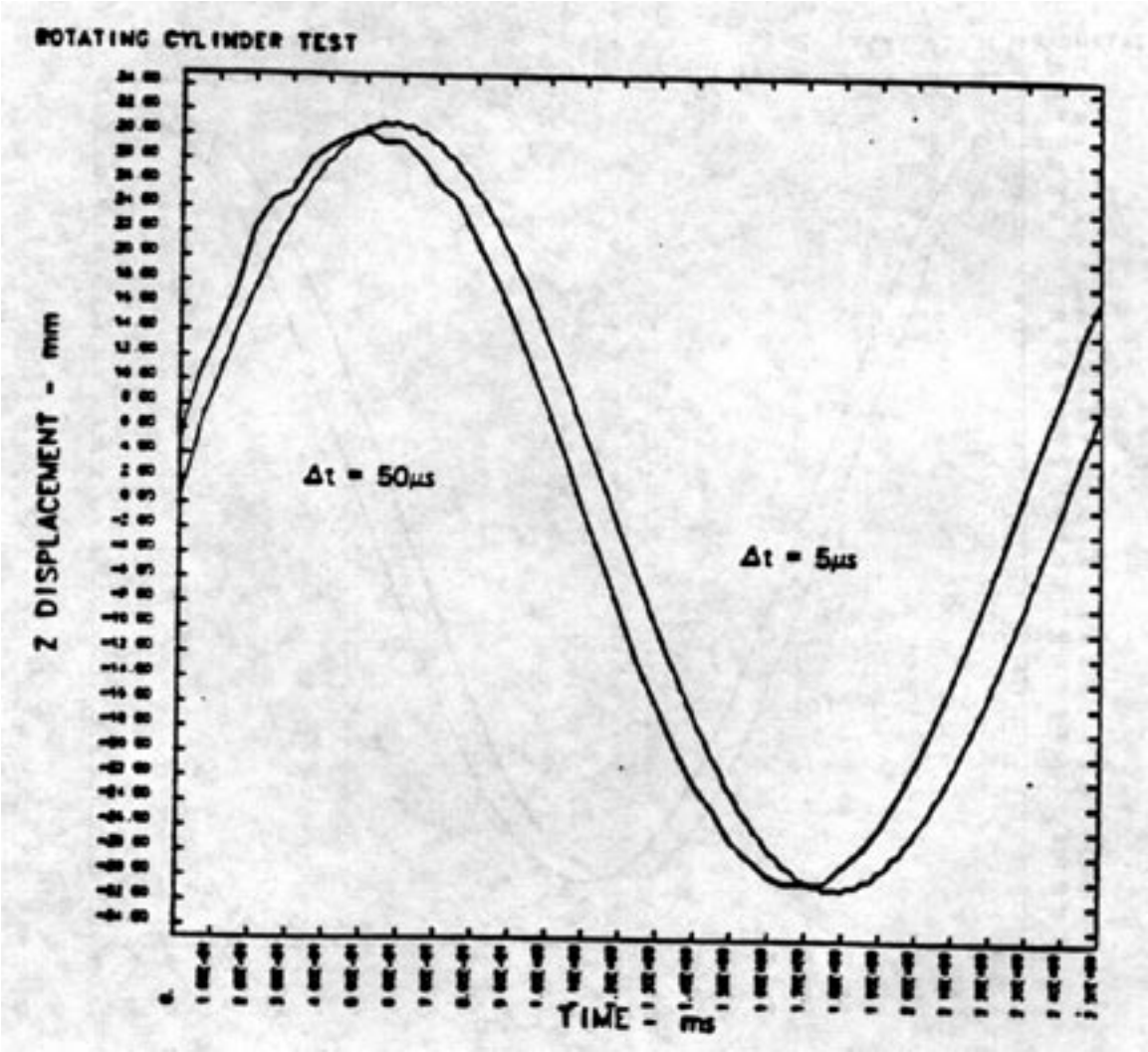

Figure 18
Effect of time step on *z*-displacement at node 1.

7.2 TENSION TEST SIMULATION

In this example, a quasistatic NIKE2D simulation is used to model the necking of steel specimen under uniaxial tension. The axisymmetric finite element model of the 50.8 *mm* specimen is shown in Figure 19. The material behavior is assumed to be elastoplastic with $E = 206.9$ *GPa*, $\nu = 0.29$, and an effective stress vs. effective plastic strain relationship as shown in Table 3. Displacement boundary conditions are prescribed to produce a change of length ΔL of 14 *mm* in 100 equal time increments. The NIKE2D analysis results are compared to a HEMP (see Giroux [1973]) calculation reported by Norris et al. (1978). The HEMP calculation took 29,000 steps to reach the same state of deformation.

The NIKE2D deformed shapes at various times are shown in Figure 20. As ΔL reaches 14 *mm*, the aspect ratios of the elements in the neck region become large. However, the calculation remains well behaved, and the radial stress approaches zero at the outer radius as expected. Figure 21 shows the normalized neck radius a/a_0 plotted versus axial engineering strain $\Delta L/L_0$. NIKE2D results are compared to reported HEMP results and to experimental data, and all are in excellent agreement. Contours for stress and effective plastic strain are shown in Figure 22, and again compare quite favorably with the results reported by Norris et al. (1978).

Table 3.
Elastoplastic stress-strain data

Effective Plastic Strain $\bar{\varepsilon}^p$	Effective Stress σ (*GPa*)
0.0000	0.450
0.0050	0.470
0.0178	0.514
0.0378	0.590
0.0678	0.642
0.1478	0.700
0.4980	0.790
1.0000	0.840

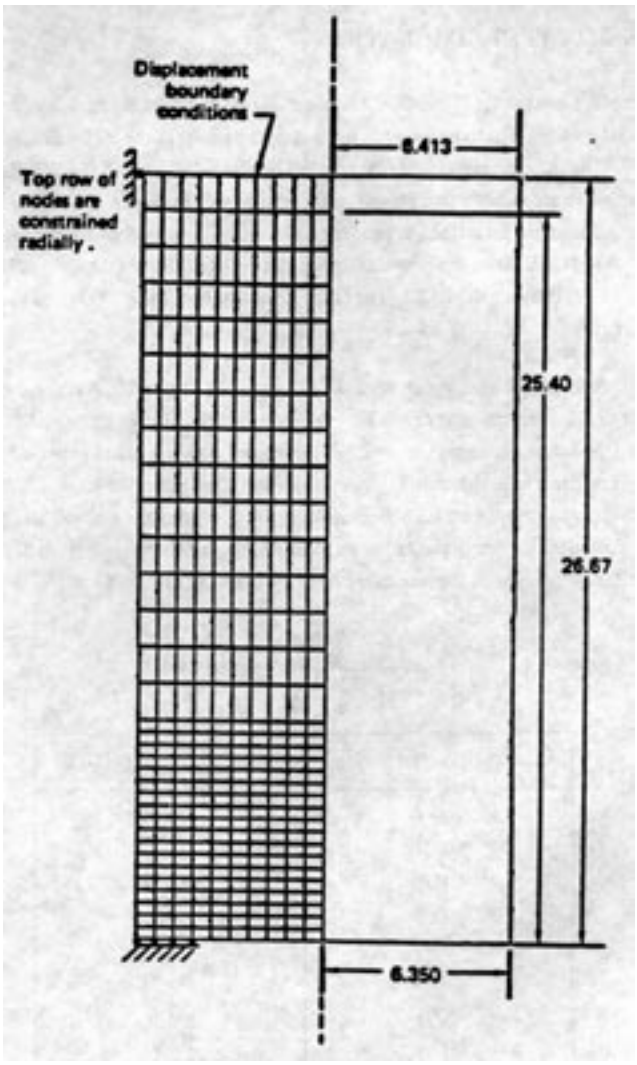

Figure 19
Finite-element model of uniaxial tension specimen. All dimensions are in millimeters.

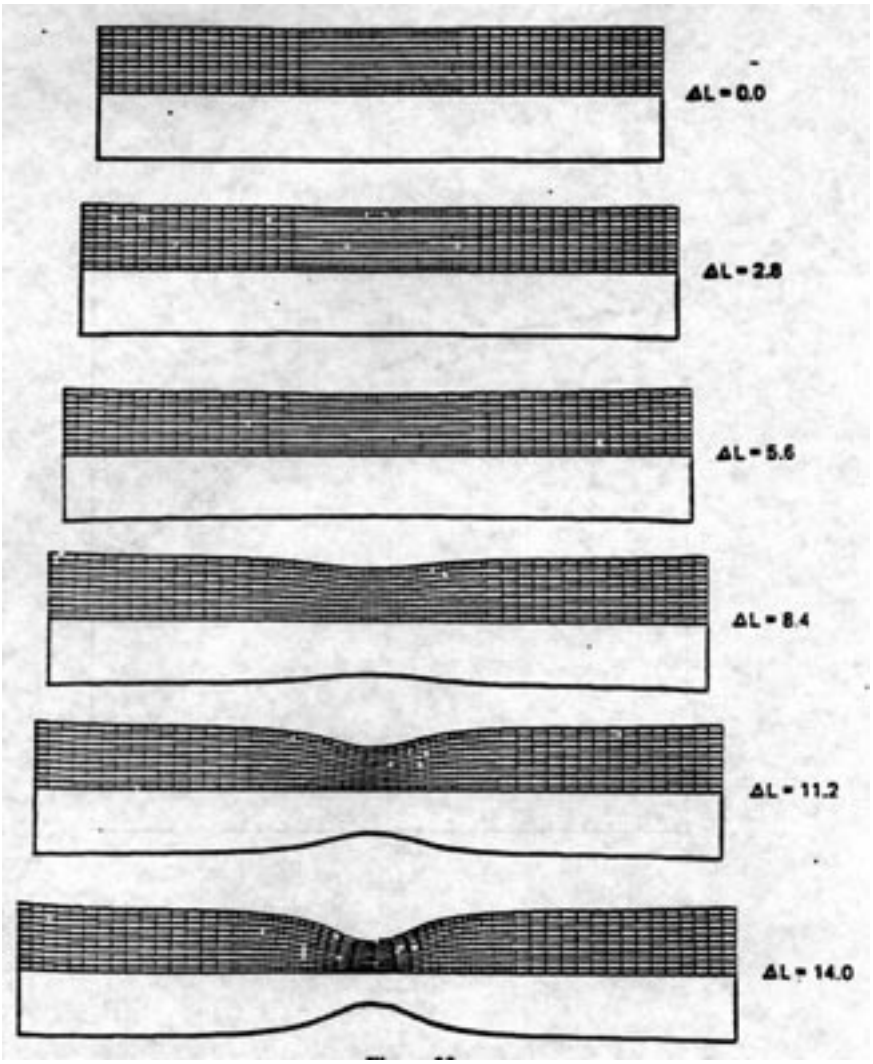

Figure 20
Deformed shapes at various times

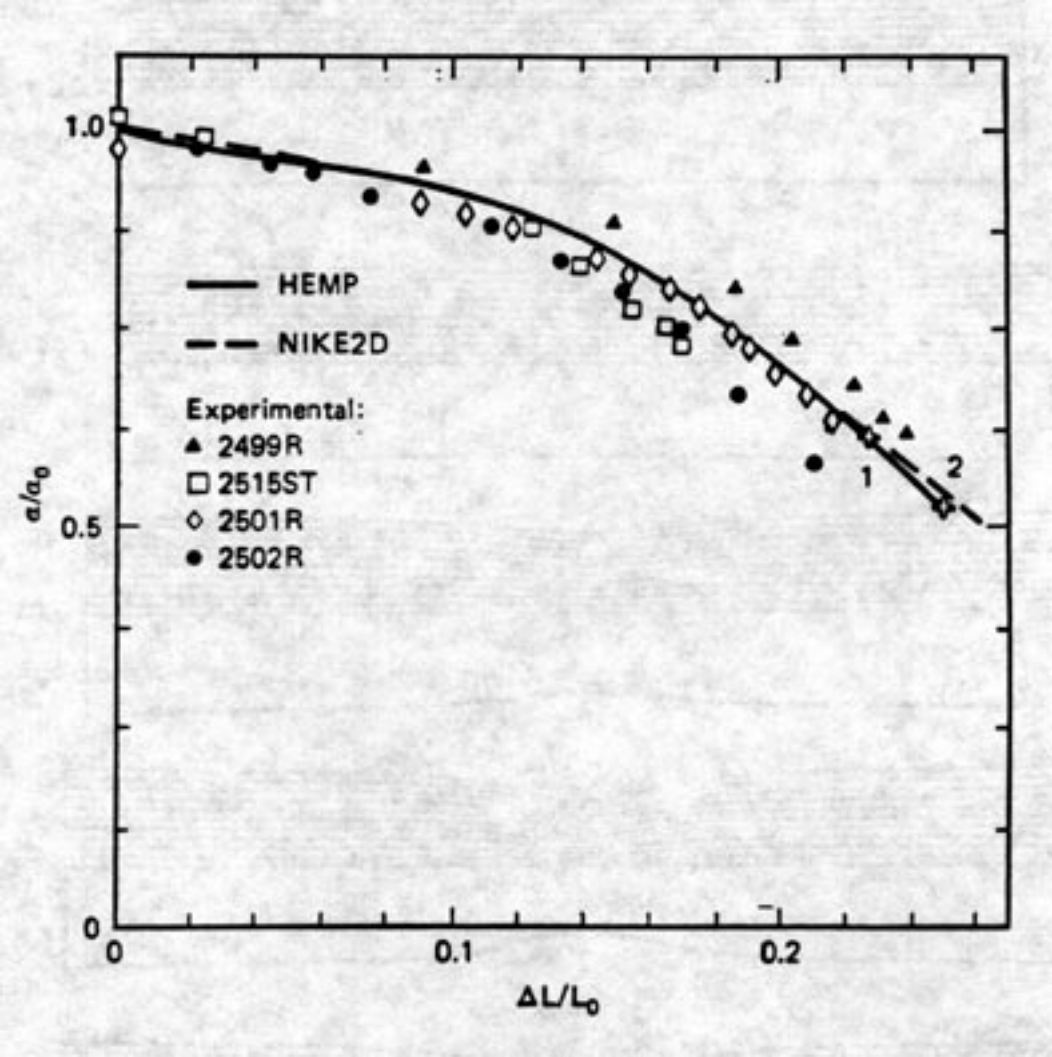

Figure 21
Normalized neck radius a/a_0 versus axial engineering strain $\Delta L/L_0$.

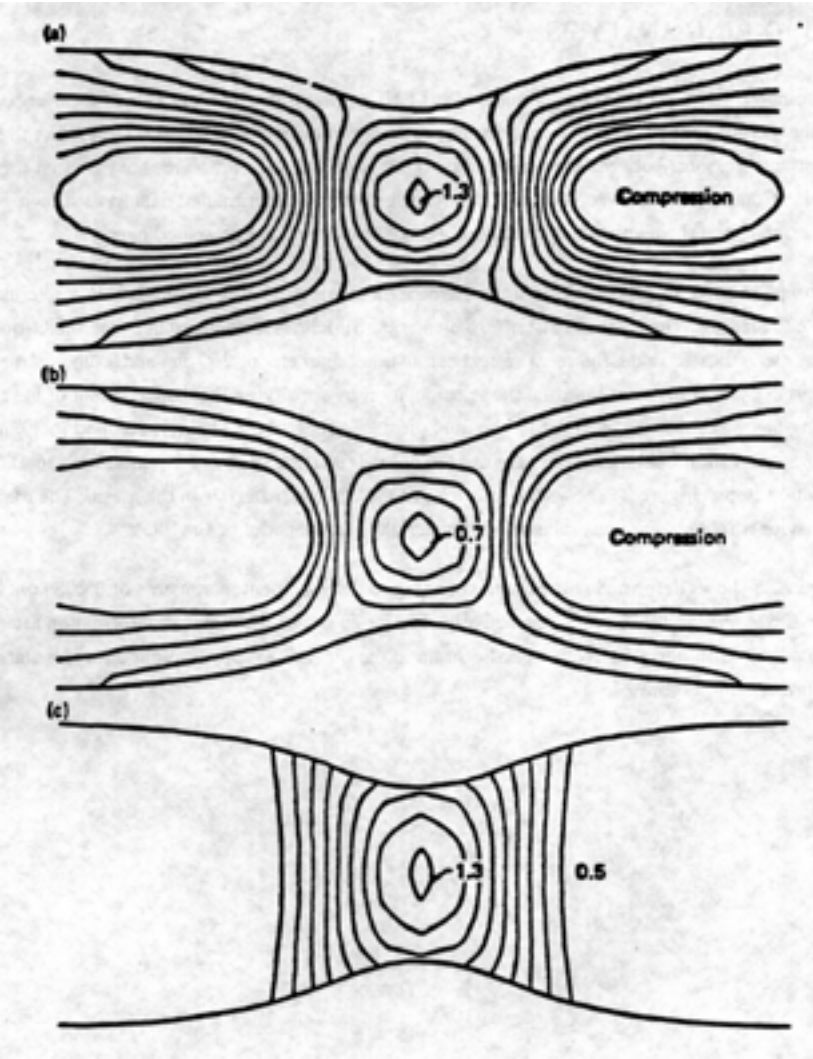

Figure 22
Contours of stress and strain at a/a_0 = 0.54:
(a) axial stress, (b) mean tensile stress, (c) effective plastic strain.

7.3 O-RING ANALYSIS

A comprehensive program was completed at LLNL to investigate the leak rate of a variety of seal-flange configurations. Quasistatic calculations were performed with NIKE2D to predict the interface pressures between the seals and flanges. High interface pressures are essential for tight seals. Comparisons between NIKE2D analysis results and experimental data have shown good agreement, and the results of a typical seal-flange calculation are presented here.

Figure 23 shows an axisymmetric finite element model of a metallic O-ring seal in a steel flange prior to loading. The mesh consist of 378 elements. Slidelines are defined between the O-ring and flange as indicated in the figure. The seal has an outer diameter of 260 *mm* and a tube diameter of about 2.5 *mm*. Loads are imposed in the calculation by specifying the displacement of the nodes along the top of the flange such that the final displaced state of 0.832 *mm* is reached in 20 increments. Ten additional increments are used to unload from the peak deformation for a total of 30 solution steps. Figure 24 shows the locations of the various materials in the mesh. The material behavior is modeled as elastoplastic with material parameters defined in Table 4.

Figure 25 shows deformed shapes corresponding to displacement increments of 0.208 *mm*, 0.416 *mm*, 0.624 *mm*, and 0.832 *mm*, respectively. Figure 26 shows the residual deformation after unloading. Contours of effective plastic strain in the Inconel X-750 are plotted for this state of deformation in Figure 27.

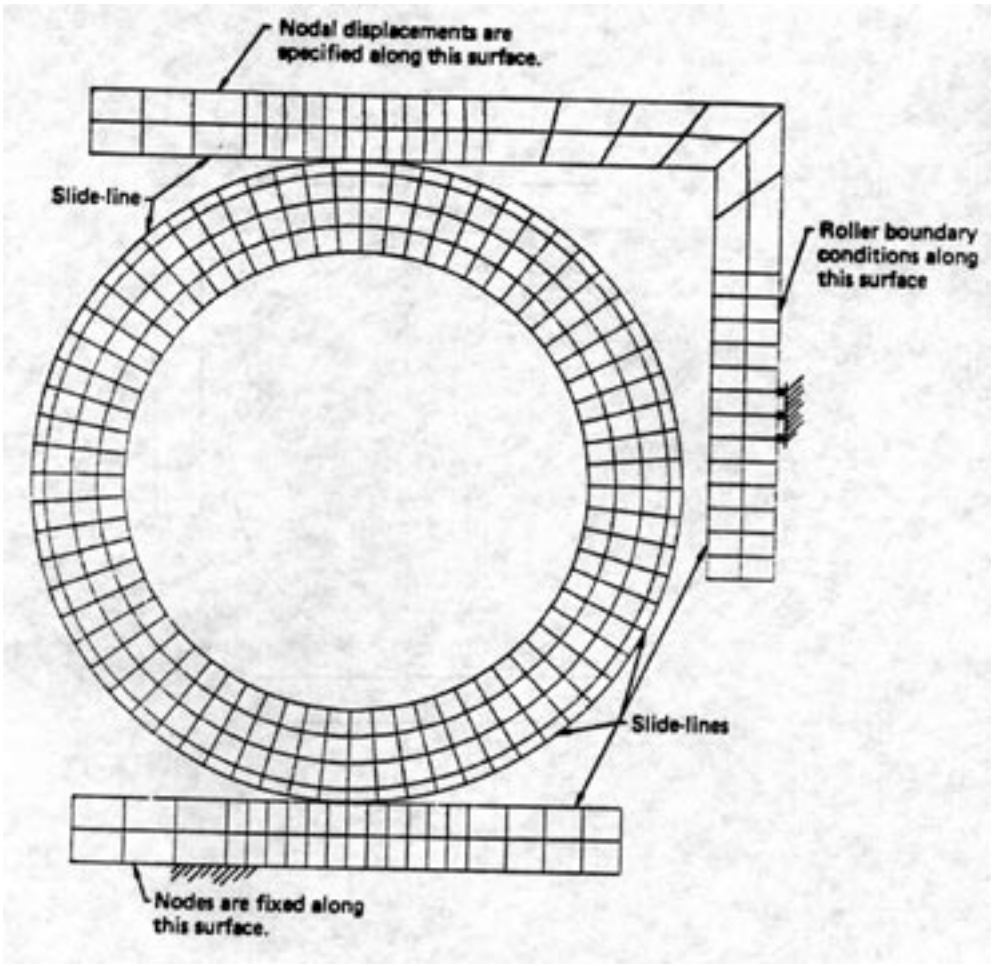

Figure 23
Axisymmetric finite element model of metallic O-ring.

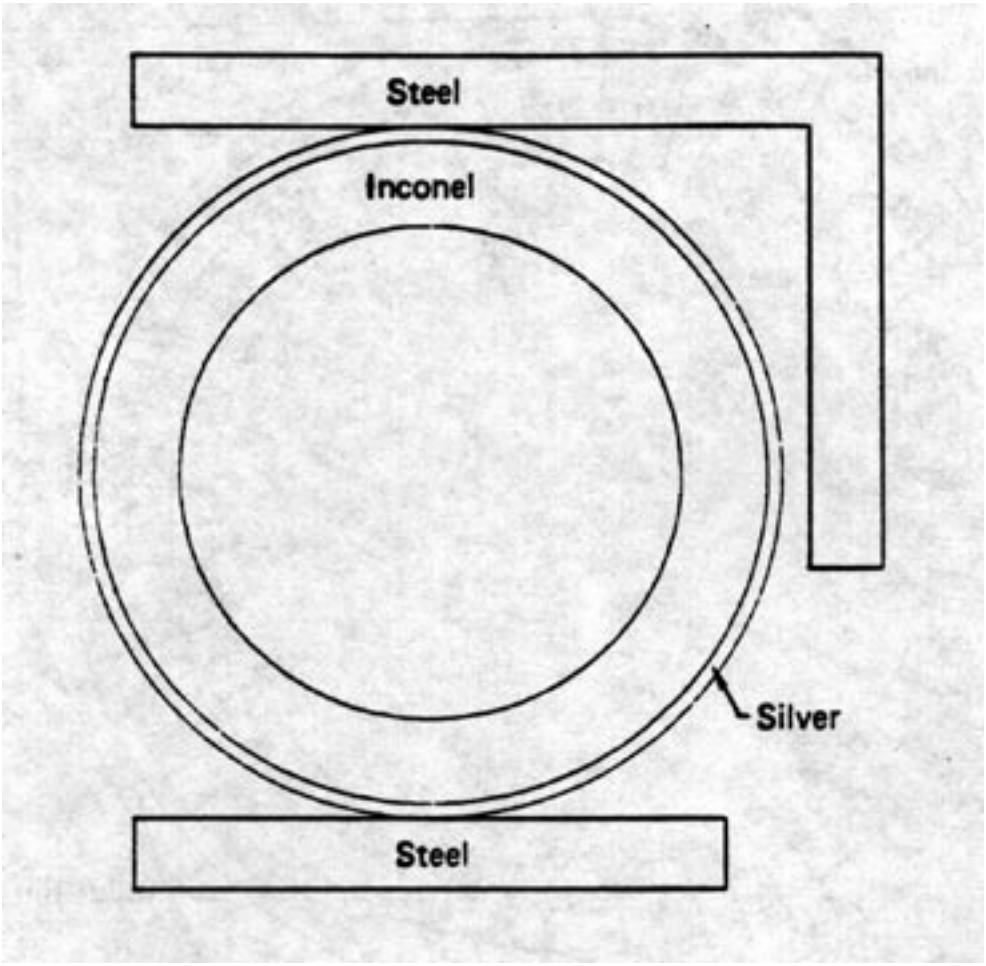

Figure 24
Location of materials used in O-ring mesh.

Table 4.
Material parameter values for O-ring calculation.

Parameter	Silver	Inconel x-750	Steel
E (GPa)	72.4	207.0	207.0
υ	0.37	0.30	0.30
σ_0 (GPa)	0.055	0.621	0.207
E_P (GPa)	0.144	0.689	0.689
β	1.0	1.0	1.0

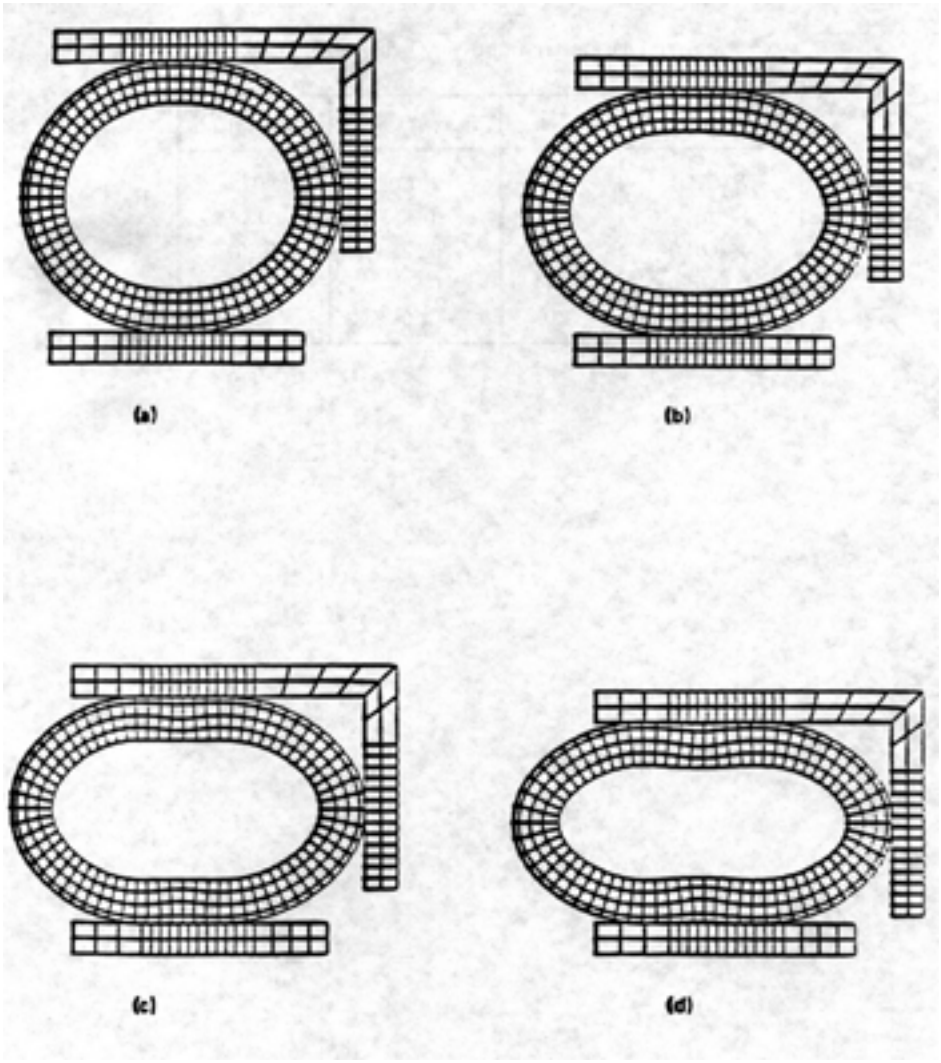

Figure 25
Deformed shapes corresponding to flange displacements of (a) 0.208 *mm*, (b) 0.416 *mm*, (c) 0.624 *mm*, and (d) 0.832 *mm*.

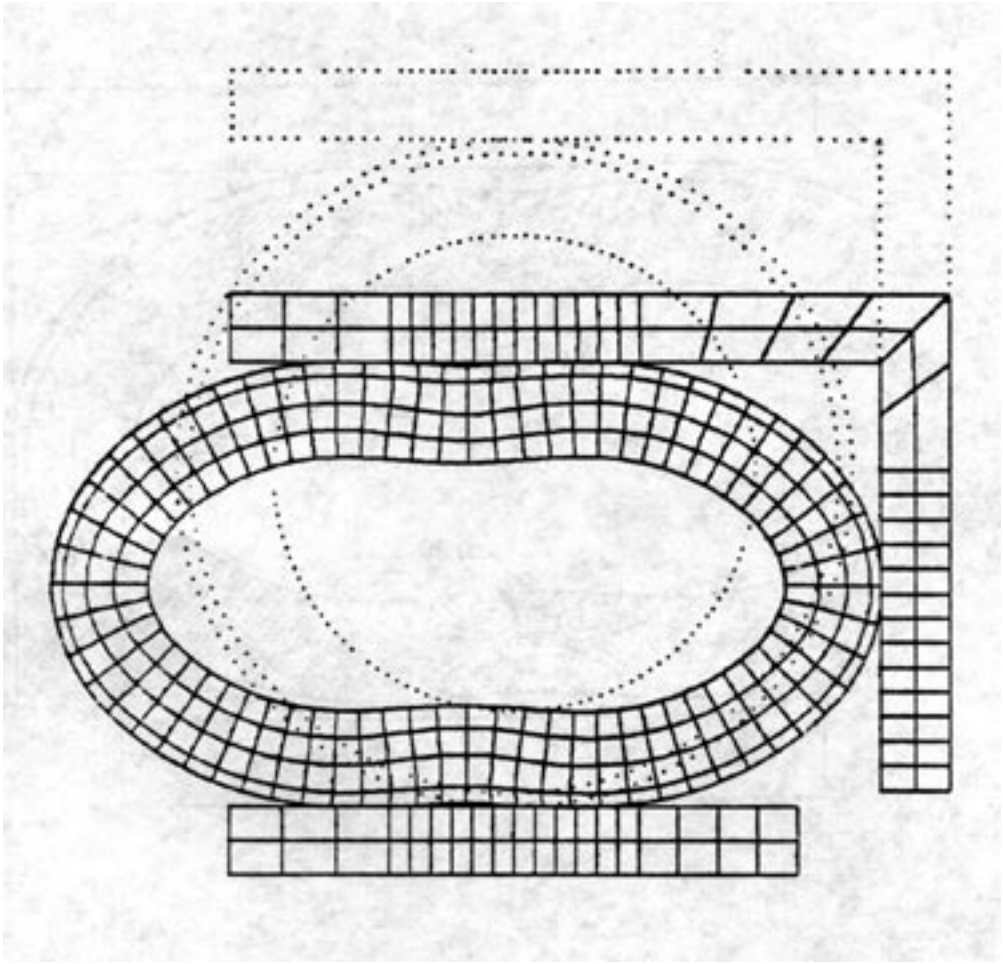

Figure 26
Deformed shape of O-ring after unloading.

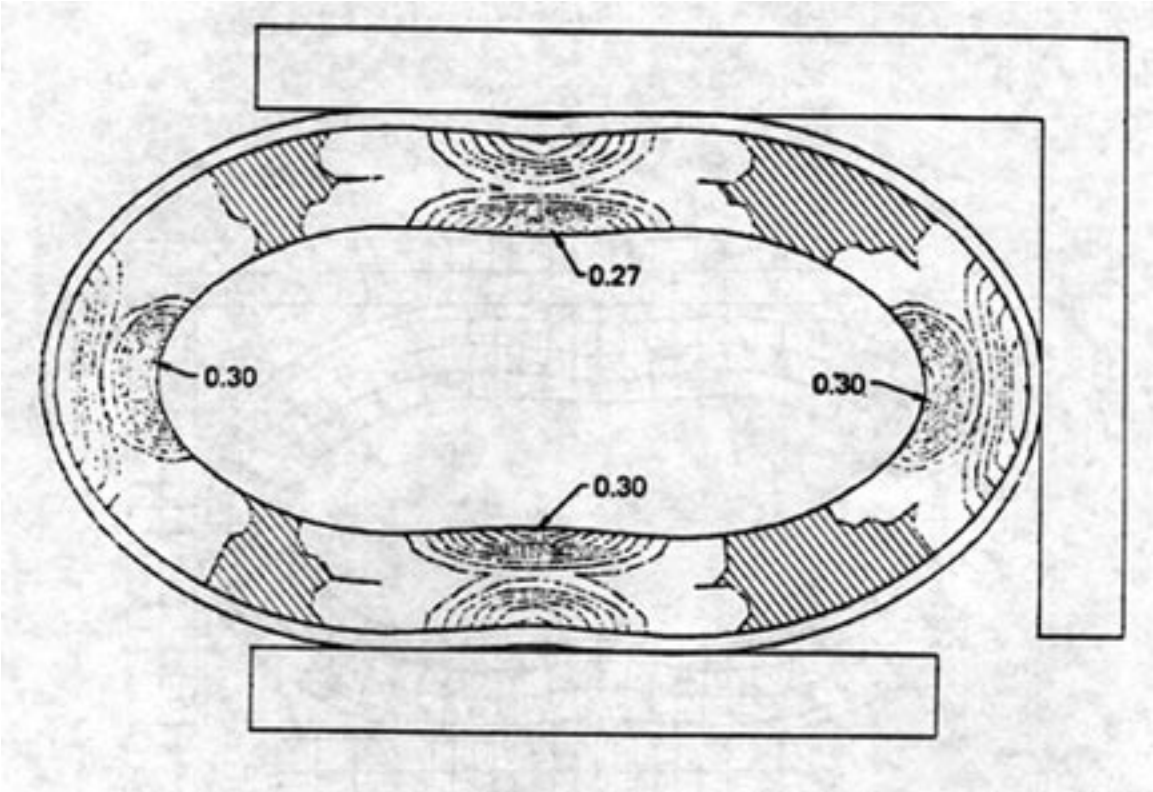

Figure 27
Contours for effective plastic strain in the Inconel X-750.
Elastic regions are shaded and the contour interval is 0.03 *mm/mm*.

7.4 BAR IMPACT ON A RIGID BOUNDARY

Computer simulations of a cylindrical bar impacting on a rigid wall are sometimes used to identify yield strengths of materials (e.g. Wilkins [1973]). Calculations with explicit codes like HEMP or DYNA2D may be costly since the governing Courant time-step size is controlled by the wave transient time across the smallest element. Elements at the impact end decrease in size, often considerably, and the time-step size drops. Because NIKE2D is unconditionally stable, its application to this class of problems is tempting. However, for NIKE2D to be competitive with explicit methods, a large time step size is required. As a result, details of elastic-plastic wave propagation response may be lost. In this example, NIKE2D and DYNA2D are applied to a bar impact problem, and their relative performance is evaluated.

A bar of radius 3.2 *mm* and length of 32.4 *mm* is modeled with 250 elements as shown in Figure 28. Roller boundary conditions are specified along the axis of symmetry and at the impact end. The initial z-velocity is 0.227 *mm*/μs. The material is assumed to be elastoplastic with E= 117.0 *GPa*, $\upsilon = 0.350$, $\sigma_0 = 0.4$ *GPa*, $E_p = 0.1$ *GPa*, $\beta = 1.0$, and $\rho = 8930$ kg/m^3. Isotropic hardening is assumed. Eighty time steps of 1 μs are used in the NIKE2D calculation with a convergence tolerance of 10^{-4}. DYNA2D requires over 13,000 time steps to complete the problem to 80 μs.

The time history of rigid body z-velocity is shown in Figure 29. Figure 30 shows the deformed shape at 80 μs. Comparing the results of NIKE2D and DYNA2D, the final length and final width of the impacting bar differ slightly. Physical quantities such as effective stress, pressure, and effective plastic strain are in excellent agreement. The maximum effective plastic strain occurs in the centerline element at the impact end and is computed as 3.18 *mm*/*mm* by NIKE2D, and as 3.05 *mm*/*mm* by DYNA2D. Contours of effective plastic strain at 80 μs are shown in Figure 31 where only minute differences between NIKE2D and DYNA2D can be discerned.

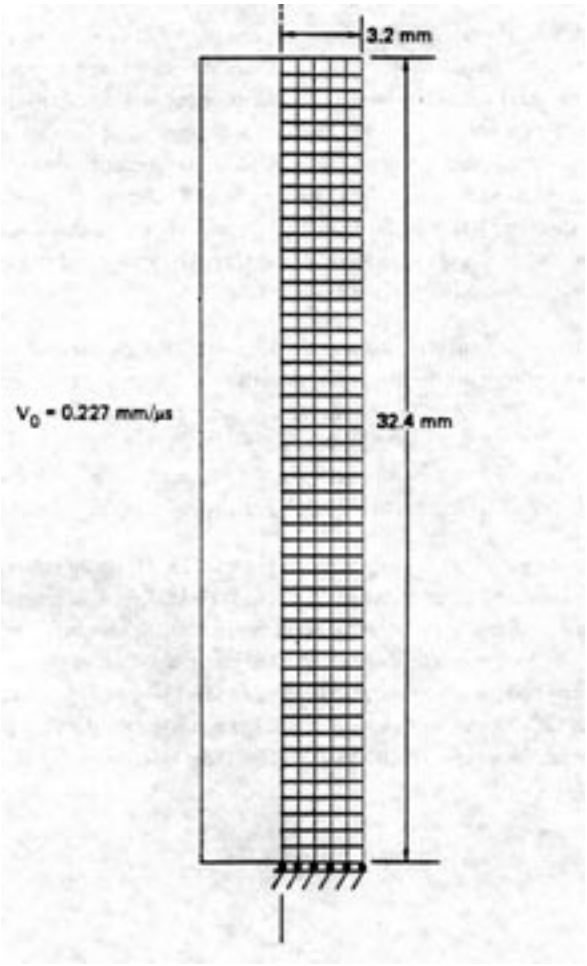

Figure 28
Finite element mesh used in bar impact calculations.

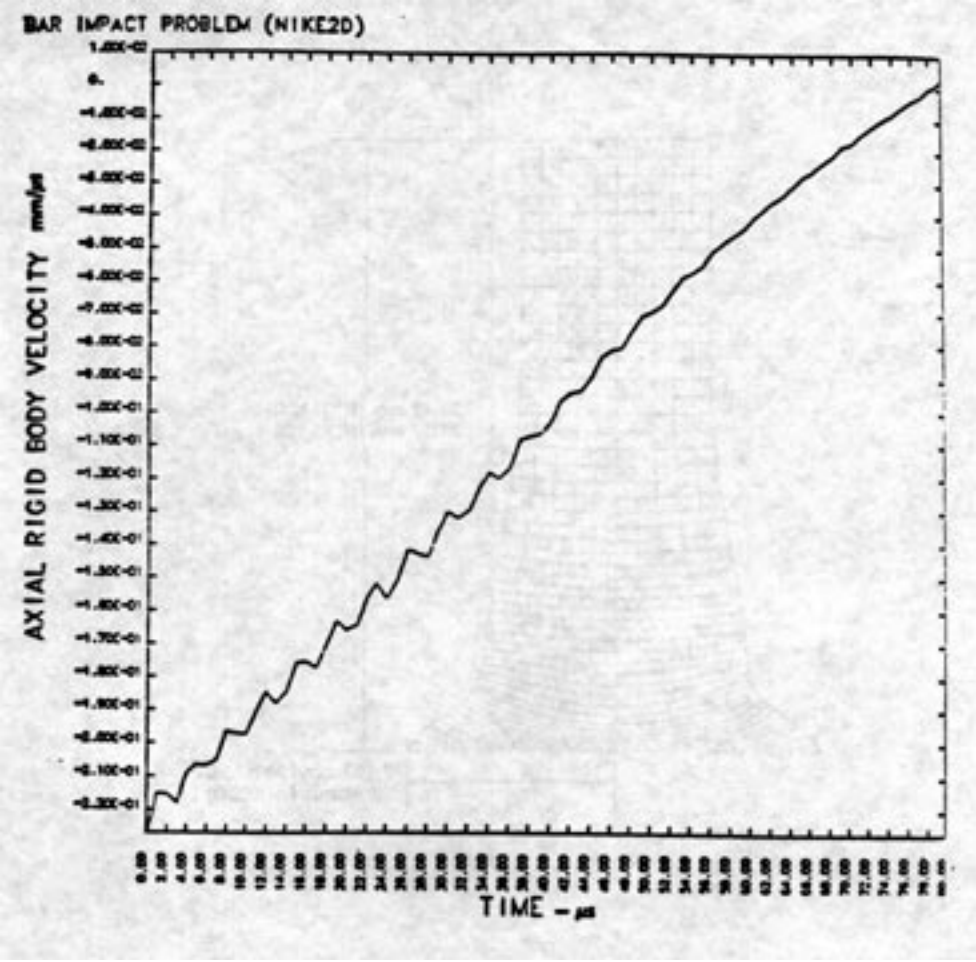

Figure 29
Rigid body velocity of bar.

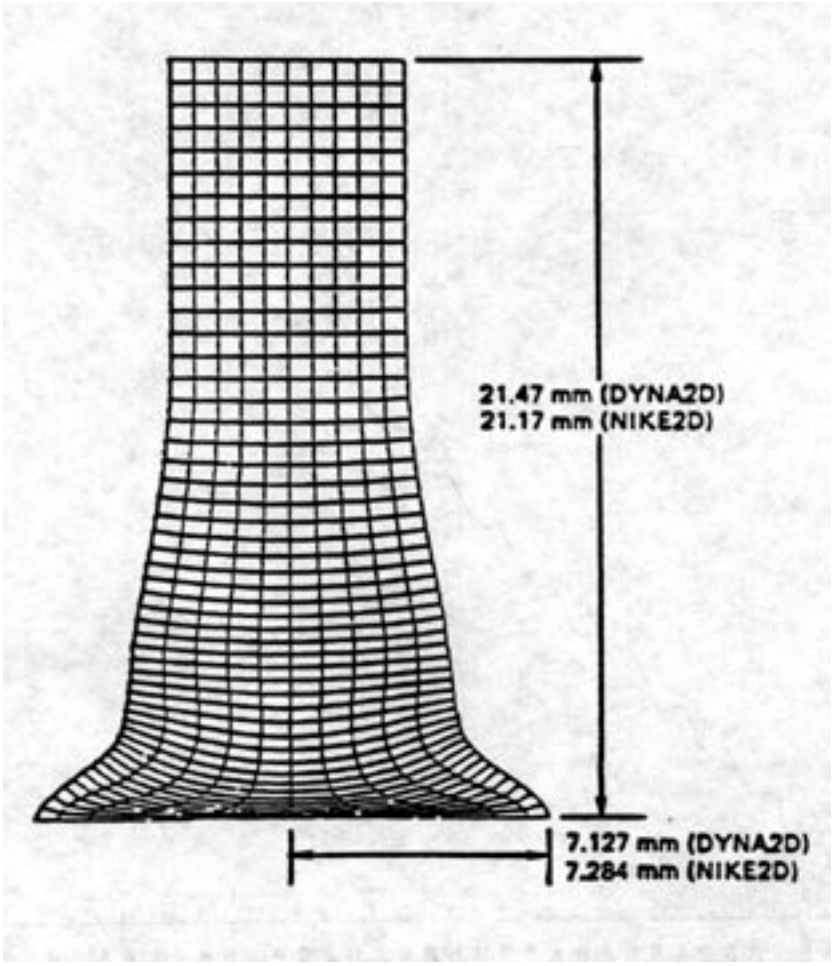

Figure 30
Final configuration at 80 μ*s* as computed by DYNA2D and NIKE2D.

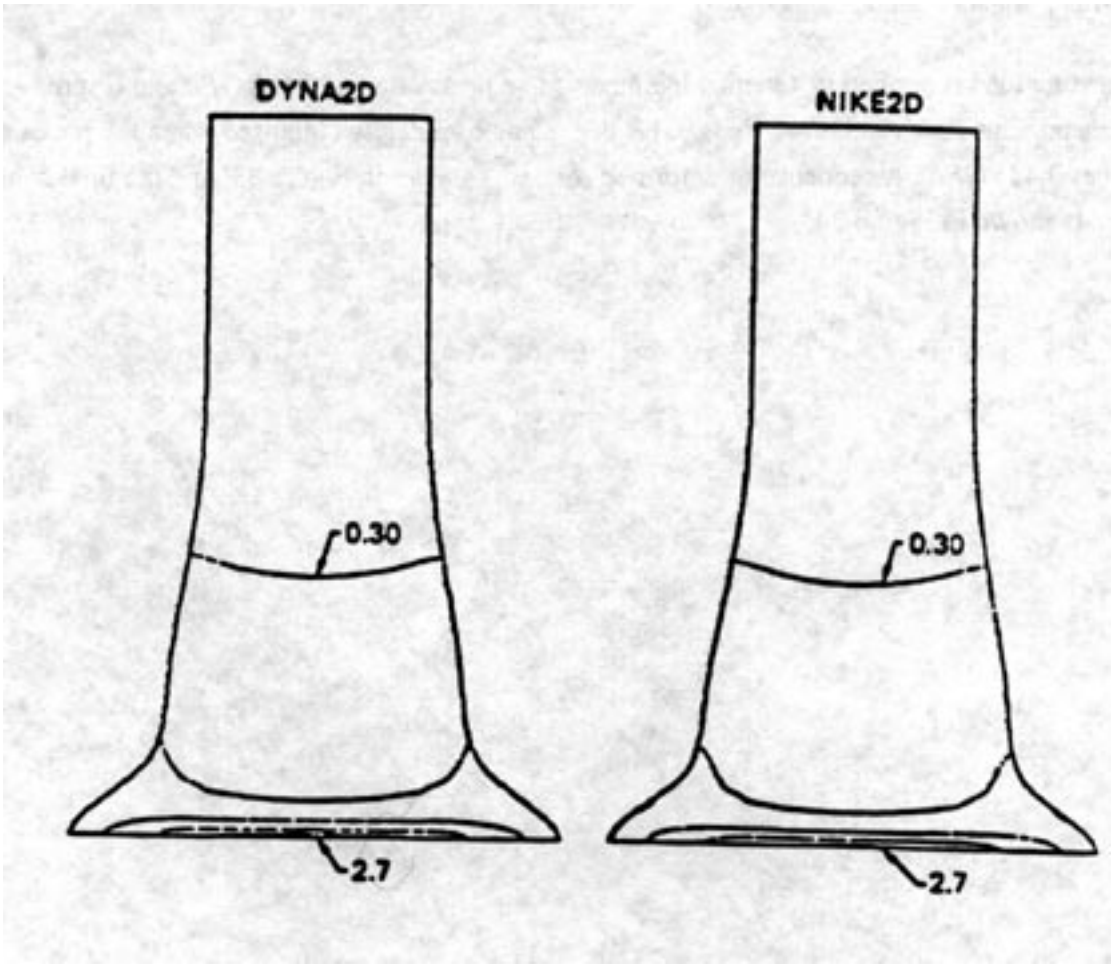

Figure 31
Contours of effective plastic strain at 80 μs. The contour interval is 0.60 *mm*/*mm*.

7.5 BELLOWS FORMING ANALYSIS

This example, contributed by Streit (1982), illustrates a problem involving a large amount of sliding along the contact interface. The purpose of the calculation is to determine the pressure required to collapse the stainless steel sleeve into the elastic die. Figure 32 shows the finite element mesh and boundary conditions.

A pressure load is applied in 43 equal increments to a peak value of 0.580 *GPa* and is removed in two increments for a total of 45 steps. The sleeve has completely collapsed when the pressure reaches 0.483 *GPa*. A sequence of deformed shapes is shown in Figure 33, and the final configuration is shown in Figure 34.

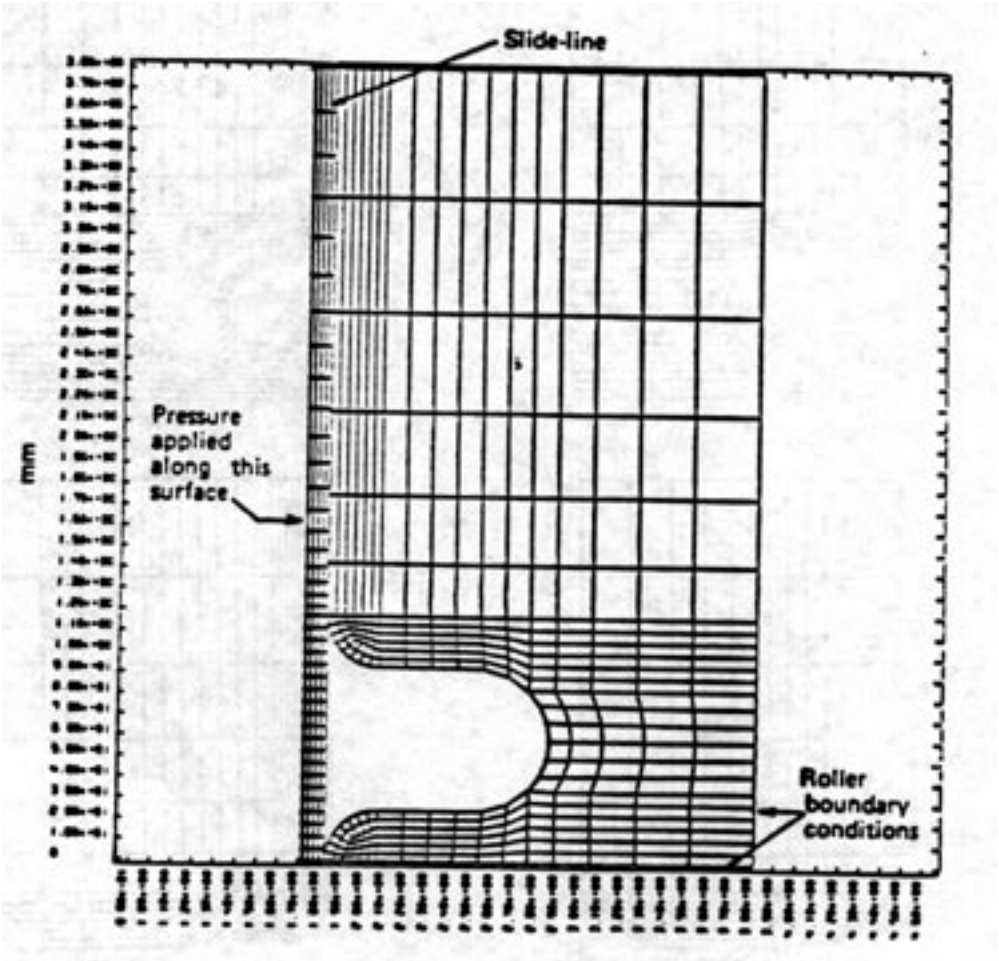

Figure 32
Finite element model for bellows forming problem.

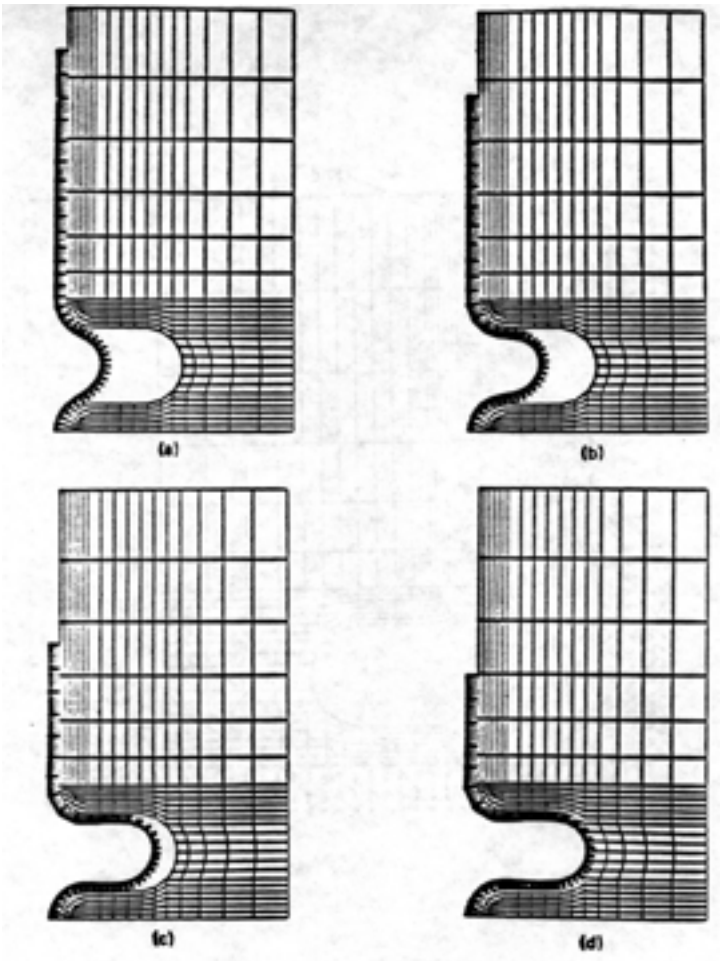

Figure 33
Deformed shapes corresponding to pressures of
(a) 0.138 *GPa*, (b) 0.276 *GPa*, (c) 0.414 *GPa*, and (d) 0.552 *GPa*.

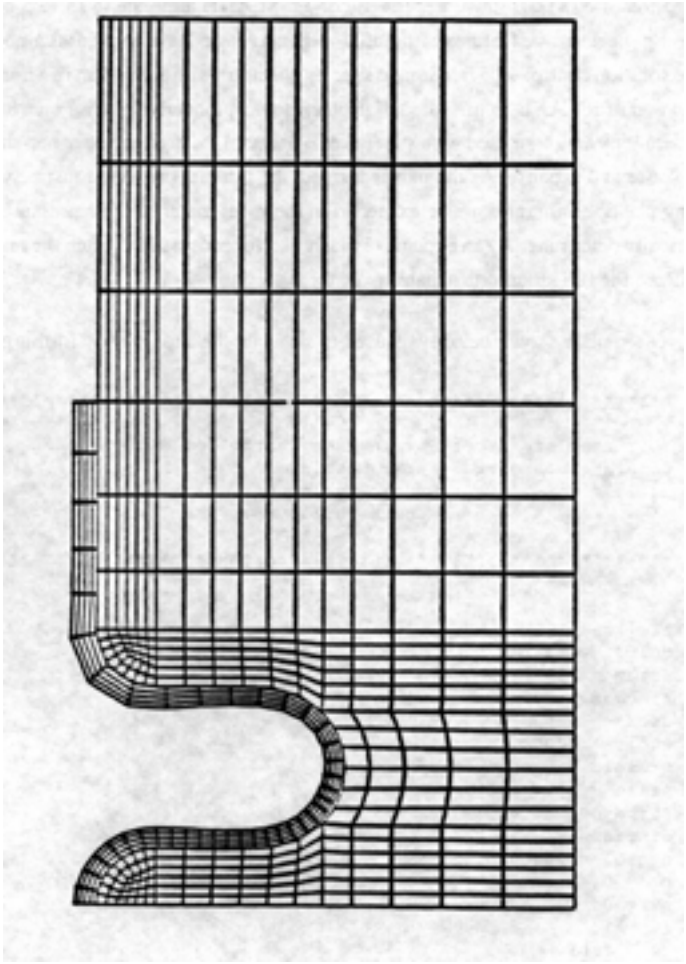

Figure 34
Final deformed shape after removal of pressure.

7.6 SUPERPLASTIC FORMING

This application of NIKE2D illustrates the use of an ISLAND template to solve a process control problem using the adaptive features of the ISLAND language. It demonstrates a powerful aspect of adaptive solution control - the freedom to specify constraints on a problem in a nonclassical way. The application of ISLAND to this class of problems was pioneered by Dr. Peter Raboin. Blow-forming operations are often used with superplastic materials to produce near-net-shape parts with minimum waste and expense. As the part is formed, the internal pressure must be varied in order that limiting plastic strain rates not be exceeded in the sheet material. This pressure variation has been historically determined by an expensive trial and error process, and often the resulting process has not utilized the full strain rate capability of the material.

The ISLAND template shown below was used to simulate the superplastic forming operation:

```
C ************************************************************************
c
c          template name: Strain Rate Controlled Blow-forming
c     template designers: Peter Raboin
c                         Bruce Engelmann
c                         Robert Whirley
c
c *************************** Initialization ***************************
c
global
   initialize
      delt_t = 1.
      nstep = 200
      timemax = 200.
      dtol = .0005
      etol = .0005
      presold = 0.
      prate = 10.
      strtarget = .01
      finerate = .5
      strtol = .00001
      p1 = 0.
      p2 = 0.
      f1 = 1.
      f2 = 1.01
      phase2 := false
   end
c
```

```
c ******************************Definition ******************************
c
   define
      c1 := disnormstp lt dtol
      e1 := engnorm lt etol
      converged := c1 or e1
      restrue := resnorm le 1.
      strrate = ecomp 43 materials 1 1
      strainfunc = strtarget - strrate
      funcpos := strainfunc gt 0.
      deltpres = prate * delt_t
      pressure = presold + deltpres
      s1 = p1 * f2
      s2 = p2 * f1
      s3 = s1 - s2
      s4 = f2 - f1
      secant = s3 / s4
      absfunc = abs strainfunc
      bangit := absfunc lt strtol
   end
c
c******************************** Set *********************************
c
   set
      idisplay 1
      iprint 1
      iplotdata 1
      iresdump 10
      ibackfile 1
      islandplot pressure strrate prate &
                 disnormstp engnorm resnorm
   end
c
c ************************ Timestep Procedure ************************
c
timestep
   batch
      timeloop 0 nstep timemax
      calltrial
      presold = pressure
      updateloop
      display summary
      done
   end
c
```

```
c ************************ Timetrial Procedure ***************************
c
timetrial
   batch
      loadset 1 pressure
      callsolve delt_t
      p1 = prate
      f1 = strainfunc
      prate = prate + finerate while funcpos
      prate = prate = finerate until funcpos
      loadset 1 pressure
      callsolve delt_t
      loop 10
      p2 = prate
      f2 = strainfunc
      prate = secant
      loadset 1 pressure
      callsolve delt_t
      p1 = p2
      f1 = f2
      endloop
   end
c
c ************************ Solution Procedure ***************************
c
solution
   override
      while converged
        display pressure
        display strrate
        until phase2
          nextstep while funcpos
          phase2 := .true.
          nexttrial
        enduntil
        nextstep while bangit
        nextrial
      endwhile
   end
   batch
      loop 15
      bfgs 10 while reform
      reform 1
      endloop
      display pressure
      display strrate
      nextstep while bangit
      nextrial
   end
timestep
   start
c
c ***********************************************************************
```

This solution template was developed to adjust the internal pressure at each step so that a target effective plastic strain rate was achieved. The time history of applied pressure computed with ISLAND is shown in Figure 35. The mesh configuration at the beginning, middle, and end of the simulation is shown in Figure 36. Figure 37 shows the time history of effective plastic strain rate averaged over the critical sheet material. Experience has shown this time variation of pressure to be an extremely difficult function to determine by trial and error analysis. Thus, ISLAND was used to effectively solve an external constraint equation that limited the plastic strain rate, in addition to controlling the normal solution of the nonlinear finite element equations at each step. The important results from this analysis are not only the predicted deformed shape and strain rates in the sheet material, but also the pressure variation computed with ISLAND to achieve the desired shape. The pressure variation can then be directly used in production manufacturing to confidently produce blow-formed superplastic parts with a minimum of trial and error.

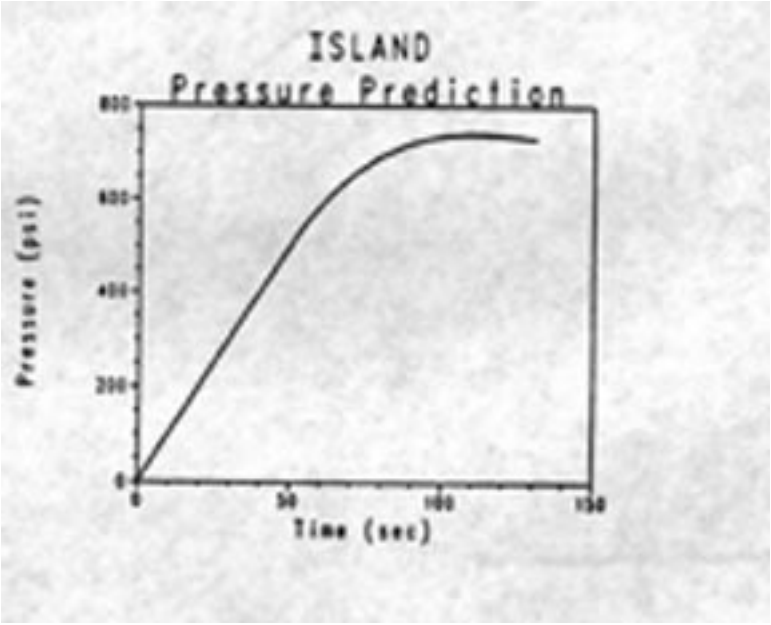

Figure 35
Time variation of pressure used to achieve the desired part using a blow-forming process with a superplastic material. These values were computed with ISLAND to satisfy an external inequality constraint on the average plastic strain rate within the critical sheet material.

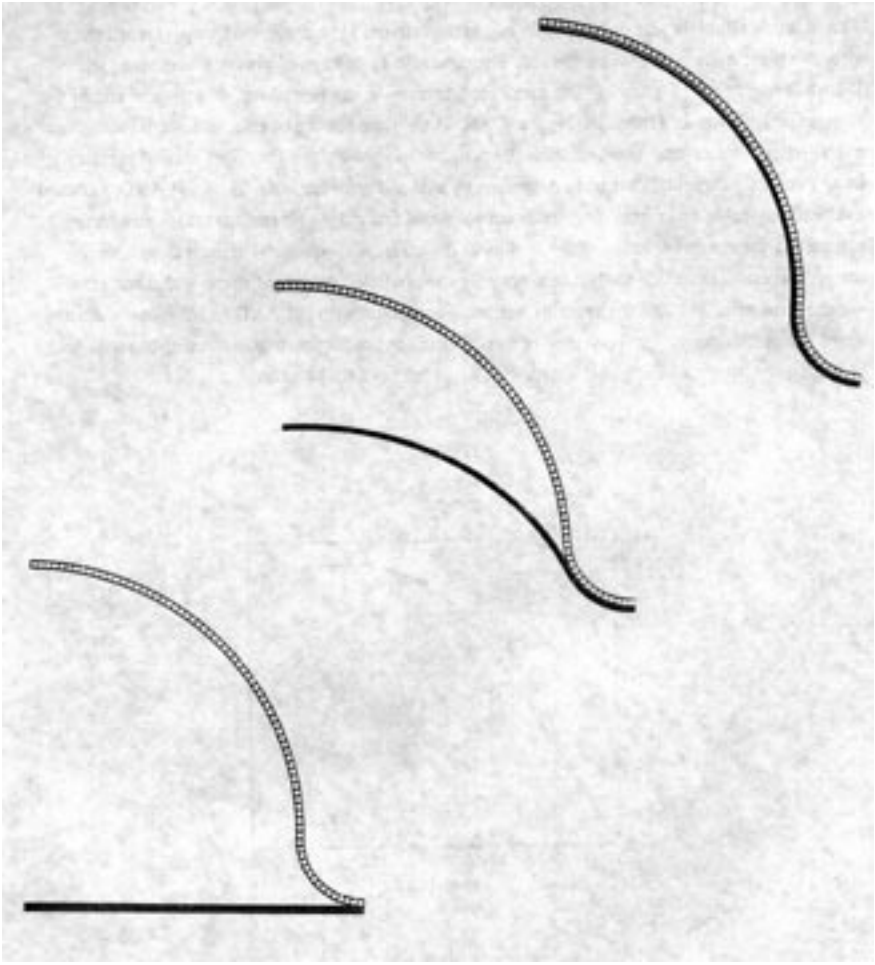

Figure 36
Predicted geometry at the beginning, middle and end of the simulation. Note the uniform wall thickness predicted in the completed part. This results from carefully controlled plastic strain rates in the sheet during the forming process.

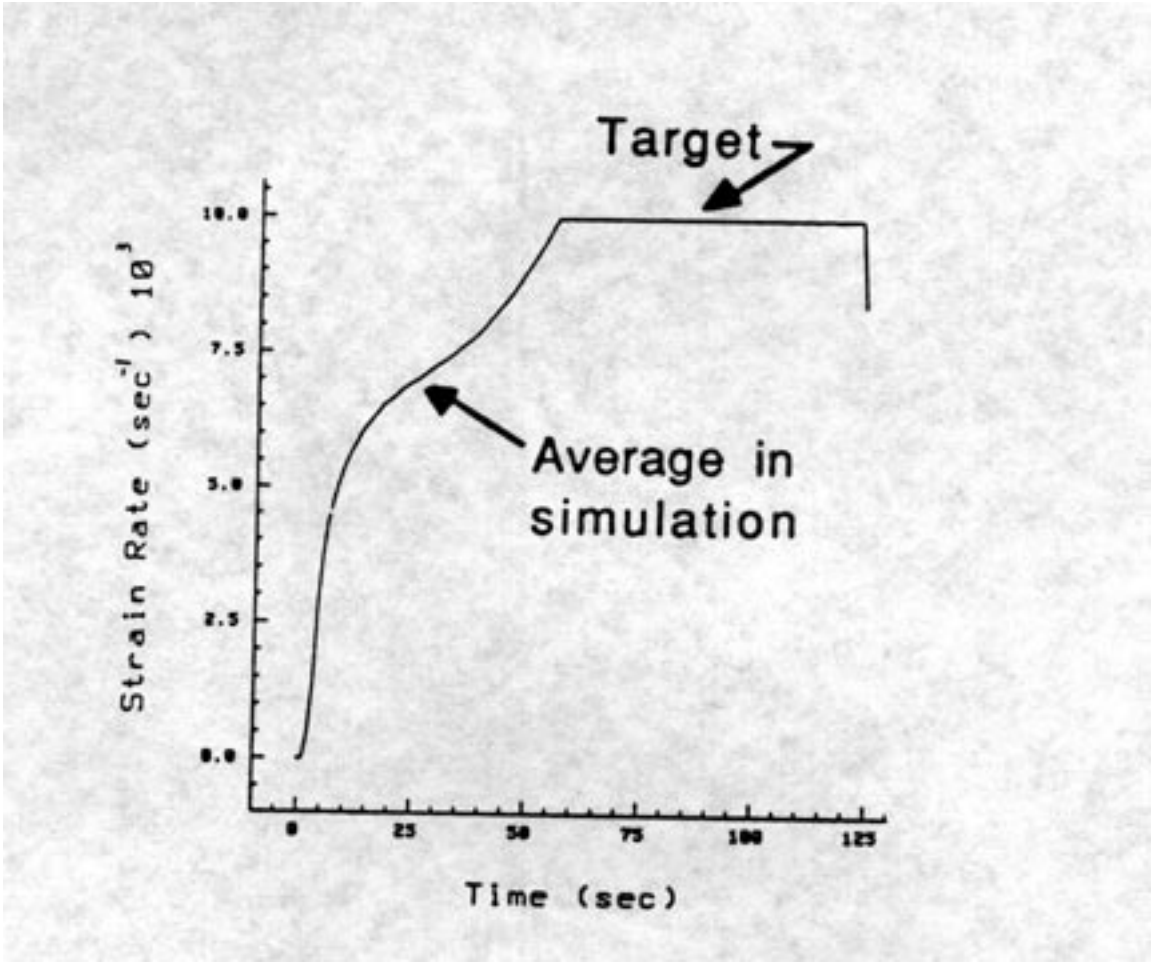

Figure 37
Time history of the average effective plastic strain rate in key regions of the sheet. ISLAND was used to limit the average effective plastic strain rate to less than 0.01.

8.0 SUBSET OF MAZE COMMANDS

The following is a description of a subset of MAZE commands used to generate analysis options in the problem definition and solution definition sections of the input file. When commands are not used, the generated default value is zero unless otherwise indicated.

af *analopt* Analysis flag on problem definition card 5. When

analopt = -2, dynamic analysis, statically initialized is indicated,

analopt = -1, dynamic analysis is indicated,

analopt = 0, quasistatic analysis is indicated,

analopt = N, eigenvalue analysis is indicated, with N eigenvalues and eigenvectors extracted.

asiz *arcsize* Initial arc length size on solution definition card 2. When

arcsize = 0, the arc length size is based on the time step size,

arcsize > 0, it represents the initial arc length size.

bwmo *ibandopt* Bandwidth minimization flag on problem definition card 5. When

ibandopt = 0, bandwidth minimization is not performed,

ibandopt = 1, bandwidth minimization is performed.

delt *stepsize* Time step size, *stepsize,* on solution definiton card 1.

dctol *dtol* Convergence tolerance on displacements, *dtol* (default value is 0.001), on solution definition card 1.

ectol *etol* Convergence tolerance on energy, *etol* (default value is 0.01), on solution definition card 1.

eff *elemform* Element formulation flag on problem definition card 4. When

elemform = 0, the B-bar form of the material tangent matrix is used,

elemform = 1, the old NIKE2D formulation is used.

iacn *methcon* Arc length constraint method on solution definition card 2. When

methcon = 0, Crisfield's constraint method is used,

methcon = 1, Ramm's constraint method is used.

iadc *idispflag* Arc length displacement control flag on solution definition card 2. When

idispflag = 0, displacement norm is used,

idispflag > 0, it is the node number for arc length displacement control.

iadm *idamp* Arc length damping flag on solution definition card 2. When

idamp = 0, no arc length damping is specified,

idamp = 1, arc length damping is specified.

iadr *idir* Direction for nodal arc length displacement control on solution definition card 2. When

idir = 1, r-direction is used for control,

idir = 2, z-direction is used for control.

iaum *munload* Arc length unloading method on solution defintion card 2. When

munload = 1, BFGS updates are used during unloading,

munload = 2 Broyden updates are used during unloading,

munload = 3, DFP updates are used during unloading,

munload = 4, Davidon symmetric updates are used during unloading,

munload = 5, modified Newton procedure is used during unloading.

iepd *iplotflag* Element plot database flag on problem definition card 4. When

iplotflag = 0, element energy is stored in the plot database,

iplotflag = 0, element thickness is stored in the plot database,

iplotflag = 0, element temperature is stored in the plot database.

igm *igeometry* Geometry type on problem definition card 5. When

igeometry = 0, an axisymmetric geometry is indicated,

igeometry = 1, a plane strain geometry is indicated,

igeometry = 2, a plane stress geometry is indicated.

igs *istifflag* Geometric stiffness flag on solution definition card 3. When

istifflag = 0, the geometric stiffness is not used,

igeomflag = 1, the geometric stiffness is used.

ioosf *icoreflag* Out-of-core solution flag on problem definition card 5. When

icoreflag = 0, in-core solution of finite element equations is performed,

icoreflag = 1, out-of-core solution of equations is performed.

itcurve *numcurve* Load curve for temperature vs. time on problem definition card 4. Parameter *numcurve* is the load curve number.

itrf *refopt* Reference temperature flag on problem definition card 4. When

refopt = 0, nodal reference temperatures are not specifed,

refopt = 1, nodal reference temperatures are specified.

lst *lstol* Line search tolerance, *lstol,* on solution definition card 3.

msrf *imsrf* Maximum number of stiffness reformations per time step, *imsrf*, on solution definition card 1.

naus *nunload* Number of arc length unloading steps, *nunload,* on solution definition card 2.

nbei *inbei* Number of time steps between equilibrium iterations, *inbei,* on solution definition card 1.

nbsr *inbsr* Number of time steps between stiffness matrix reformations, *inbsr,* on solution definition card 1.

neig *igeomtype* Geometry type on problem definition card 5. When

igeomtype = 0, axisymmetric geometry is specifed

igeomtype = 1, plane strain geometry is specified

igeomtype = 2, plane stress geometry is specified

nibsr *inibsr* Maximum number of equilibrium iterations allowed between stiffness matrix reformations, *inibsr,* on solution definition card 1.

nip1 *gamma* Newmark paramter γ on problem definition card 5. Parameter *gamma* has a default value of 0.5.

nip2 *beta* Newmark paramter β on problem definition card 5. Parameter *beta* has a default value of 0.25.

nsmd *mthsol* Standard solution method flag on solution definition card 1. When

mthsol = 1, BFGS updates are used,

mthsol = 2 Broyden updates are used,

mthsol = 3, DFP updates are used,

mthsol = 4, Davidon symmetric updates are used,

mthsol = 5, modified Newton procedure is used,

mthsol = 6, arc length method is used,

mthsol = 7, arc length method with line search is used,

mthsol = 8, arc length method with BFGS updates is used,

mthsol = 9, arc length method with Broyden updates is used,

mthsol = 10, arc length method with DFP updates is used,

mthsol = 11, arc length method with modified BFGS updates is used,

mthsol = 12, arc length method with Davidon symmetric updates is used.

nstep *numsteps* Number of time steps, *numsteps,* on solution definition card 1.

pcm *ipercent* Percent of computer to be used on problem definition card 5. Parameter *ipercent* specifies the maximum percent of computer memory to be used, when applicable.

plti *intplot* Step interval, *intplot,* for plotting on solution definition card 1.

prti *intprint* Step interval, *intprint,* for printing on solution definition card 1.

rffc *redfac* Reduction factor for frictional slidelines, *redfac,* on solution definition card 3.

rlt *reztol* Rezoner least squares fit tolerance, *reztol,* on solution definition card 3.

sbrf *intres* Step interval *intres* for regular restart dumps on solution definition card 1.

siar *intrez* Step interval, *intrez,* for automatic rezoning on solution definition card 1.

sm *methsol* Solution method on problem definition card 5. When

methsol = 0, a fixed step strategy is indicated,

methsol = 1, an adaptive ISLAND strategy is indicated.

sst *stifftol* Slideline stiffness insertion tolerance, *stifftol,* on solution definition card 3.

teo thermopt Thermal option flag on problem definition card 4. When

teo = 0, no thermal effects are considered,

teo = 1, nodal temperatures are spatially invariant and are determined from a load curve at each step,

teo = 2, nodal temperatures are determined from specified nodal vectors and a load curve at each step,

teo = -1, nodal temperatures are determined by reading in a new temperature state from a TOPAZ2D plotfile at each time step,

teo = -2, nodal temperatures are interpolated from temperature states in a TOPAZ2D plotfile,

teo = -3, initial nodal temperatures are assigned the nodal reference temperature and the final temperatures are determined from a steady-state TOPAZ2D plotfile.

title *charstring* Title definition on problem definition card 1. Character string *charstring* is the analysis heading to appear on the output.

ACKNOWLEDGEMENTS

First, the author would like to express his deep appreciation to Ms. Pat Marten for her patience and skillful typing in the preparation of this report. The clerical support of Ms. Nikki Falco and Ms. Valli James is also gratefully acknowledged.

Second, since many of the developments in NIKE2D have been a collaborative effort of all the members of the Methods Development Group, I would like to thank Dr. Robert G. Whirley, Dr. Bradley N. Maker, Dr. Robert M. Ferencz, Mr. Thomas E. Spelce, and Dr. Jerry Goudreau. In addition, the day to day feedback from Dr. Peter J. Raboin and other members of the analysis community is very much appreciated.

Finally, I would like to again acknowledge Dr. John O. Hallquist for his extensive contributions to both computational mechanics and the development of the NIKE2D code.

REFERENCES

Bammann, D. J., "An Internal Variable Model of Viscoplasticity," Int. J. Eng. Sci., 22, pp. 1041-1053, (**1984**).

Bammann, D. J., and G. J. Johnson, "A Strain Rate Dependent Flow Surface Model of Plasticity," to appear, (**1990**).

Bathe, K. J., Finite Element Procedures in Engineering Analysis, Prentice-Hall, (1982).

Bathe, K. J., E. L. Wilson, and R. H. Iding, "NONSAP, A Structural Analysis Program for Static and Dynamic Responses of Nonlinear Systems," Rept. No. UCSESM 74-3, University of California, Berkeley, (**1974**).

Chen, W. F. and Baladi, G. Y., *"*Soil Plasticity: Theory and Implementation*"*, Elsevier, New York, (**1985**).

Crisfield, M. A., "A Fast Incremental/Iterative Solution Procedure that Handles Snap Through," Computers and Structures, 13, pp. 55-62, (**1981**).

Engelmann, B. E., and R. G. Whirley, "ISLAND: Interactive Solution Language for An Adaptive Nike Driver - User Manual," University of California, Lawrence Livermore National Laboratory, Rept. UCID, (**1991**).

Engelmann, B. E., R. G. Whirley, and A. B. Shapiro, "PALM2D: A Nonlinear Finite Element Program for the Coupled Thermomechanical Response of Solids in Two Dimensions," University of California, Lawrence Livermore National Laboratory, Rept. UCID-21868, (**1990**).

Flower, E. C., and D. J. Nikkel, Jr., "A guide to Using Material Model #11 in NIKE2D: An Internal Variable, Viscoplasticity Model," University of California, Lawrence Livermore National Laboratory, Rept. UCRL-ID-105245, (**1990**).

Gibbs, N. E., W. G. Poole, Jr., and P. K. Stockmeyer, "An Algorithm for Reducing the Bandwidth and Profile of a Sparse Matrix," SIAM J. Num. Anal., 13, 236, (**1976**).

Giroux, E. D., HEMP User's Manual, Lawrence Livermore National Laboratory, Rept. UCRL-51079, (**1973**).

Goudreau, G. L., and J. O. Hallquist, "Recent Developments in Large Scale Finite Element Hydrocode Technology," J. Comp. Meths. Appl. Mechs. Eng., 30, pp. 725-757, (**1982**).

Hallquist, J. O., "A Numerical Treatment of Sliding Interfaces and Impact," in Computational Techniques for Interface Problems, AMD Vol. 30, K. C. Park and D. K. Gartling (eds.), ASME, New York, (**1978**).

Hallquist, J. O., "MAZE - An Input Generator for DYNA2D and NIKE2D," University of California, Lawrence Livermore National Laboratory, Rept. UCID-19029, (**1983**).

Hallquist, J. O., "NIKE2D: A Vectorized Implicit, Finite Deformation, Finite Element Code for Analyzing the Static and Dynamic Response of 2-D Solids with Interactive Rezoning and Graphics," University of California, Lawrence Livermore National Laboratory, Rept. UCID-19677, (**1986**).

Hallquist, J. O., "NIKE2D: An Implicit, Finite Deformation, Finite Element Code for Analyzing the Static and Dynamic Response of Two-Dimensional Solids," University of California, Lawrence Livermore National Laboratory, Rept. UCRL-52678, March, (**1979**).

Hallquist, J. O., "User's Manual for DYNA2D - An Explicit Two-Dimensional Hydrodynamic Finite Element Code with Interactive Rezoning," University of California, Lawrence Livermore National Laboratory, Rept. UCID-18756, Rev. 3, (**1987**).

Hallquist, J. O., G. L. Goudreau, and D. J. Benson, "Sliding Interfaces with Contact-Impact in Large-Scale, Lagrangian Computations," Comp. Meths. Appl. Mechs. Eng., 51, pp. 107-137, (**1985**).

Hallquist, J. O., and J. L. Levatin, "ORION: An Interactive Color Post-Processor for Two Dimensional Finite Element Codes," University of California, Lawrence Livermore National Laboratory, Rept. UCRL-19310, (**1985**).

Hughes, T. J. R., "Generalization of Selective Integration Procedures to Anisotropic and Nonlinear Media," *Int. Journal for Numerical Methods in Engineering*, Vol. 15, No. 9, pp. 1413-1418, (**1980**).

Hughes, T. J. R., "The Finite Element Method," Prentice-Hall, Englewood Cliffs, N. J., (**1987**).

Isenberg, J., Vaughn, D. K., and Sandler, I., “Nonlinear Soil-Structure Interaction,” EPRI Report MP-945, Weidlinger Associates, December, (**1978**).

Jones, R. E., "QMESH: A Self-Organizing Mesh Generation Program: Rept. SLA-73-1088, Sandia National Laboratories, Albuquerque, N.M., (**1974**).

Kenchington, C. J., "A Non-Linear Elastic Material Model for DYNA3D," Proceedings from DYNA3D User Group Conference 1988, London, pp. 28-39, September 29, (**1988**).

Key, S. W., "A Finite Element Procedure for Large Deformation Dynamic Response of Axisymmetric Solids," *Computer Methods in Applied Mechanics and Engineering*, 9, pp.195-218, (**1974**).

Key, S. W., "HONDO - A Finite Element Computer Program for the Large Deformation Dynamic Response of Axisymmetric Solids," Rept. No. 74-0039, Sandia Laboratories, Albuquerque, New Mexico, (**1974**).

Key, S. W., J. H. Biffle, and R. D. Kreig, "A Study of the Computational and Theoretical Differences of Two Finite Strain Elastic-Plastic Constitutive Models," U. S.-Germany Symposium on Finite Element Analysis, Massachusetts Institute of Technology, Cambridge, MA, (**1976**).

Krieg, R. D., "Numerical Integration of Some New Unified Plasticity - Creep Formulations," SMiRT-4, M6/4, (**1977**).

Krauss, T., private communication, Deformation Control Technology, Inc., Cleveland Ohio, (**1990**).

Maker, B. N., R. M. Ferencz, and J. O. Hallquist, "NIKE2D: A Nonlinear, Implicit, Three-Dimensional Finite Element Code-User's Manual," University of California, Lawrence Livermore National Laboratory, Rept. UCRL-MA-105268, (**1991**).

Marsden, J. E., and T. J. R. Hughes, Mathematical Foundations of Elasticity, Prentice-Hall, (**1983**).

Matthies, H,. and G. Strang, "The Solution of Nonlinear Finite Element Equations," Int. Journal for Numerical Methods in Engineering, Vol. 14, No. 11, pp. 1613-1626, (**1979**).

Nagtegaal, J. C., D. M. Parks, and J. R. Rice, "On Numerically Accurate Finite Element Solutions in the Fully Plastic Range," *Comput. Methods Appl. Mech. Eng.,* 4, 153, (**1974**).

Norris, D. M., Jr., B. Moran, J. K. Scudder, and D. F. Quinones, J. Mech. Phys. Solids, 26, pp. 1-19, (**1978**).

Raboin, P. J., "A Deformation-Mechanism Material Model for NIKE2D," University of California, Lawrence Livermore National Laboratory, Rept. UCRL-104202, (**1990**).

Ramm, E., "Strategies for Tracing Nonlinear Response Near Limit Points," Europe-U. S. Workshop: Nonlinear Finite Element Analysis in Structural Mechanics, Eds. Bathe, Stein, and Wunderlich, Springer-Verlag, Berlin, pp. 63-89, (**1980**).

Riks, E., "An Incremental Approach to the Solution of Snapping and Buckling Problems," International Journal of Solids and Structures, Vol. 15, pp. 529-551, (**1979**).

Sandler, I. S., and D. Rubin, "An Algorithm and a Modular Subroutine for the Cap Model," *International Journal of Numerical and Analytic Methods in Geomechanics*, Vol. 3, pp. 173-186, (**1979**).

Schweizerhof, K. H., private communication, (**1986**).

Schweizerhof, K. H., and E. Ramm, "Combining Quasi-Newton and Arc-Length Methods for the Analysis of Nonlinear Problems into the Postlimit Range," unpublished paper, (**1986**).

Schweizerhof, K. H., and P. Wriggers, "Consistent Linearization for Path Following Methods in Nonlinear FE Analysis," to be published in Comp. Meth. Appl. Mech. and Engng., (**1987**).

Shapiro, A. B., "TOPAZ3D: A Three-Dimensional Finite Element Heat Transfer Code," University of California, Lawrence Livermore National Laboratory, Rept. UCID-20484, (**1985**).

Shapiro, A. B., and A. L. Edwards, "TOPAZ2D Heat Transfer Code Users Manual and Thermal Property Data Base," University of California, Lawrence Livermore National Laboratory, Rept. UCRL-ID-104558, (**1990**).

Simo, J. C., J. W. Ju, K. S. Pister and R. L. Taylor, "An Assessment of the Cap Model: Consistent Return Algorithms and Rate Dependent Extension," *Journal of Engineering Mechanics*, Vol. 114, No. 2, pp. 191-218, (**1988**).

Simo, J. C., P. Wriggers, K. H. Schweizerhof, and R. L. Taylor, "Finite Deformation Postbuckling Analysis Involving Inelasticity and Contact Constraints," Innovative Methods for Nonlinear Problems, Eds. Liu, Belytschko, and Park, Pineridge, Press Int. Ltd., Swansea, pp. 365-387, (**1984**).

Spelce, T. E., and J. O. Hallquist, "TAURUS: An Interactive Post-Processor for Analysis Codes NIKE3D, DYNA3D, TOPAZ3D, and Gemini," University of California, Lawrence Livermore National Laboratory, Rept. UCID, (**1990**).

Streit, R. D., private communication, Lawrence Livermore National Laboratory, (**1982**).

Stillman, D. W., and J. O. Hallquist, "INGRID: A Three-Dimensional Mesh Generator for Modelling Nonlinear Systems," University of California, Lawrence Livermore National Laboratory, Rept. UCID-20506, (**1985**).

Taylor, R. L., E. L. Wilson, and S. J. Sackett, "Direct Solution of Equations by Frontal and Variable Band Active Column Methods," Europe-U. S. Workshop: Nonlinear Finite Element Analysis in Structural Mechanics, Eds. Bathe, Stein, and Wunderlich, Springer-Verlag, Berlin, pp. 63-89, (**1980**).

Walker, H. F., "Numerical Solution of Nonlinear Equations," University of California, Lawrence Livermore National Laboratory, Rept. UCID-18285, (**1979**).

Whirley, R. G., and B. E. Engelmann, "A Numerical Implementation of the Gurson-Tvergaard Void Growth Model," University of California, Lawrence Livermore National Laboratory, Rept. UCID, (**1991**).

Whirley, R. G., and B. E. Engelmann, "Development of a Kelvin Viscoelastic Model for DYNA3D," University of California, Lawrence Livermore National Laboratory, Rept. UCID, (**1991a**).

Whirley, R. G., and B. E. Engelmann, "Development of a Ramberg-Osgood Elastoplastic Model for DYNA3D," University of California, Lawrence Livermore National Laboratory, Rept. UCID, (**1991b**).

Whirley, R. G., and B. E. Engelmann, “Generalized Rayleigh Damping in Implicit and Explicit Nonlinear Finite Element Analysis,” University of of California, Lawrence Livermore National Laboratory, Rept UCID, (**1991d**).

Whirley R. G., and B. E. Engelmann, “A Vectorized Numerical Implementation of a Two-Invariant Cap Model Including Kinematic Hardening,” University of California, Lawrence Livermore National Laboratory, Rept. UCID, (**1991e**).

Whirley, R. G., B. E. Engelmann, and B. N. Maker, "A Slightly Compressible Mooney Rivlin Material Model for NIKE3D," University of California, Lawrence Livermore National Laboratory, Rept. UCID, (**1991**).

Whirley, R. G., and J. O. Hallquist, "DYNA3D: A Nonlinear, Explicit, Three-Dimensional Finite Element Code for Solid and Structural Mechanics," University of California, Lawrence Livermore National Laboratory, Rept. UCID-00000, (**1991**).

Whirley, R. G., and G. A. Henshall, "Creep Deformation Structural Analysis Using an Efficient Numerical Algorithm," University of California, Lawrence Livermore National Laboratory, Rept. UCRL-JC-104747, (**1990**).

Wilkins, M. L., "Calculations of Elastic-Plastic Flow," University of California, Lawrence California, Lawrence Livermore National Laboratory, Rept. UCRL-7322, Rev. I, (**1969**).

Wilkins, M. L., "Impact of Cylinders on a Rigid Boundary," J. of Appl. Phys., 44, (**1973**).

Zienkiewicz, O. C., L. Xi-Kui, and S. Nakazawa, "Iterative Solution of Mixed Problems and the Stress Recovery Procedures," Comp. Appl. Num. Meths., 1, pp. 3-9, (**1985**).